

**APPENDIX A: WHITE PAPERS DEVELOPED AS A RESULT OF ISSUES
RAISED IN WORKSHOP #1**

Discreet Charleston earthquake source.

Pro: Pradeep Talwani

Con: Gill Bollinger

Discreet fault sources within the ETSZ.

Pro: Martin Chapman

Con: Klaus Jacob

Discreet local fault sources for Vogtle

Pro Kevin Coppersmith

Con: Pradeep Talwani

(DRAFT)

**ARGUMENTS FOR A DISCRETE CHARLESTON, SOUTH CAROLINA,
EARTHQUAKE SOURCE ZONE**

by
**Pradeep Talwani
and
Ronald Marple**

Sections a – c are intentionally not included

d. Stratigraphy

Auger-hole and well data along the ZRA to the north and south of Lake Moultrie reveal uplifted stratigraphy. Investigation of the anomalously-oriented, early Pleistocene Summerville barrier and underlying shallow marine sediments near Summerville reveals that they were deposited on a NNE-trending, buried structural high, which is reflected in the pre-Plio-Pleistocene surface near Summerville (Weems and Obermeier, 1990) (Fig. 3).

In northeastern South Carolina, the base of a prominent, widespread clay unit (lagoonal/bay environment, Woollen, 1978) within the Black Creek Formation (Upper Cretaceous) is upwarped ~45 m beneath the northern end of the ZRA between the Lynches and Pee Dee rivers (Fig. 4). Further south along the east side of the ZRA between the Lynches and Santee rivers, this Upper Cretaceous horizon exhibits a west-side-up flexure, which suggests faulting or folding of this horizon. However, the contours in the southwestern part of the map area are poorly constrained due to the lack of subsurface data in this area. This linear, NNE-trending area of upwarped, Upper Cretaceous sediments between the Santee and Pee Dee rivers is aligned with the inferred uplift associated with the Summerville barrier to the south (Fig. 3).

e. Shallow seismic reflection data

Shallow seismic reflection data are available along certain portions of the ZRA. The EXXON Exploration Company acquired a seismic reflection profile across the South Carolina Coastal Plain (unpublished data) during the mid 1980s that traverses the ZRA between the Black and Lynches rivers (Fig. 5). These data reveal two steeply-dipping faults about 3.8 km apart that are approximately centered on the ZRA (Fig. 5). Displacements along the steep, west-dipping fault toward the east side of the ZRA decrease from about 20 ms (about 20 m) for the deepest (720 ms, about 720 m) continuous reflector (Jurassic-age basalt flow?) to about 8 ms (8 m) for the reflector at about 320 ms (~320 m) depth (Fig. 5). The reflectors above appear gently upwarped. The fault to the west dips steeply to the east and displays small (< 10 ms) displacements to within about 340 ms (~340 m) of the surface. These two faults are nearly centered on the upwarped Upper Cretaceous sediments along the ZRA (Fig. 5), which suggests that the two faults on the EXXON profile are part of a buried active fault system, uplift along which produced the upwarped Upper Cretaceous sediments and the ZRA.

Additional shallow seismic reflection surveys were acquired near Summerville. Three seismic reflection surveys acquired by the U.S. Geological Survey in the early 1980s near Summerville (e.g., SC-4, SC-6, and SC-10; Fig. 2) revealed three possible faults (Gants and Cooke faults, and the edge of the missing 'J' of Fig. 2; Hamilton et al., 1983) that are nearly centered on the ZRA. The Gants and Cooke faults, both of which coincide with the linear aeromagnetic anomaly, are characterized by west-side-up offsets of about 50 m in a Jurassic-age basalt layer at a depth of about 700 to 750 m (Hamilton et al., 1983). Marple and Talwani (1993) reinterpreted the edge of the missing 'J' as an offset in the Jurassic-age basalt at about 750 m depth. Three shallow, high resolution seismic reflection profiles that were acquired across the ZRA near Summerville in 1993 by the University of South Carolina also revealed

buried faults with small west-side-up offsets and/or upwarped sediments (Marple, 1994) (Fig. 2). A few of these coincide with the linear magnetic anomaly (Fig. 2), which suggests the presence of a NNE-trending buried fault zone beneath the ZRA near Summerville.

f. Microseismicity

Using instrumentally-recorded seismicity data from the MPSSZ, Talwani (1982, 1986) identified two intersecting faults in the Summerville area, the north-northeast-trending Woodstock fault and the northwest-trending Ashley River fault (Fig. 3). The Woodstock fault dips steeply to the west and is associated with right-lateral, oblique, strike-slip motion whereas the Ashley River fault is associated with reverse motion, upthrown to the southwest (Madabhushi and Talwani, 1993). During the period between 1980 and 1990 the seismicity was concentrated primarily near the intersection of these faults (Madabhushi and Talwani, 1993). Although the seismicity between 1991 and early 1995 was located near the main cluster of microseismic activity, more recent seismicity (1995 and 1996) lies farther from this cluster along the trend of the Woodstock fault as defined by Talwani (1982).

g. Paleoseismology

Recent analyses of all available paleoseismological data suggest that there may have been at least six and possibly 7 paleoearthquakes in the outer South Carolina Coastal Plain. A search was carried out for paleoliquefaction features within fluvial deposits inland near the Edisto River and Bowman, although none were found. The only paleoliquefaction features that have been found in South Carolina lie along the coast northeast and southwest of Charleston (Weems et al., 1986; Amick and Gelinas, 1991; Rajendran and Talwani, 1993). The ages of the paleoearthquakes are $110, 546 \pm 17, 1001 \pm 33, 1641 \pm 89, 3548 \pm 66, 5038 \pm 166$ and $5300 - 6300$ years before present (Talwani and Amick, in preparation). The discovery of sandblows of similar ages near Charleston and to its northeast and southwest argue for a source near Charleston. However, sandblows for the event dated at 1641 ± 89 were found only in the north near Georgetown and Myrtle Beach, and not near Charleston, which argues for a seismic source north of Charleston. These observations suggest that the seismic source associated with the seismicity near Charleston extends to the northeast, possibly along the Woodstock fault. No evidence of a source of prehistoric earthquakes was found towards the northwest.

h. Conclusions

Based on all the data presented in the sections above, we conclude that the seismic activity in Charleston is associated with a NNE-trending fault along the ZRA. A fault length of 50 to 60 km is required to generate an Mw 7.3 earthquake (Johnston's (1996) estimate of the 1886 Charleston earthquake). The extent of the buried fault associated with the ZRA and other features described above provide an adequate length for an Mw 7.3 earthquake.

III. EVIDENCE OF TECTONIC ACTIVITY

Evidence of tectonic activity is divided into loosely-defined time scales, which cover the last 1,000,000 years. These different lines of evidence include the ZRA, upwarped Plio-Pleistocene deposits, paleoearthquakes, releveling, current seismicity and GPS investigations.

a. Holocene to 1,000,000 years

Evidence of tectonic activity along the ZRA during this time range comes from a variety of observations. The upwarped floodplains along the Santee, Lynches and Pee Dee rivers (Fig. 1) indicate tectonic activity between about 100,000 years and Holocene time. Observations of surficial deposits combined with changes in the cross-valley shapes of the Santee and Lynches river valleys along their arc-shaped curves suggest local uplift along the ZRA since at least Penholoway time (~750,000 years, McCartan et al., 1990) and through Holocene time.

b. Thousands of years to present

Paleoliquefaction data suggest that there was earthquake activity at least as far back as 5,000 years. Historical seismicity has been documented for about the last 300 years. In view of the current seismicity we conclude that there has been tectonic activity for at least the last 5,000 years. Additional evidence of local tectonic activity for the last 100 years comes from an evaluation of the releveling data in the area. These data suggest localized uplift south of Summerville.

Results of recent GPS surveys show that there is localized high strain accumulation in the MPSSZ. The calculated strain rate is about two orders of magnitude greater than the background. The direction of compression obtained from GPS is in good agreement with the direction of SHmax inferred from other data (e.g., Zoback et al., 1986).

c. Conclusions

Data presented above provide evidence for tectonic activity over approximately the last 1,000,000 years.

IV. EVIDENCE FOR A DISCRETE SOURCE

Between Summerville and Middleton Place we have evidence of a northwest-trending fault along the Ashley River. The northwest trend terminates near Summerville along the north-northeast trend of the Woodstock fault/ZRA. No evidence for a NW-trending fault was found northwest of Summerville. In the sections above we showed that integration of a variety of data support the existence of a NNE-trending buried fault along the ZRA. The length of this NNE-trending Woodstock fault/ZRA is adequate to generate the Mw 7.3 estimated for the 1886 Charleston, SC, earthquake. A variety of data indicate that there has been tectonic activity on this feature for at least 1,000,000 years. Currently, the most seismically active part of this feature is its southern end where it intersects with the Ashley

River fault. This is also where localized high strain accumulation was observed by a GPS study. S_H max is favorably oriented with respect to the Woodstock fault to generate right-lateral strike slip faulting.

Based on all these observations we conclude that the seismicity near Charleston is associated with a discrete, ~50-km-long, NNE-trending source--the Woodstock fault.

REFERENCES

- Amick, D.C., and Gelinis, R., 1991, The search for evidence of large prehistoric earthquakes along the Atlantic seaboard: *Science*, v. 251, no. 4994, p. 655-658.
- Hamilton, R.M., Behrendt, J.C., and Ackermann, H.D., 1983, Land multichannel seismic reflection evidence for tectonic features near Charleston, South Carolina, in Gohn, G.S., ed., *Studies related to the Charleston, South Carolina, earthquake of 1886; tectonics and seismicity*: U.S. Geological Survey Professional Paper 1313, p. 11-118.
- Johnston, A.C., 1996, Seismic moment assessment of earthquakes in stable continental regions—III. New Madrid 1811-1812, Charleston 1886 and Lisbon 1755: *Geophysical Journal International*.
- Madabhushi, S., and Talwani, P., 1993, Fault plane solutions and relocations of recent earthquakes in Middleton Place Summerville seismic zone near Charleston, South Carolina: *Bulletin of the Seismological Society of America*, v. 83, no. 5, p. 1442-1466.
- Marple, R.T., 1994, Discovery of a possible seismogenic fault system beneath the Coastal Plain of South and North Carolina from an integration of river morphology and geological and geophysical data [Ph.D. dissert.]: Columbia, University of South Carolina, 354 p., 13 plates.
- Marple, R.T., and Talwani, P., 1993, Evidence of possible tectonic upwarping along the South Carolina coastal plain from an examination of river morphology and elevation data: *Geology*, v. 21, no. 7, p. 651-654.
- McCartan, L., Weems, R.E., and Lemon, E.M., Jr., 1990, Quaternary stratigraphy in the vicinity of Charleston, South Carolina, and its relationship to local seismicity and regional tectonism, in *Studies Related to the Charleston, South Carolina, Earthquake of 1886-Neogene and Quaternary Lithostratigraphy and Biostratigraphy*: U.S. Geological Survey Professional Paper 1367-A, p. A1-A39.
- Phillips, J.D., 1988, Buried structures at the northern end of the early Mesozoic South Georgia basin, South Carolina, as interpreted from aeromagnetic data, in Froelich, A.J., and Robinson, G.R., eds., *Studies of the early Mesozoic basins of the eastern United States*: U.S. Geological Survey *Bulletin* 1776, p. 248-252.
- Rajendran, C.P., and Talwani, P., 1993, Paleoseismic indicators near Bluffton, South Carolina: An appraisal of their tectonic implications: *Geology*, v. 21, p. 987-990.
- Talwani, P., 1982, An internally consistent pattern of seismicity near Charleston, South Carolina: *Geology*, v. 10, p. 655-658.
- Talwani, P., 1986, Seismotectonics of the Charleston region, in *Proceedings, National Conference on Earthquake Engineering, 3rd*: Earthquake Engineering Research Institute, v. 1, p. 15-24.
- Weems, R.E., and Obermeier, S.F., 1990, The 1886 Charleston earthquake -- An overview of geologic studies, *Proceedings, Water Reactor Safety Information Meeting, 17th*: U.S. Nuclear Regulatory Commission NUREG/CP-0105, p. 289-313.

- Weems, R.E, Obermeier, S.F., Pavich, J.J., Gohn, G.S., Rubin, M., Phipps, R.L., and Jacobson, R.B., 1986, Evidence for three moderate to large prehistoric Holocene earthquakes near Charleston, South Carolina: Proceedings, 3rd U.S. National Conference on Earthquake Engineering, Earthquake Engineering Research Institute, v. 1, p. 197-208.
- Woollen, I.D., 1978, Structural framework, lithostratigraphy and depositional environments of Upper Cretaceous sediments of eastern South Carolina [Ph.D. dissert.]: Columbia, University of South Carolina, 276 p.
- Zoback, M.L., Nishenko, S.P., Richardson, R.M., Hasegawa, H.S., and Zoback, M.D., 1986, Mid-plate stress, deformation and seismicity, in Vogt, P.R., and Tucholke, B.E., eds., The Geology of North America, volume M: Boulder, Colorado, Geological Society of America, The Western North Atlantic region, p. 297-312.

FIGURE CAPTIONS

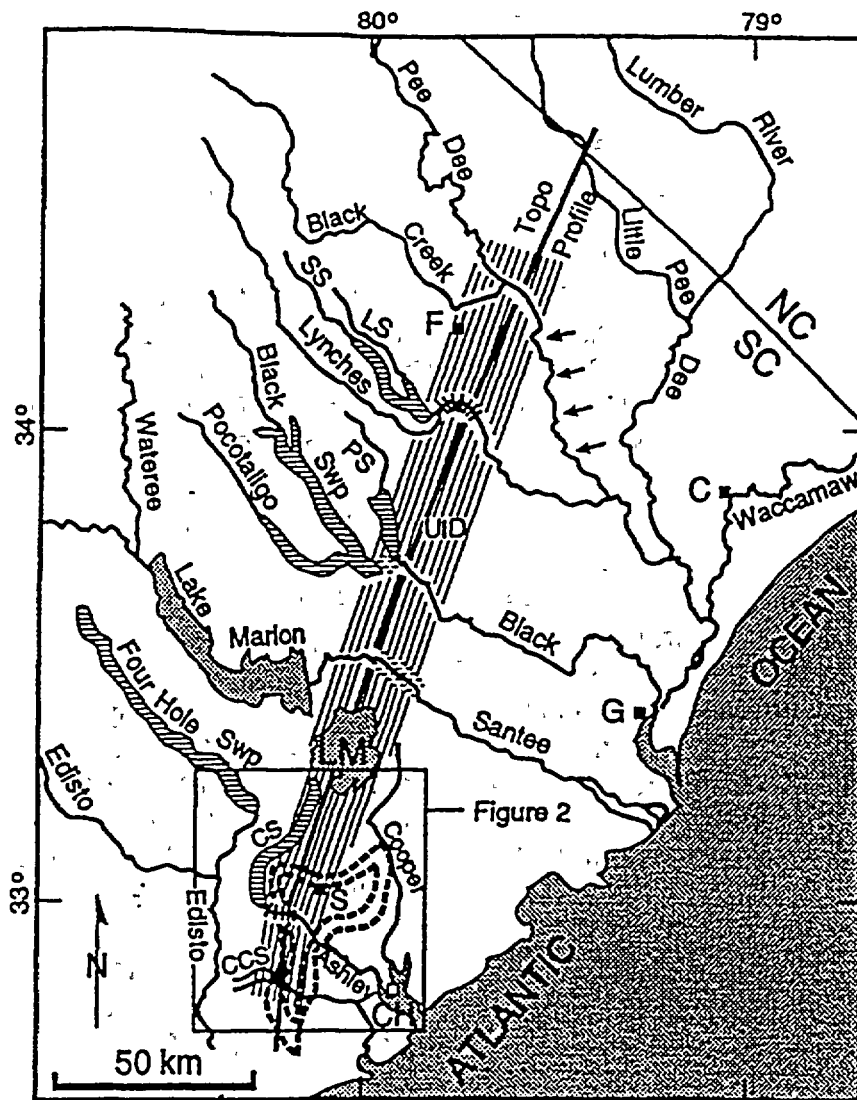
Figure 1: The "zone of river anomalies" (ZRA, NNE-trending striped area), anastomosing stream patterns, pre-1886 sand blow sites (stars, modified from Obermeier et al., 1987, and Prowell and Obermeier, 1991) and Sloan's isoseismals of the 1886 Charleston, S.C., earthquake (dashed closed contours near Summerville-S, after Dutton, 1890). The arrows along the north side of the Pee Dee River downstream of the ZRA denote that part of the river that is flowing against the southwest side of its valley. U/D denotes location of the easternmost fault of the two buried faults inferred on the EXXON seismic reflection profile (unpublished data) (see Fig. 5). C-Conway, CCS-Caw Caw Swamp, CH-Charleston, CS-Cypress Swamp, F-Florence, G-Georgetown, LM-Lake Moultrie, LS-Lake Swamp, PS-Pudding Swamp, S-Summerville, SS-Sparrow Swamp. Location of figure 2 is shown.

Figure 2: Locations of seismicity (1974-1996, black dots) compared with the "zone of river anomalies" (ZRA, NNE-trending stripes) and locations of various geological features. Ashley River fault (ARF) and Woodstock fault (WF) shown as dashed lines (from Talwani, 1986). Gray area denotes topographically high areas inferred from topographic profiles (see Fig. 4 of Marple and Talwani, 1993). Line 9 shows part of releveling line from Yemassee (Y) to Charleston (Ch) (from Poley and Talwani, 1986). The area of uplift inferred along Line 9 is dashed. Buried faults and areas of upwarped sediments inferred from seismic reflection data are denoted by U/D and U?, respectively. J-western edge of missing 'J' horizon, C-Cooke fault, G-Gants fault (Hamilton et al., 1983). Ch-Charleston, LM-Lake Moultrie, ML-linear magnetic anomaly inferred from aeromagnetic data of Phillips (1988), S-Summerville.

Figure 3: Spatial comparison of Summerville barrier (bold contour), ZRA (between parallel dashed lines), and linear aeromagnetic anomaly (ML) with the contour map of the base of the Plio-Pleistocene deposits (from Weems and Obermeier, 1990) in the Summerville area. Note the coincidence of the linear magnetic anomaly, Summerville barrier, ZRA, and the NNE-trending structural high on the base of the Plio-Pleistocene sediments (black area, >40 ft contour) between Lake Moultrie and Summerville. LM-Lake Moultrie, M-Moncks Corner, S-Summerville.

Figure 4: Spatial comparison of the ZRA (striped area) with the structure contour map of the base of a clay unit in the Black Creek Formation in northeastern South Carolina and the postulated area of uplift between Lake Moultrie and the Ashley River (black area). Contours in hundreds of feet with respect to mean sea level. Contours modified from Woollen's (1978) map (figure 6.8.8, p. 207). Note the distortion of the contours along or just east of the ZRA. CS-Cypress Swamp, S-Summerville.

Figure 5: Portion of seismic reflection profile acquired by EXXON (unpublished data) that crosses the ZRA. Note the two steeply-dipping buried faults (steeply dipping thin lines) about 3.8 km apart. See figure 1 for location of fault on the east side of this profile.



LEGEND

+++++		
incised river channel	dissected floodplain	anastomosing stream patterns

Figure 1

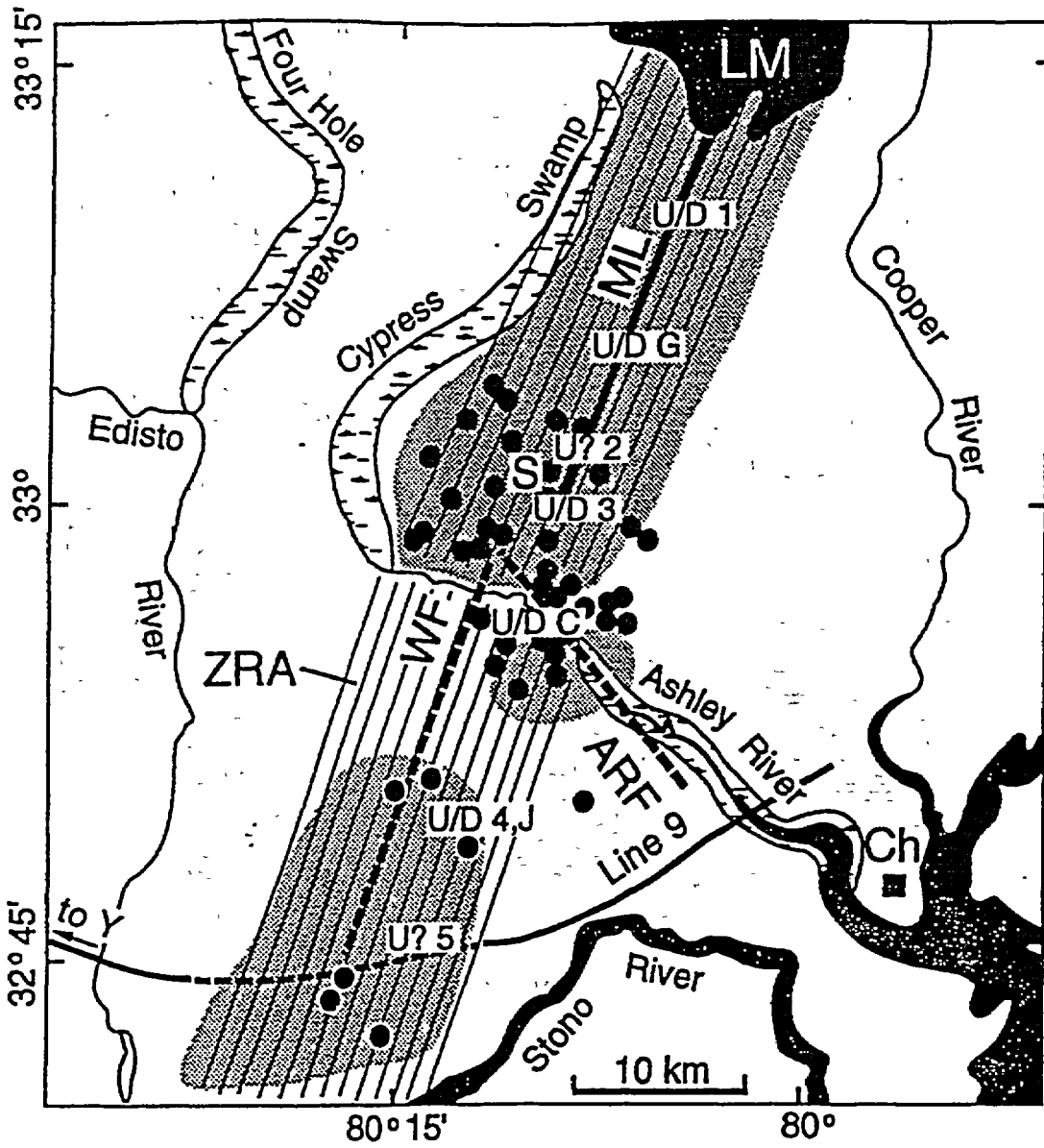


Figure 2

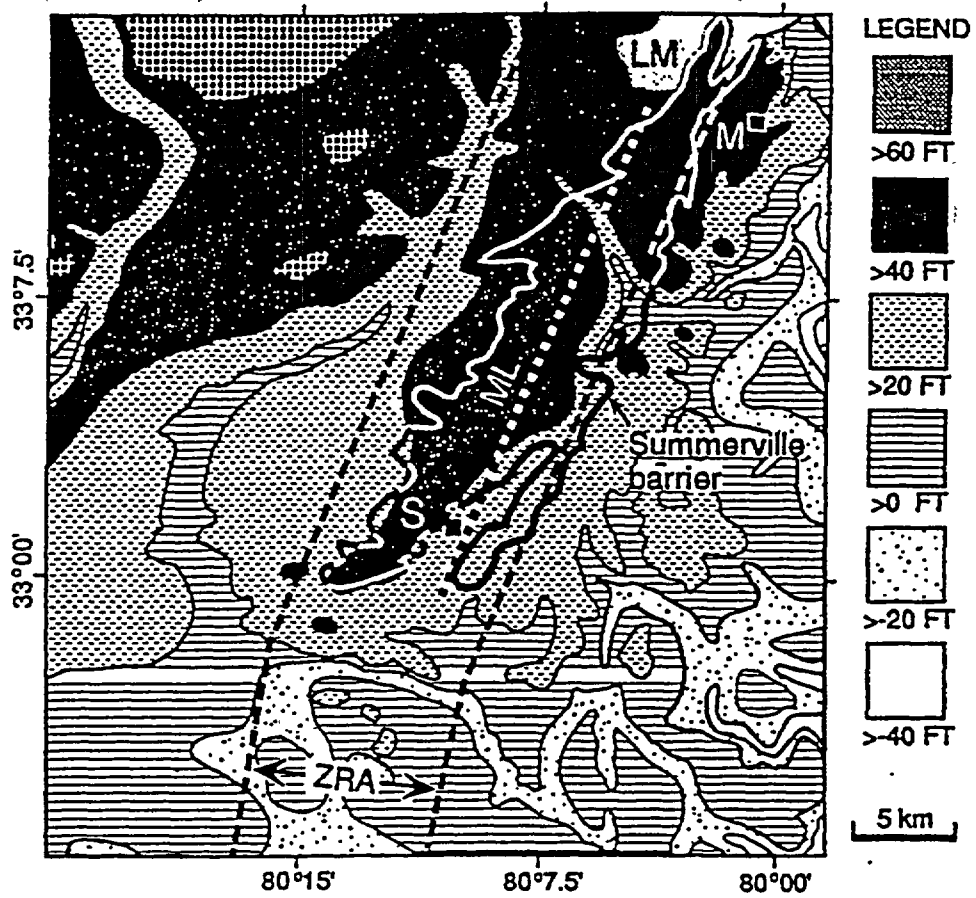


Figure 3

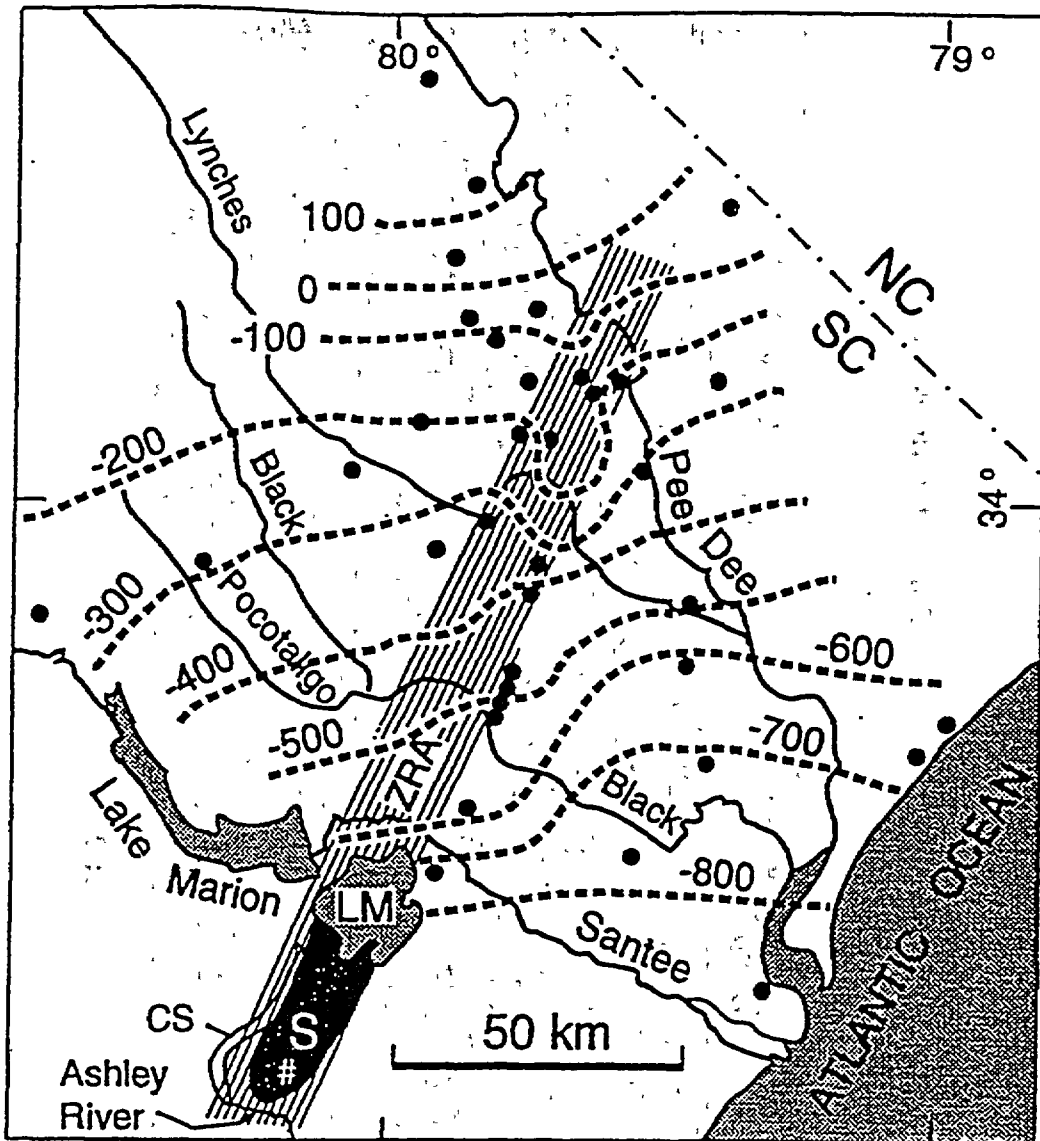
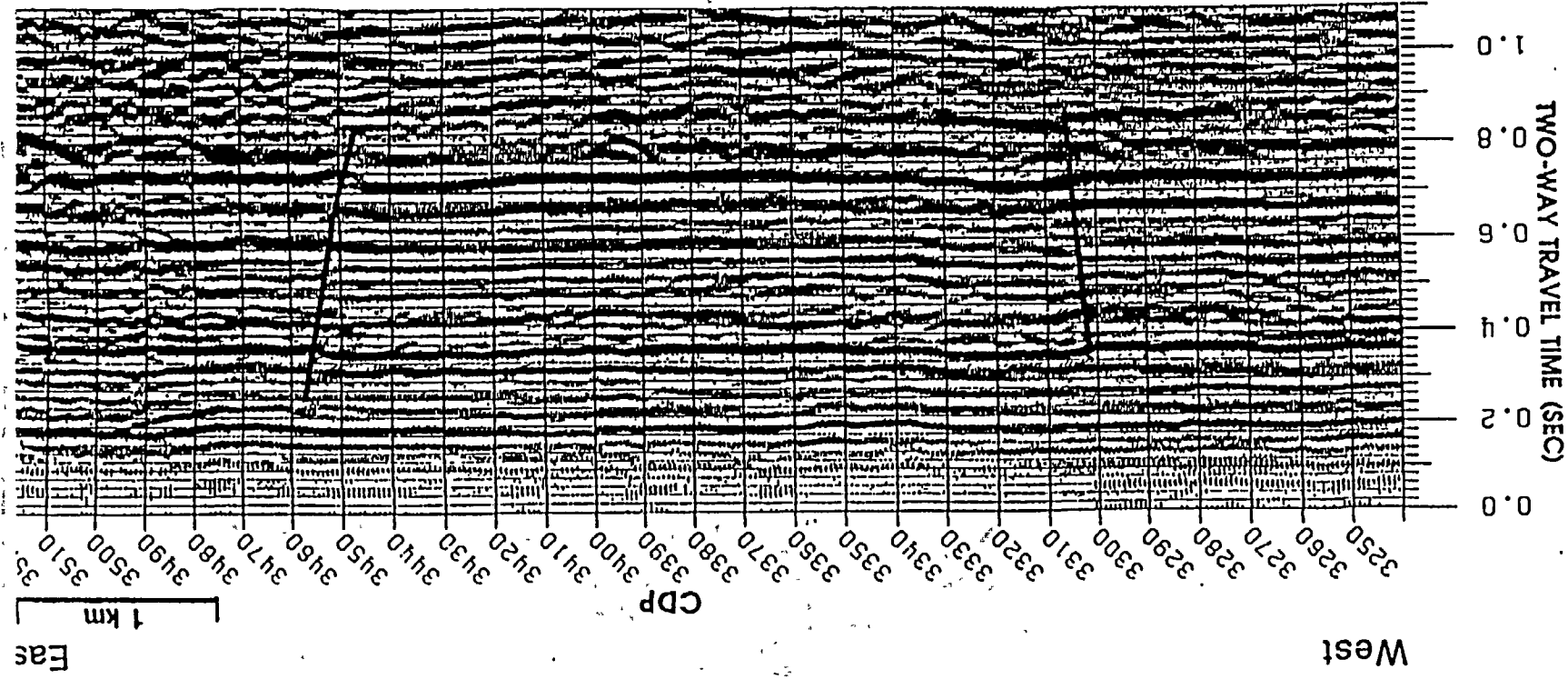


Figure 4



Courtesy of EXXON Exploration Company, Houston

Figure 5

THE CASE FOR A LARGE EARTHQUAKE (M=7+) IN SOUTH CAROLINA AWAY FROM THE CHARLESTON AREA

Gil Bollinger

Introduction

The large 1886 Charleston, South Carolina earthquake (M 7.3, MMI X) dominates the seismicity of that state and its host region. It is an especially singular event in that the next largest earthquake, the 1897 Giles County, Virginia shock, was some one-and-a-half magnitude units and two MMI levels smaller (M 5.7, MMI VIII). South Carolina has a further seismological distinction in that the entire state exhibits a low level of diffuse historical and recent earthquake activity while adjoining North Carolina and Georgia are much less active. I emphasized this fact in a 1973 BSSA paper with the definition of a northwest trending South Carolina-Georgia Seismic Zone. Subsequent instrumental and network monitoring has continued to document earthquake occurrence both in the Charleston area and throughout that northwest zone, including episodes of reservoir-induced seismicity.

Given the singular occurrence of a large earthquake at the apparent terminus of a relatively isolated zone of seismicity the question of the earthquake potential throughout the remainder of that zone arises naturally. This paper will argue that the entire zone should be considered to have a M 7+ capability.

Spatial Considerations

The spatial character of historical and recent seismicity in South Carolina can be characterized as clusters at Charleston and Bowman and a diffuse distribution throughout the remainder of the state, particularly in the Piedmont portion. Comparison of my original definition of seismic zones based primarily on historical seismicity with recent SEUSSN Bulletins showing the activity over the past two decades documents the spatial stationarity of earthquake occurrence in South Carolina over that time period. The only 'newcomer' is the low energy level cluster at Bowman

which has an on again/off again habit since its initial activity in the early 1970's. In terms of energy release, however, the Charleston Zone accounts for some 90+% of the state's strain energy release budget.

As noted above, in 1973 I zoned all of the seismicity in South Carolina, plus a small amount in Georgia, into a South Carolina-Georgia Seismic Zone. In 1992 (USGS Bulletin 2017), given the increase in locational accuracy by the region's networks, I separated the clusters and the diffuse activity into three separate zones labeled Charleston, Bowman and South Carolina Piedmont & Coastal Plain. Recent paleoseismic results indicate possible prehistoric liquefaction producing loci northeast of Charleston and maybe southwest of Charleston also. Both of those sites are in the Coastal Plain and should be considered for zonal status even though one possible explanation for the paleoliquefaction there is amplification by some form of crustal focusing.

The spatial isolation of South Carolina seismicity with respect to the northeast, southwest and southeast directions defines a distinct seismotectonic regime that includes the region's largest known earthquake at its southeast terminus. Charleston's seismic activity appears to be due to a set of intersecting structures. Talwani and his co-workers (Eqke Notes, 1986) have presented extensive evidence for two intersection faults which they term the Woodstock and Ashely River faults. Phillips (USGS Bull. 1776, 1988) interpreted potential field data to show a circular impact-type structure intersecting a throughgoing Triassic basin border fault at Summerville, near the presumed epicenter of the 1886 shock. An intersection feature would certainly explain the concentrated character of the recent seismicity. The sporadic earthquakes at Bowman are also clustered but no probable structures have been identified there.

At least some portion of the diffuse South Carolina Piedmont seismicity carries one or two proposed explanations. Zoback et al (GSA Geol. No. Am., 1986) finds a very high level of horizontal stress in the upper few kilometers of the high-velocity crystalline Piedmont rocks. He argues that this stress regime could result in a 'skin effect' of shallow microseismicity that has no associated large earthquake potential. Talwani (see, e.g., Seism.

Res. Ltrs., 1996) has studied the small central Piedmont and upper Coastal Plain earthquakes (M about 4 or less) with respect to their tectonic and potential field settings. He finds such earthquakes often located on the flanks of intrusive structures and invokes a stress-concentration type of causality -- again without large earthquake potential. Finally, the South Carolina Piedmont is unique in the host southeastern U.S. because of its multiple instances of reservoir-induced seismicity (see, e.g., Talwani, Pure & Appld. Geoph., 1984) which also tends to be shallow and associated with high stress levels.

If all of the spatially diffuse South Carolina Piedmont is indeed due to one or both of the proposed mechanisms then only the Charleston locale and perhaps the paleoliquefaction sites have the capability to generate a large earthquake within the state. There are, however, a number of throughgoing structural features in the state, e.g., Triassic basin marginal faults, Modoc fault, etc. that require only an intersecting fault, intrusion or dike to have an adequate strain volume for a Charleston-sized shock. In principle, the Bowman cluster or any of the skin effect/stress amplification earthquakes could be at such an intersection that is currently only experiencing only a very low rate of strain deformation. This type of situation would be similar to the lack of historic and current seismicity that presently exists at the non-Charleston paleoliquefaction sites within the state.

Temporal Considerations

The temporal behavior of South Carolina's seismicity displays the following three different habits :

- (1) Charleston locale - Some 300 years of persistent seismicity (earliest earthquake 1698) with one large historic shock 110 years ago,
- (2) Coastal Plain northeast and southwest of Charleston - Paleoliquefaction sites indicating focusing from Charleston and/or the occurrence of moderate to large prehistoric earthquakes. There is little or no associated historic or recent earthquake activity at these sites and
- (3) Coastal Plain and Piedmont northwest of Charleston - 200+ years of sporadic, low energy level earthquakes and no large historic earthquake.

No prehistoric data available. On/off clustered activity in the Bowman area.

In terms of recurrence rates, we have the following (Bollinger, USGS Bull. 2017, 1992) :

Charleston Zone	Log Nc = 1.69 - 0.77mb	Observed Mmax ~ 7.3
Bowman Zone	Log Nc = 1.34 - 0.78mb	Observed Mmax ~ 4.5
SC P/CP Zone	Log Nc = 1.86 - 0.80mb	Observed Mmax ~ 4.8

Interestingly, while there is the expected large difference in the zonal observed Mmax's and seismicity levels (a-values), the proportions of small to large shocks that have occurred are all at a b-value of about 0.8. Comparing these a-values and b-values with those from the host region (SE US) and geological provinces (Coastal Plain and Piedmont) (Bollinger, IGR, 1989) :

SE US	Log Nc = 3.12 - 0.84mb,
Piedmont	Log Nc = 2.18 - 0.81mb,
Coastal Plain	Log Nc = 2.22 - 0.78mb,

we again find the same b-value (0.8) and the expectably very different a-values. Thus, within the resolution of the historical seismicity data base, significant differences are not found between the region and its various subdivisions in the small-to-large earthquake proportions. This provides no spatial or temporal constraints or preferences on the occurrence of a large earthquake in the region.

Geologic Considerations

The tectonic setting at Charleston is almost certainly non-unique. Therefore, similar settings probably exist elsewhere in the region - perhaps in the South Carolina Piedmont - and are candidates for future large shocks.

The rate of the Charleston source, about 1/500 yr, would leave obvious structural evidence (Cenozoic mountains) over geologic time frames. Such evidence is not found at Charleston which implies an episodic, 'on/off' source. This allows for the presence of currently 'off' sources elsewhere in

the region, including the South Carolina Piedmont, that can turn 'on' in the future.

Given the same plate motions driving the seismicity over much of the past few tens of millions of years (Klitgord and Schouten, GSA, The Geol. of No. Am., 1986) then the eastern U.S. seaboard, including Charleston, has probably maintained the same approximate rate of seismicity over that time interval. Therefore, before Charleston turned on, any accumulated strain deformation was released elsewhere, most likely along the belt of Mesozoic extensional faults which includes the South Carolina Piedmont (R. Wheeler, written comm., 1996). Such sources can, in principle, turn 'on' again.

In high strain-rate interplate areas the faulting tends to be rather organized with earthquakes repeating themselves - but there are occasional outliers. It may be that in low strain-rate intraplate areas the long term variance of the faulting process is very large which results in a spatially uniform, long term seismicity (M. Chapman, written comm., 1996). Surely, there should also be the occasional 'outlier' shocks there. Such a seismic environment could host more than one large earthquake source in an area the size of the state of South Carolina.

Possible Locations for Large South Carolina Earthquakes

If the the temporal habits described above are indeed applicable to South Carolina's next large earthquake then assigning a large earthquake potential outside of the Charleston locale requires either that,

- (1) The new source area(s) have exhibited persistent historical seismicity similar to the Charleston area or,
- (2) They have exhibited no appreciable strain release during historic and recent time similar to the paleoliquefaction sites.

If the previously discussed spatial habits are diagnostic, then,

- (3) Only the recent clustered activity at Bowman allows for a possible new large earthquake site.

The geologic considerations presented have argued that,

(4) The Charleston source's tectonic non-uniqueness, 'on/off' recurrence nature from lack of structural/topographic features, the probable presence of other pre-Charleston 'on/off' sources elsewhere in response to long-term, uniform plate motions and low, intraplate strain-rate effects in the region; all allow for the occurrence of a large earthquake in the South Carolina Piedmont.

The (1) and (3) possibilities restrict new sources to the Bowman locale. In the (2) possibility, however, the prehistorically active and historically inactive paleoliquefaction sites, if due at least in part to large earthquakes, open the entire South Carolina Coastal Plain area to that level of hazard. Possibility (4) and the fact that there are no prehistoric indicators on the South Carolina Piedmont to define seismicity there argue for the potential occurrence of a large (M 7+) in the South Carolina Piedmont.

AN ARGUMENT IN SUPPORT OF THE CONTENTION THAT A MAJOR
EARTHQUAKE COULD OCCUR IN EASTERN TENNESSEE

by
Martin C. Chapman

Introduction

The eastern Tennessee seismic zone is defined primarily on the basis of small, instrumentally recorded earthquakes that have occurred since regional seismic networks became operational in the area beginning in 1981. The zone lies mostly within the Valley and Ridge province of eastern Tennessee, but extends from northwestern Georgia to near the intersection of the Tennessee, Virginia and Kentucky borders (e.g., Powell et al., 1994). For the period 1981 through 1994, this zone has dominated the recorded seismicity of the southeastern U.S., in sheer number of events. This is partly due to the network detection capability. But when one examines only the larger shocks (Figure 1) the zone remains the most outstanding feature on the regional seismicity map.

Most, if not all of the earthquakes occur beneath the Appalachian thrust sheets, at depths from 5 to 20 km, and therefore indicate a relatively thick section of seismogenic (brittle) crust (Bollinger et al., 1985, 1991; Vlahovic et al 1996). No surface expression of the seismicity has been recognized.

Focal mechanisms indicate that strike-slip is the dominant mode of faulting throughout the seismic zone, with most well-constrained mechanisms showing right-lateral or left-lateral motion on N-S or E-W striking planes, respectively (Johnston et al, 1985, Teague et al 1986, Davison, 1988; Li, 1994; Chapman et al., 1996). A smaller population of events exhibit right-lateral and left-lateral motion on planes striking NE-SW or NW-SE,

respectively (Chapman et al. 1996). The largest historical shock in the zone is mblg 4.6. (Bollinger, 1973; Bollinger et al., 1976; Reinbold and Johnston, 1987).

The Potential for Large Shocks

Kagan and Jackson (1994) give, for the general case, the following conditions that seem reasonable pre-requisites for assigning a high likelihood for future large earthquakes.

- 1) Geological evidence of large earthquakes in the past few thousand years.
- 2) Geodetic or geological evidence of stress accumulation.
- 3) Seismological evidence of large earthquakes in the last few centuries (historical seismicity).
- 4) Seismological evidence of earthquakes in the last few years or decades.

As noted by Kagan and Jackson (1994), the conditions often give contradictory signals. The following discussion will deal with these four conditions in turn.

1) Geological Evidence

We have no geological evidence for past large earthquakes in eastern Tennessee. In assessing the implication of this, the observation that seismicity is occurring at depth, beneath a detachment surface must be considered. This, combined with the great thickness of brittle crust, may represent a situation where the rupture of a magnitude 7.0 shock could be contained entirely within the basement. Given the intra-plate setting, surface expression of repeated shocks might be masked or removed

entirely by erosion, particularly if mechanisms were strike-slip with return periods on the order of several thousand years. Also, lack of geological evidence is relevant to this issue only if it can be argued, with reasonable confidence, that evidence would be in hand if the requisite geologic features actually exist. Clearly, the extent to which geological investigations have been made, or are possible, is an important consideration. For example, the fact that no paleoliquefaction relics have been recognized to date may reflect a lack of deposits susceptible to liquefaction, rather than the absence of large shocks in the past.

2) Stress Accumulation

Accurate geodetic estimates of strain rate are not available for eastern Tennessee. There is some geological evidence for post Cretaceous uplift in the region, based on erosion rates of the order 40m/million yr (Bartholomew and Mills, 1993).

3) Historical Seismicity

The earliest recorded shock in eastern Tennessee was in 1777. There is no record of an eastern Tennessee earthquake with magnitude exceeding 4.6. The lack of moderate earthquakes in the historical past is a potential argument against future large shocks in the seismic zone. To examine this, I use the Virginia Tech catalog of southeastern U.S. earthquakes to develop a recurrence relation for the area shown by the dashed lines in Figure 1. After removing obvious dependent events, the numbers of earthquakes are summed by decade and binned by magnitude as shown in Table 1.

TABLE 1
Number of Earthquakes by decade
Eastern Tennessee Seismic Zone

date	Magnitude mblg					
	2.0-2.4	2.5-2.9	3.0-3.4	3.5-3.9	4.0-4.4	4.5+
1994-90	35	19	5	0	0	0
1989-80	59	27	15	4	2	0
1979-70	1	3	2	4	0	1
1969-60	0	3	1	2	1	0
1959-50	0	0	6	4	3	0
1949-40	0	3	2	2	1	0
1939-30	0	0	1	2	0	0
1929-20	0	0	0	2	0	0
1919-10	0	2	3	3	1	0
1909-00	0	0	1	2	1	0
1899-90	0	0	0	0	0	0
1889-80	1	0	1	0	0	0
1879-70	0	2	0	0	1	0
1869-60	0	1	0	0	0	0
1859-50	0	0	0	0	0	0
1849-40	0	0	0	1	0	0
-----	-	-	-	-	-	-
1777	0	0	1	0	0	0

1981

Assuming stationary temporal behavior, I judge (from Table 1) that the catalog is ~~complete for magnitudes 2.0 to 3.5 for the past 15 years; for magnitudes 3.5 to 3.9 it appears complete back to 1900; for magnitudes greater than 4.0 it appears complete to 1879.~~ A least squares fit to the logarithms of the cumulative annual rates gives $\text{Log } N = 3.23 - 1.07 \text{ mblg}$. The data and the regression line are shown in Figure 2. Further assuming that the earthquakes represent a Poisson process, with rates for various magnitudes given by the above equation, I address the question of whether or not the lack of moderate shocks in the historical record has any real significance to the issue of possible large shocks in eastern Tennessee. I ask: how far back in time would the historical record of (complete) seismicity have to extend in order for it to have a more than 0.5 probability of recording the occurrence of at least 1 event

of say, M greater than 7.0? The probability of one or more events in time t is given by $P = 1 - \exp(-Nt)$. Solving for t with $N = 5.5 \times 10^{-5}$ (for mblg = 7.0) and $P = 0.5$ gives $t = 12,600$ years. Results for mblg = 6.0 and mblg = 5.0 are 1,030 and 88 years, respectively. The required catalog dates are as follows:

$t(m=7.0|P=0.5) = 12,600$ years, 10,604BC,
 $t(m=6.0|P=0.5) = 1,066$ years, 930AD,
 $t(m=5.0|P=0.5) = 91$ years, 1905AD.

Clearly, the existing catalog is much too short to have any relevance for magnitudes 6 and greater. However, it appears that at the magnitude 5 level, the catalog MAY be long enough to yield some marginally significant information. It is likely that the catalog is in fact complete for $M > 5$ back to at least 1870, and possibly somewhat earlier. Using the 1870 date as the completeness limit (i.e., setting $t = 126$ years) we get:

$P(\text{at least 1 } M > 5.0 \text{ event} | 126 \text{ years}) = 0.62.$

This is another way of saying that the return period of $M > 5.0$ is 126 years. Let us consider the possibility that the catalog is complete for $M = 5.0$ all the way back to 1840.

$P(\text{at least 1 } M > 5.0 \text{ event} | 156 \text{ years}) = 0.69.$

Although 0.69 is large enough to suggest that eastern Tennessee is slightly overdue for the occurrence of a magnitude 5.0 or larger shock, it is not a statistically significant basis for an argument in favor of a limited maximum magnitude.

For the seismic history to have any bearing on the "Large Earthquake" problem, we need a catalog of length such that the absence of $M > 5$ events is significant at (the very least) the 90%

level: i.e, the catalog would have to be complete for magnitude 5.0 (and contain no $M > 5.0$ events) back to

$t(m=5.0|P=0.9) = 303 \text{ years, } 1693\text{AD.}$

Assuming that a catalog complete to the days of earliest colonial presence in the area was in hand, an argument favoring a limited maximum magnitude on the basis of that catalog would have to recognize that the Poisson process is a critical assumption.

In summary, there is an appreciable probability of not observing moderate or large shocks during the historical period, and arguments either for (or against) the likelihood of earthquakes significantly larger than the historical maximum of 4.6 are highly equivocal, if based on the catalog alone. Finally, it is worth mentioning that the magnitude 5.0+ earthquake of February 21, 1916 which is listed in most catalogs (e.g., Stover and Coffman, 1993) as centered near Waynesville, North Carolina, produced very nearly the same maximum intensity effects over an extended area of Sevier County, Tennessee, well to the west (Figure 3). In my opinion, the possibility exists that this shock actually occurred somewhere in the Smoky Mountains near the Tennessee - North Carolina border.

4) Recent Seismicity

On the basis of the above arguments, I contend that the information provided by the instrumentally recorded seismicity during the past 15 years currently represents the most viable basis for assessing the potential for large shocks in eastern Tennessee.

In addition to the salient features mentioned in the introduction, the instrumentally located seismicity exhibits other properties which are pertinent to this discussion.

- Unequivocal correlation of the seismicity with major potential field anomalies and crustal velocity anomalies.
- A high degree of consistency of focal mechanism solutions within the spatially extended seismic zone.
- Correlation and mutual consistency of earthquake spatial location, epicenter directional alignment, and focal mechanism solutions.

The correlation between seismicity and the New York - Alabama potential field anomaly is well known (King and Zietz, 1978; Johnston et al., 1985; Powell et al. 1994). Johnston et al. (1985) interpreted the early results of network monitoring as suggesting the existence of a seismogenic crustal block bounded on the northwest by the NY-AL anomaly and on the southeast by the Clingman Lineament (Nelson and Zietz, 1983). After more than a decade of additional monitoring, this conceptual model can be refined.

On the basis of a statistical examination of the epicenter locations and focal mechanism solutions, Chapman et al., (1996) find that much of the seismicity is organized along several NE-trending, en-echelon alignments, which lie along and to the southeast of the potential field anomaly. The NE-trending alignments are responsible for the overall trend of the seismic zone, but do not tell the whole story. The picture is complicated by evidence for easterly-trending alignments, the most prominent of which is at 35.5 deg. N, where a significant number of earthquakes have occurred on both sides of the NY-AL anomaly.

Chapman et al. (1996) interpret the network data as suggesting the existence of a set of northeast-trending basement faults intersected by an east-trending conjugate set (Figure 4). The faults are inferred to be steeply dipping, with mostly right

lateral motion on the NE set, whereas left-lateral slip is inferred for the east-trending set. It is important to note that this interpretation is based on the entire data set, including earthquakes as small as magnitude 0.0; however, as shown in Figure 4, the larger magnitude shocks have occurred along and near the intersections of the inferred faults.

A 3D velocity inversion of the network data by Vlahovic et al. (1996) indicates that the potential field anomalies are spatially correlated with velocity anomalies that extend vertically through the inversion volume (25 km). An integrated interpretation of the velocity and potential field data is being performed by Gordana Vlahovic. At this point, it appears that the juxtaposition of crustal scale potential field and velocity anomalies with a spatially extensive and highly organized zone of seismicity is no coincidence. I argue here that the recent shocks are illuminating two sets of basement faults, one of which trends sub-parallel to major structural/lithologic elements of the crust. The relationship between the faults inferred on the basis of the seismicity and the large scale crustal features responsible for the potential field and velocity anomalies is likely complex, due to the very complex tectonic history of the Appalachians. In fact, there is no strong, presumptive reason to expect anything approaching a one-to-one correlation between the gross structural framework of the crust (that is probably responsible for the potential field/velocity anomalies) on the one hand, and currently seismogenic faults on the other. The reason is that the modern stress field will act to preferentially re-activate favorably oriented faults. In this particular case a clear correlation does exist, involving the NE-trending inferred faults. The east-west trending epicenter alignments may be illuminating (comparatively minor?) cross cutting features more favorably aligned to the modern direction of maximum shear stress. Regardless of the likely complex relationships between currently

seismogenic structures and the gross tectonic fabric, the lengths of the inferred faults are more than sufficient to produce a major shock. In my opinion, this is to be expected given that the velocity and potential field data suggest that this area may be the site of a major Late Paleozoic (or Precambrian) shear zone or Eocambrian zone of extension (Powell et al., 1994).

References

- Bartholomew, M.J. and H.M. Mills, (1993). Old courses of the New River: Its Cenozoic migration and bedrock control inferred from high level stream gravel, *Bull. Geological Soc. Am.*, 103, 73-81.
- Bollinger, G.A. (1973). Seismicity of the southeastern United States, *Bull. Seism. Soc. Am.*, 63, 1785-1808.
- Bollinger, G.A., C.J. Langer and S.T. Harding (1976). The eastern Tennessee earthquake sequence of October through December, 1973, *Bull. Seism. Soc. Am.*, 66, 525-547.
- Bollinger, G.A., M.C. Chapman, M.S. Sibol and J.K. Costain (1985). An analysis of earthquake focal depths in the southeastern U.S., *Geophysical Research Letters*, 12, 785-788.
- Bollinger, G.A., A.C. Johnston, P. Talwani, L.T. Long, K.M. Shedlock, M.S. Sibol and M.C. Chapman (1991). Seismicity of the southeastern United States; 1698 to 1986, in Slemmons, D.B., E.R. Engdahl, M.D. Zoback and D.D. Blackwell, eds., *Neotectonics of North America, Decade Map Vol. 1*, Geological Society of America, Boulder Co., 498 p.
- Chapman, M.C., C.A. Powell, G. Vlahovic, and M.S. Sibol (1996). The nature of faulting in eastern Tennessee inferred from a statistical analysis of focal mechanisms and epicenter location, submitted to *Bull. Seism. Soc. Am.*

- Davison, F.C. (1988). Stress Tensor Estimates Derived from Focal Mechanism Solutions of Sparse Data Sets: Applications to Seismic Zones in Virginia and Eastern Tennessee, Ph.D. thesis, Virginia Polytechnic Institute and State University, Blacksburg, VA, 189 p.
- Herrmann, R.B. (1979). Surface wave focal mechanisms for eastern North American earthquakes with tectonic implications, *Journ. Geophys. Res.*, 84, 3543-3552.
- Johnston, A.C., D.J. Reinbold and S.I. Brewer, (1985). Seismotectonics of the southern Appalachians, *Bull. Seism. Soc. Am.*, 75, 291-312.
- Kagan, Y.Y. and D.D. Jackson (1994). Long-term probabilistic forecasting of earthquakes, *Journal of Geophysical Research*, 99, B7, 13,685-13,700.
- King, E.R., and I. Zietz (1978). The New York - Alabama lineament: geophysical evidence for a major crustal break beneath the Appalachian basin, *Geology*, 6, 312-318.
- Li, Hongsheng (1994). Focal Mechanism Analysis of Eastern Tennessee Seismic Zone Earthquakes, Master's Degree thesis, University of Memphis, Memphis, TN.
- Nelson, A.E. and I. Zietz (1983). The Clingman lineament, other aeromagnetic features and major lithotectonic units in part of the southern Appalachian mountains, *Southeastern Geology*, 24, 147-157.
- Powell, C.A., G.A. Bollinger, M.C. Chapman, M.S. Sibol, A.C. Johnston and R.L. Wheeler (1994). A seismotectonic model for the 300 kilometer long eastern Tennessee seismic zone, *Science*, 264, 686-688.
- Reinbold, D.J. and A.C. Johnston (1987). Historical seismicity in the southern Appalachian seismic zone, U.S. Geological Survey Open-File Report 87-433, 859 p.
- Stover, C.W and J.L. Coffman (1993). Seismicity of the United States, 1568-1989 (Revised), U.S. Geological Survey Prof. Paper 1527.

Teague, A.G., G.A. Bollinger and A.C. Johnston (1986). Focal mechanism analyses for eastern Tennessee earthquakes (1981-1983), *Bull. Seism. Soc. Am.*, 76, 95-109.

Vlahovic, G, C.A. Powell, M.C. Chapman and M.S. Sibol (1996). P and S wave velocity structure and hypocenter locations in the eastern Tennessee seismic zone, *Abst., Sesimological Research Letters*, 67, no.2, 59.

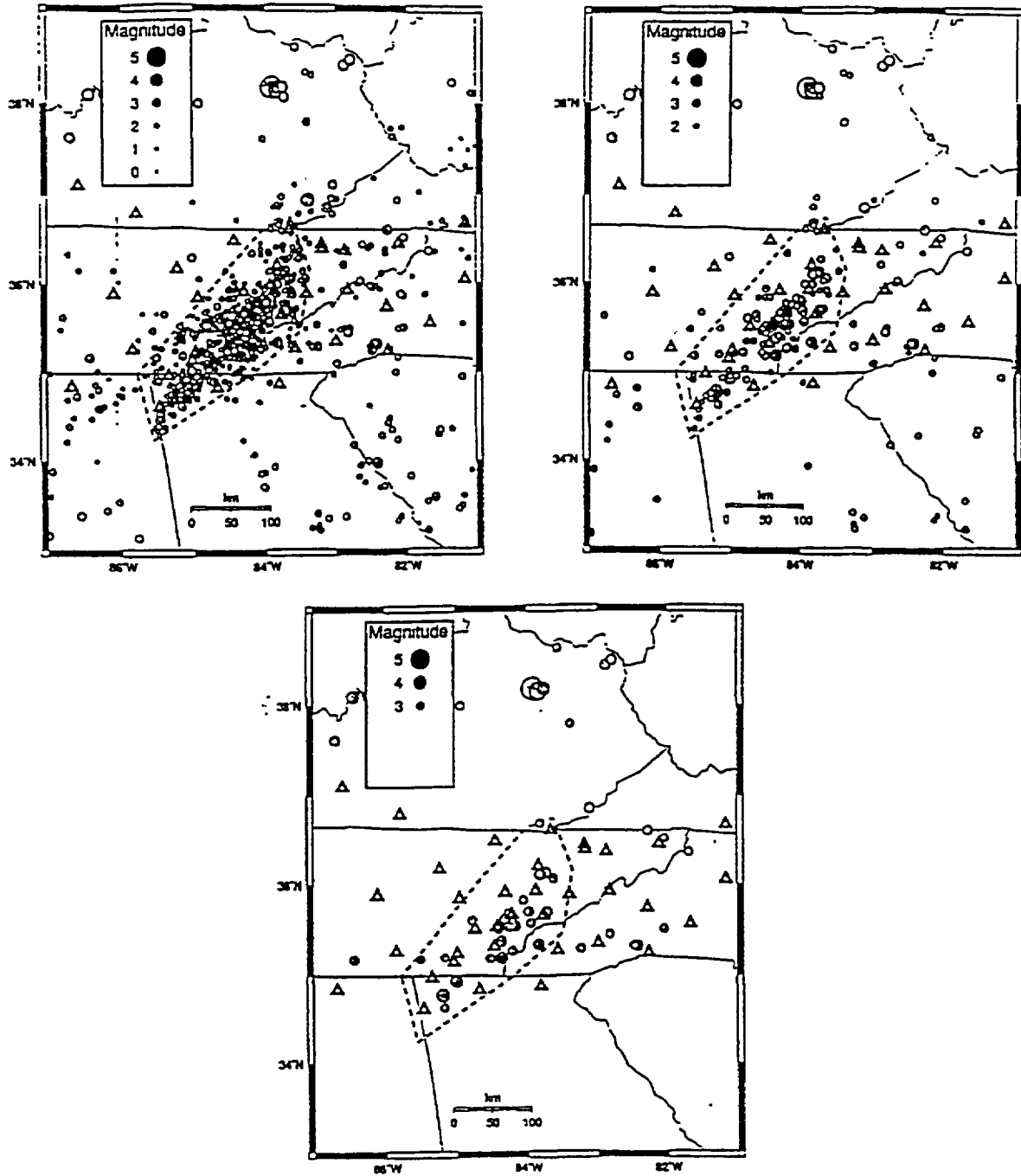


Figure 1: Circles indicate the epicenters of instrumentally detected and located earthquakes in eastern Tennessee and the surrounding region 1977-present. Three different magnitude thresholds are shown, to illustrate the effect of network detection capability. The eastern Tennessee seismic zone is indicated by the dashed line. TVA and University of Memphis seismic network stations are shown by the triangles.

Eastern Tennessee Seismic Zone

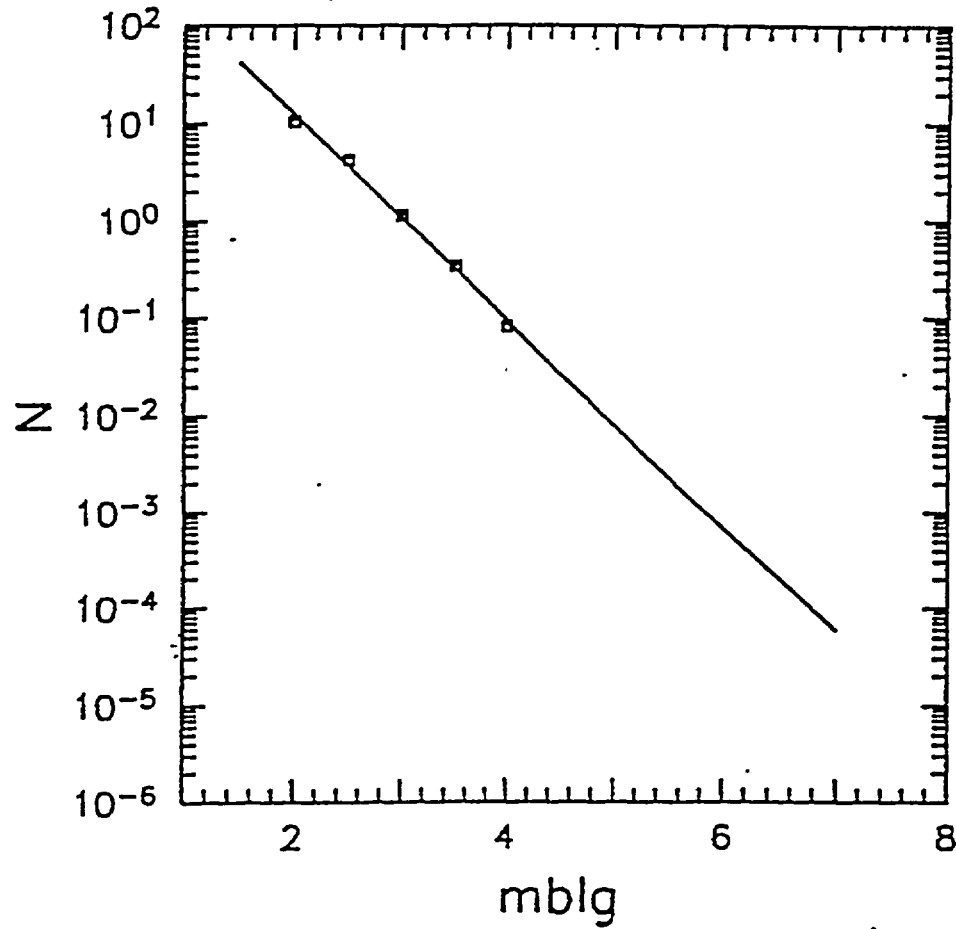


Figure 2: Estimated cumulative annual rates for earthquakes in the eastern Tennessee seismic zone, versus mblg magnitude. The solid line shows a least squares fit to the data, which are shown by the squares.

Figure intentionally omitted

Figure 3: Isoseismal map for the February 21, 1916 earthquake in the southern Appalachians. (from Stover and Coffman, 1993).

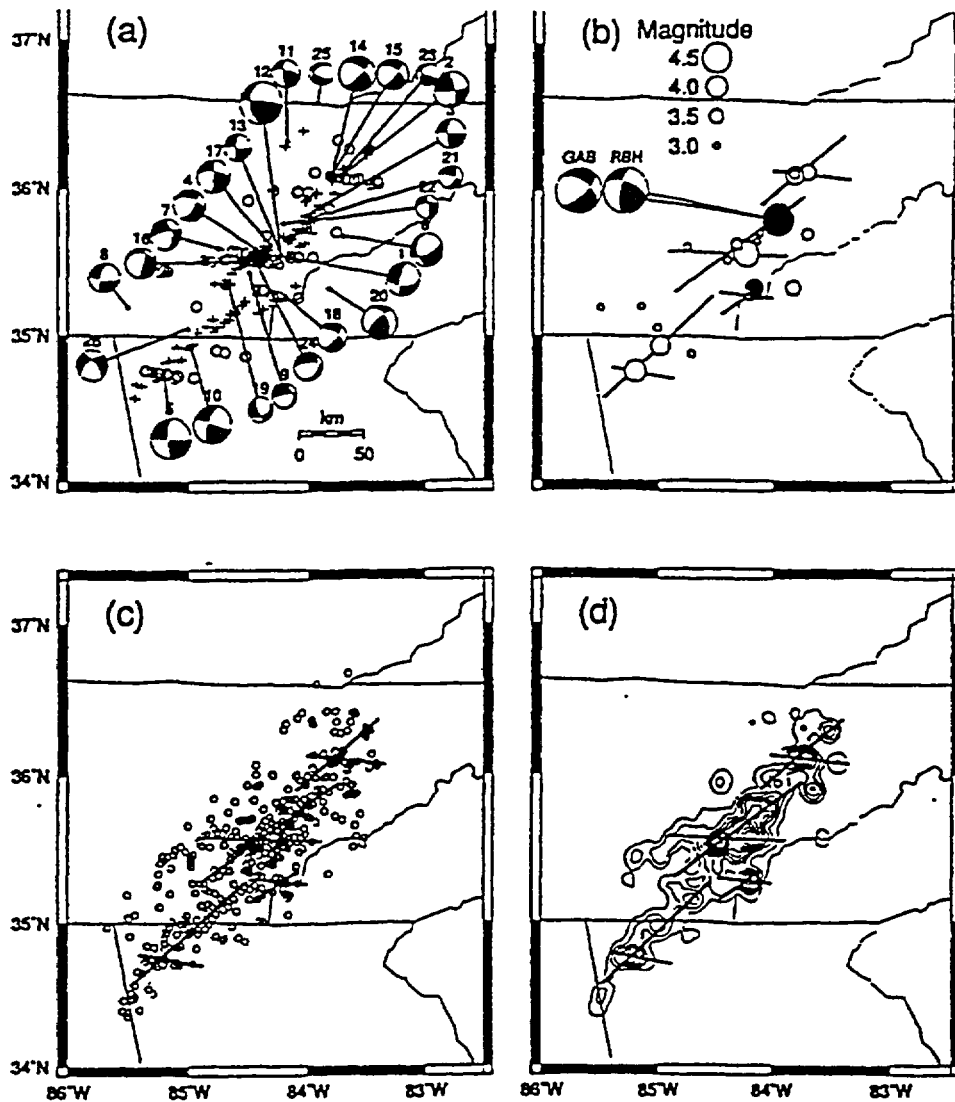


Figure 4: (a) Combined results of sorting the eastern Tennessee earthquake catalog using scale lengths of 20 and 30 km, for 20 degree azimuth ranges centered on N50E (crosses) and N95E (circles). Lower hemisphere focal mechanism solutions have the compressional quadrants shaded. (b) Bold lines indicate faults inferred from (a). The unshaded circles indicate epicenters of instrumentally located earthquakes with magnitudes greater than 3.0, 1983-1995. The large shaded circles represents the Nov. 30, 1973 Maryville earthquake. The smaller shaded circle represents the July 5, 1995 Tellico Plains earthquake. Focal Mechanisms of the Maryville shock derived by Bollinger et al., (1976) and Herrmann (1979) are indicated by GAB and RBH, respectively. (c) Circles show the 474 relocated epicenters. (d) Contours depict the epicenter density function derived using a 10 km kernel half-width.

DRAFT DRAFT DRAFT DRAFT

Invited Arguments Against the Hypothesis that
Major Earthquakes Occur in the Eastern Tennessee Seismic Zone
(ETSZ)

OR:

ESTIMATING THE UPPER-BOUND MAGNITUDE OF THE ETSZ.

by

Klaus H. Jacob
Lamont-Doherty Earth Observatory of Columbia University
Palisades NY 10964
E-mail: jacob@ldeo.columbia.edu

PREAMBLE.

The author was assigned to the task of presenting the arguments AGAINST the likelihood for a large earthquake in the ETSZ. Martin Chapman was assigned to the task to present the opposite arguments, i.e. IN SUPPORT of the notion that the ETSZ can produce "major" earthquakes. That paper is referred to simply as Chapman, (1996) or "PRO" paper.

SUMMARY

In search for arguments for a low upper-bound magnitude M_u for the ETSZ, the low maximum magnitude of $M_{blg}=4.6$ historically observed is the only strong argument in favor of low upper-bound magnitude levels for the ETSZ. Most other arguments lead to M_u values in excess of $M=6$. For this reason we propose a wide range of M_u values, from $M_u = 5$ to 8, to which we assign subjective weights for use in a logic-tree approach.

Introduction.

The ETSZ is at most 300 km long, about 50 km wide, and extends in depth from about 3 to 25 km, with most of the seismicity located below the Paleozoic thrust decollement in presumably cratonic basement which is likely to be at least 1 Billion years old. The tectonic province is known as the Valley and Ridge province of the Appalachians formed of Paleozoic metasedimentary folded thrust sheets above the decollement. The largest event observed for the ETSZ in historic time is the $M_{blg}=4.6$ of 1973 earthquake near Alcoa-Maryville (Bollinger et al, 1991).

What is the upper-bound magnitude earthquake that can be generated by the ETSZ ?

There are several fundamental ways to argue about the upper-bound magnitude M_u of a seismic source zone or seismotectonic province. Possible constraints include:

(1) Catalogs and Seismicity - Magnitude extrapolations to Long Recurrence Periods. A common procedure is to use earthquake catalogs for a region and extrapolating by some statistical procedure or recurrence period argument what the upper bound M_u would or should be. Examples are work by Veneziano (1988?) as part of the EPRI and NCEER studies of seismicity in the CEUS. Martin Chapman (1996), in his PRO paper, used simple recurrence relations assuming the Poisson model

of seismicity and the exponential Gutenberg Richter relation of frequency of occurrence vs. magnitude. He estimated the probabilities of observing certain threshold magnitudes during various (past) periods of exposure time, most of them much longer than the actual catalog duration. Extrapolating a least-square-fit recurrence relation for the entire ETSZ to annual probabilities of $10^{-2}/\text{yr}$ yields magnitudes of about $M_{blg}=5.1$; for $10^{-3}/\text{yr}$ it yields about $M_{blg}=6.0$; and for $10^{-4}/\text{yr}$ it yields about $M_{blg}=6.8$.

(2) Geological Province Arguments. In this case the seismic zone is placed into a type of geological province for which global statistical evaluations have been made. The principle is to replace limited catalog time with plenty of (global) space in the hope to catch the largest possible earthquakes elsewhere in a comparable geologic setting. An example is the approach that EPRI (1994) took for its study of the large-earthquake potential in stable continental regions (SCR). The ETSZ is located in the Appalachian Valley and Ridge province which can be categorized as a Paleozoic thrust and fold belt underlain by unextended cratonic crust. The EPRI (1994) study assigns an upper bound $M=6.8\pm 0.3$ to non-extended crust, craton; and a $M=6.4\pm 0.2$ to non-extended crust, fold belt (Paleozoic- Mesozoic). The latter choice seems the most fitting category for the ETSZ (i.e. upper bound $M=6.4 \pm 0.2$).

(3) Strain energy arguments. Geodetic strain rates in the eastern US, although not known for the ETSZ in particular, are estimated from VLBI and GPS measurements to be of the order of 10^{-14} to 10^{-15} /sec which implies about 0.3 to 0.03 microstrains / year. For instance: recent GPS measurements in the NMSZ (Zoback et al., 1996, unpublished data) indicate a mean of 0.11 microstrain / year (95 % confidence intervals are from 0.04 to 0.20 microstrains / year) for a region about 55km in width across the NMSZ.

Annual strain rate, $\partial e/\partial t$, and annual moment rate, $\partial Mo/\partial t$, are related by

$$\partial Mo/\partial t = 2\mu V \partial e/\partial t$$

where V, the strained Volume, is assumed to have an average shear modulus μ .

The strain rate for the ETSZ is not known. But if we assume for the moment that the geodetic rate were the same as that for the NMSZ (!); and if we assume the volume V of the ETSZ proper to be about 300 by 50 by 20 km cubed or $V=3 \times 10^5 \text{ km}^3 = 3 \times 10^{20} \text{ cm}^3$, and the shear modulus to be of the order $\mu = 3.7 \times 10^{11} \text{ dyne/cm}^2$. This combined with the relation

$$M = 2/3 \log Mo (\text{dyne cm}) - 10.7$$

would imply an average annual rate of moment of $2.22 \times 10^{25} \text{ dyne cm/y}$ or the equivalent of a $M_w=6.2$ every year (!), which obviously is not even achieved by the NMSZ. If no seismic moment would be released in the ETSZ by smaller earthquakes, this moment rate would imply every thousand years a magnitude $M=8.2$. Such events would have most likely be detected by their paleo-seismic / geologic effects in the ETSZ area and beyond. Hence we do not believe such high strain rates are currently accumulating, which -by the way- would be geodetically detectable in a decade or less. On the other hand we are not certain whether sufficient paleoseismic and geologic work has been done in and around the ETSZ to exclude that $M=7$ to 8 earthquakes have not occurred in the last 10,000 years or so.

The historically detectable seismic moment rate (determined from the seismic network data), according to Chapman (1996, Figure 2) is about one $M_{blg}=4$ event every 10 years. If we equate (for convenience rather than accuracy) M_{blg} with M, then this level of seismicity corresponds to a moment release on the order of

$$\partial Mo/\partial t = 1.122 \times 10^{21} \text{ dyne cm / y}$$

and to a "seismic" strain rate of only

$$\partial e/\partial t = \partial Mo/\partial t / (2\mu V) = (1.122 \times 10^{21} \text{ dyne cm / y}) / (2 \times 3.7 \times 10^{11} \text{ dyne/cm}^2 \times 3 \times 10^{20} \text{ cm}^3)$$

$$\partial e/\partial t \approx 5 \times 10^{-6} \text{ microstrain / y}$$

or five orders of magnitude lower than what is currently being observed in the NMSZ. This seems an extraordinarily small strain rate. Almost certainly there is more strain either being accumulated elastically, or being released by aseismic creep in the ETSZ than is being released seismically. This clearly warrants future GPS measurements in the area.

One possible analogy comes to mind in this context. The region may be -for one reason or another- a "creeping inclusion" into the generally competent fully brittle eastern US crust. Similarly the creeping section of the Andreas Fault (SAF) north of Parkfield CA, is an anomaly amongst the otherwise brittle segments of the SAF. Creep in the ETSZ could be induced by pressure solution. The surrounding rock matrix may respond to stress changes related to the volume changes associated with the pressure solution by limited brittle stress release in relatively small earthquakes. The creeping section of the San Andreas fault is by number of earthquakes the most seismically active, and most well defined fault segment of the SAF, but only for earthquakes in the order of $M=3$ or less. No larger earthquakes ($M>5$) are known to have ever occurred on this SAF segment. Why the process of creep in the ETSZ volume -if present- should be activated there and not elsewhere in the eastern US crust or along other portions of the New York - Alabama lineament remains of course a mystery. But so is the reason for the creeping section of the SAF.

Another option to explain the ETSZ activity is analogous to what is known for the NMSZ and the Charlevoix/St. Lawrence River SZ in Quebec, Canada. The current small-earthquake activity in these active areas is "aftershock" seismicity to recent large $M=7$ to 8 earthquakes. In the case of the ETSZ the large earthquake would have occurred recently, yet prehistorically. But once again we have to ask: where is the paleoseismic / geologic evidence for this past large earthquake (or sequence of quakes).

To close this issue, the strain argument is inconclusive in providing constraints on the size of future earthquakes in the ETSZ, at least until geodetic / GPS measurements are being made at and surrounding the ETSZ. Such geodetic measurements would hopefully indicate whether and how strain accumulates elastically in the ETSZ compared to what strain is being seismically released; or whether and how strain is aseismically released; and how strain rates in the ETSZ compare to measured rates in regions outside the ETSZ. We would expect that GPS can elucidate the issue whether the ETSZ coincides with a strain rate anomaly in the CEUS, and whether the observed strain is compatible with the seismic strain release during the last few decades, or not. Additionally, paleoseismic studies may need to be intensified in and around the ETSZ.

At this time we do not feel that magnitude constraints can be inferred from the strain argument.

4. Detailed Seismicity and Focal Mechanism Patterns.

Chapman et al. (1996) have analyzed and correlated the strike of focal mechanism planes in the ETSZ with spatial patterns of epicenters (but not of hypocenters) to infer the existence of extended faults, and their dimensions and orientations. They find two preferred orientations of subvertical strike-slip faults: (1) a NE striking right-lateral strike-slip set of en-echelon faults whose individual strikes virtually coincide with the maximum horizontal stress direction S_1 (about $N56E$; personal communication by L. Seeber, based on inversion of the 26 focal mechanisms presented by

Chapman et al., 1996). In order for these NE striking faults to slip, one must infer very low effective stress to be associated with them, i.e. they appear to be very weak, possibly implying high pore pressure. (2) a nearly E-W striking, left-lateral-slipping set which is oriented at about 40 degrees with respect to the maximum horizontal compressional axis S1 (and with respect to the first set of faults as well). Since the volume of ETSZ basement rock appears to undergo NE-SW compression, then these E-W striking left-lateral, left-stepping faults could be considered a set of cross faults in an overall right-lateral NE-trending ETSZ shear zone. These cross faults may indicate blocks in a "bookshelf" tectonic regime where the individual blocks undergo clockwise rotation.

The length of the E-W striking fault sets appears somewhat shorter (<30km) than that of the NE-striking sets (>50km). This inference needs to be qualified since only 2-d epicenter information instead of 3-d hypocenter information was analyzed for alignment by Chapman et al. (1996).

While from the pattern of apparent fault alignment it appears unlikely that there exists a single through-going NE-striking fault, the apparent sub-fault dimensions of L=50km length towards NE, and up to L=30km towards E, if activated in single ruptures, could accommodate earthquakes with moments on the order of:

$$M_0 = k \Delta s w^2 L$$

where k is a constant with an amplitude of order of k=1; it varies in detail for dip-slip and strike-slip fault geometries and for different ratios of fault width w to fault length L; with reasonable assumptions for k, w, L and stress drop Δs ,

$$\begin{aligned} M_0 &= k \Delta s w^2 L \\ &= 1 \times 50 \text{ bar} \times (20 \text{ km})^2 \times 40 \text{ km} = \\ &= 1 \times 50 \times 10^6 \text{ dyne/cm}^2 \times (2.0 \times 10^6 \text{ cm})^2 \times 4.0 \times 10^6 \text{ cm} = \\ &= 8 \times 10^{26} \text{ dyne cm.} \end{aligned}$$

This moment corresponds to a (moment-) magnitude of $M = 7.2$. Hence, fault length segmentation as presented by Chapman et al. (1996) for the ETSZ is hardly an argument to advocate that the ETSZ is capable of only moderate ($M \leq 6$) earthquakes.

Conclusions.

1. The strongest argument for small values for the upper-bound magnitude M_u is the fact that observed historic and recent network seismicity in the ETSZ did probably not exceed magnitudes of $M_{blg} = 4.6$. Extrapolation of the Gutenberg-Richter relation $\log N = a - bM$ to recurrence periods of 100, 1,000 and 10,000 years imply M_{blg} magnitudes on the order of 5.1, 6.0 and 6.8, respectively, for the ETSZ. This presumes a temporally stationary, exponential and Poissonian-, rather than characteristic-earthquake, behavior out to these magnitudes.

2. The tectonic-province categorization using global correlations from EPRI (1994) would suggest an upper-bound magnitude of about $M = 6.4 \pm 0.2$.

3. Strain arguments are inconclusive since independent (geodetic or GPS) strain data are not available for the ETSZ and surrounding areas.

4. Focal mechanisms combined with spatial patterns of hypocenter alignments give potential maximum fault lengths on the order of at least 20 to 30 km if not 50km, especially for the NE-striking alignment directions within the ETSZ. Such fault-lengths, when combined with moderate stress drop assumptions (≈ 50 bar), yield moment magnitudes in excess of $M = 7$. Hence analysis of seismicity and focal mechanism patterns does not provide viable arguments for low upper-bound magnitude values.

In summary, we infer that maximum magnitudes for the ETSZ lie in the range from 5 to 7 and must be considered seriously, and those beyond $M=7$ marginally. For a logic-tree representation we suggest the following weighting scheme:

Upper-Bound Magnitude M_u	Weight w
5.0	0.10
5.5	0.20
6.0	0.30
6.5	0.20
7.0	0.10
7.5	0.07
8.0	0.03
Total:	1.00

References.

- Bollinger, G.A. et al. (1991). Seismicity in the southeastern U.S.; 1698 to 1986; pp. 291-308; Chapter 16 in: Neotectonics of North America; Decade Map Volume to accompany the Neotectonic Maps, Part of DNAG; Slemmons, D.B. et al. (Editors); The Geolog. Soc. of America. 1991.
- Chapman, M.C. (1996) An argument in support of the contention that a major earthquake could occur in eastern Tennessee. pp. 15; prepared for LLNL SSHAC implementation study. July (?) 1996.
- Chapman, M.C., C.A. Powell, G. Vlahovic and M. Sibol (1996). The nature of faulting in eastern Tennessee inferred from statistical analysis of focal mechanisms and epicenter locations. subm. to Bull. Seism. Soc. Am. pp. 29, April 12, 1996.
- EPRI (1987) Working Report: Methods for Assessing Maximum Earthquakes in the Central and Eastern US. EPRI Research Project 2556-1. Prepared by K.J. Coppersmith et al., based on a EPRI workshop held at Palo Alto in June 20 & 21, 1985; published January, 1987.
- EPRI (1994). The earthquakes of stable continental regions. Volume 1: Assessment of large earthquake potential. And Volume 5: Database and Maps. EPRI Report TR-102261-V1 to V5. Prepared by A.C. Johnston et al.; Dec 1994.
- Powell, C.A. et al (1994). A seismotectonic model of the 300-kilometer-long ETSZ. Science, 264. 686-688; April 29, 1994.
- Veneziano, D. (ca 1987 or 88 ?): A random-effects model for maximum earthquake magnitude. Unpublished (?) script; pp. 27; ca. 1987 or 1988 ? based on work supported by NCEER and EPRI.

DRAFT

**DOES THE PEN BRANCH FAULT POSE A
SEISMIC HAZARD?**

Dr. Pradeep Talwani

PEN BRANCH FAULT

Here I present an extended outline of the arguments against the Pen Branch Fault (PBF) being a major player contributing to seismic hazard potential at the Vogtle plant. In my view, the seismic hazard presented by the PBF is at a level equal or less than the regional background for the area, i.e., $M_{\max} \leq 4.5$.

1. Depth Constraints

The depth extent of the Pen Branch Fault and the Dunbarton basin has been obtained from a variety of seismic reflection and refraction data. These include the following:

- a. Various seismic reflection data acquired on the Savannah River Plant in the 1960s (various reports by I.W. Marine).
- b. Seismic reflection data on SRS acquired and processed by CONOCO (Chapman and DiStefano, 1989).
- c. CONOCO data reprocessed by VPI (Domoracki, 1995; Sen and Çoruh, 1992).
- d. An analyses of these data by Stieve and Stephenson, S.E. Geology, 1995; Domoracki et al., preprint and Dale Stephenson's and Alice Stieve's presentations at the Augusta meeting, 1996 (Figure 1).
- e. Seismic reflection line along the Savannah River by U.S.G.S.
- f. Seismic refraction data acquired between two wells in New Ellenton and Walterboro (Luetgert et al., SRL, 1994).
- g. COCORP reflection profile in Georgia just across the SC-GA border (Peterson et al., 1984).

Synthesis of these data (see e.g., Domoracki et al., preprint) and Figures 2 and 3 from Luetgert et al., 1994) all show that the Dunbarton basin is very shallow (~ 3-4 km) (Çoruh, Pers. Comm. to Dale Stephenson). The data also show that the PBF is also very shallow and does not wrap into the decollement.

To generate a moderate earthquake, $M \geq 5.0$ would require larger depth extent (in order to store the needed stresses). Usually a $M \sim 5.0$ event occurs at depths greater than about 10 km in southeast US.

Conclude that available data do not support the PBF having adequate depth extent to generate a $M \geq 5.0$ earthquake.

2. Geologic Constraints

Detailed geologic data have been acquired as a result of confirmatory drilling (Stieve et al., Conf. Drilling Report, 1994; Stieve and Stephenson, S.E. Geology, 1995 and Stieve, Augusta presentation, 1996).

- a. The PBF lies below the Williamsburg unconformity. Examination of sediments revealed no evidence of deformation above the unconformity. The undeformed Williamsburg unconformity is approximately 50 Ma old. Deformation on the PBF was found only below the unconformity. (The Upland unconformity is shallower than the Williamsburg unconformity).
- b. Stieve in her presentation at Augusta, also concluded that "Faulting on the PBF is older than 500 K years and therefore the PBF is a non-capable fault per 10 CFR 100 Appendix A".
- c. Investigations of quaternary geology (Geomatrix, Hanson and Bullard, 1992) consisted of longitudinal profiles of stream-channel and river terraces along the Savannah River and other tributaries crossing the PBF. They showed no nick points. The authors concluded that there was no deformation within a resolution of 3 m.

These geological observations suggest that PBF has not moved recently, or with measurable displacement. Thus they provide support for the conclusion that the PBF (or other structures) are not capable of producing $M \geq 5.0$ earthquakes.

3. Orientation With Respect to S_{Hmax}

The region is under a compressional stress regime, as such the seismogenic potential of a structure depends on its orientation with respect to S_{Hmax} . Various *in situ* data (e.g., Moos and Zoback, 1993) show that the PBF is parallel to S_{Hmax} in the area. This orientation is the least likely to produce an earthquake. Sibson (1992) has shown that for faults oriented at very small angles with respect to S_{Hmax} , extremely high pore pressures (approaching lithostat) are needed to trigger earthquakes. No evidence exists for large pore pressures at the depths at which the two small earthquakes have been located within the SRS. Thus from a purely mechanical point of view, PBF does not pose much of a seismic hazard. It also does not show a capability of generating $M \geq 5.0$ earthquakes.

We have interpreted the small earthquakes that occurred within the SRS to have occurred on small, suitably oriented, cross faults. The dimensions of these cross structures preclude earthquakes $M \geq 3.0$.

Based on the arguments presented above, I consider the Pen Branch Fault incapable of generating $M \geq 5.0$ events. Consequently I suggest that a "regional event" with $M \leq 4.5$ is adequate to cover the seismic hazard posed by PBF or other small faults encountered near SRS.

Figure intentionally omitted

Figure 1. Figure 13 of Stieve, 1996. Geologic cross-section of northwest to southeast transect through SR5 to the coast.

Figure intentionally omitted

Figure 2. From Luetgert et al. (1994).

Figure intentionally omitted

Figure 3. From Luetgert et al. (1994).

**WHITE PAPER FOR TRIAL IMPLEMENTATION PROJECT
POSITION: "INCLUDE THE PEN BRANCH AND OTHER LOCAL
FAULTS IN THE PSHA"**

Kevin J. Coppersmith

Disclaimer: The following white paper—much like a lawyers legal argument—presents a particular position and seeks only to support that position. I have intentionally tried to present an unbalanced case, giving only lip service to counter-arguments that my worthy opponent (the esteemed Prof. Talwani) will likely present. Further, I have done a poor job of citing references and providing supporting data to many of my arguments. Nevertheless, I trust that the paper will at least spark some thinking and help us reach our ultimate goal: staying awake at the next workshop.

Position: The seismic hazard analysis at the Vogtle site should include a consideration of the faults mapped in the local site vicinity as potential seismic sources.

Background

Numerous studies have been conducted in the past nine years (see Domoracki, et al., in press and A. Stieve vu-graphs for summary of geologic and geophysical studies) aimed at identifying and characterizing faults in the local SRS site vicinity. These are probably the most intensive studies ever conducted of Mesozoic normal faulting anywhere along the eastern seaboard. The studies include deep seismic reflection, shallow high-resolution seismic reflection, heat-flow interpretations, seismicity analyses from a local seismic network, geologic mapping, Quaternary geologic studies, in-situ stress measurements, etc.

The available studies indicate that the major bedrock faults in the site vicinity developed during the extensional tectonic regime associated with Mesozoic continental rifting. This rifting event was a profound orogenic event that is documented in the geologic record throughout the continental margin of eastern North America and included parts of the present mid-continent including the New Madrid region. As a profound tectonic event, the faults that accommodated the extension persisted throughout the width (thickness) of the crust. Very deep seismic reflection profiles across the continental margin document the persistence downdip of the major normal faults to at least mid-crustal depths. In many cases, no doubt, the extensional faults reactivated reverse faults associated with the compression that accompanied continental collision during the Paleozoic. However, because normal faults tend to display relatively steep dips in at least the brittle upper crust, the higher-dip Mesozoic normal faults probably only reactivated the higher-dip components of Paleozoic reverse faults.

It is not clear that every Mesozoic normal fault is a fault that exists throughout the entire crust. No doubt, many faults are antithetic to major normal faults; others could be secondary splays.

The faults identified in the local site vicinity display the classic expression of Mesozoic normal faults: east-dipping normal faults showing a down-dropped basement and bounding Triassic-age arkosic "red-beds" associated with the in-filling of these basins (in this case the Dunbarton basin). Subsequent deposition of the Cretaceous and younger Coastal Plain sediments has buried the basin. The Dunbarton Basin formed as a tilted fault block with faulting along the western margin. It is a relatively small basin compared to other mapped Triassic basins (about 30 km long) although crustal extension was sufficient to result in a minimum of ----- meters of normal slip and deposition of about ----- meters of Triassic sediment. As such, the faults bounding--and responsible for--the Dunbarton basin were large, significant faults during the time that they accommodated this extension. Based on this assessment, there is a good chance that the east-facing border fault bounding the Dunbarton Basin (known in the Coastal Plain section as the Pen Branch fault) is a significant fault that likely transects the entire continental crust. Interpretations of seismic reflection data by Domoracki et al. (in press) suggest that the Pen Branch fault may be related to the updip part of large Paleozoic reverse faults such as the Augusta fault.

As discussed by Alice Stieve and Dale Stephenson at the first TIP workshop, other faults besides the Pen Branch fault have been interpreted at the top of basement and within the Coastal Plain sediment in the SRS vicinity. These local faults, as well as the Pen Branch fault, should be considered as potential seismic sources for the TIP-PSHA for the following reasons.

1. Mesozoic normal faults persist throughout the crust and extended crust can be important to large-earthquake potential. As discussed above, the faults associated with Mesozoic continental extension are likely deep-seated high-angle structures that persist downdip throughout the seismogenic crust. Although there are probably some minor normal faults that were antithetic or secondary to the major normal faults, those faults that are clearly related to and bound known Mesozoic basins are clearly the most likely to have been the major structures (i.e., have the most cumulative slip) accommodating continental extension. An example of such a basin-bounding normal fault is the Ramapo fault that forms the northwesterly boundary of the Newark Basin.

Because the Pen Branch and associated normal faults bound the Dunbarton Basin, they are likely significant structures within the seismogenic crust (upper 15 to 20 km). That is, they likely persist as fairly high-angle (approximately 60 degree dipping) faults throughout the depth of the seismic reflection profiles given in Domoracki et al. (in press). Domoracki et al. suggest that the Pen Branch may be related to--and perhaps an extensional reactivation of--Paleozoic reverse faults such as the Augusta. They do not, however, clearly identify the Pen Branch fault at mid- to upper-crustal depths on their profiles. This is not surprising for several reasons: 1) seismic reflection data commonly

do not image steeply dipping structures well (e.g., high-angle faults are usually identified from the vertical separation and discontinuity of reflectors, rather than from reflections off the fault plane), 2) the cumulative normal slip on the Pen Branch fault is relatively small compared to that of the Augusta fault, and 3) the intensity of deformation associated with the extensional tectonism was probably far less than that associated with Paleozoic compression (e.g., the development of duplex structures postulated by Domoracki et al.). As a result the downdip extent of the Pen Branch fault is not well-imaged in the seismic data. This is a common problem in the Basin and Range province in which seismic reflection profiles provide clear images of low-angle reverse faults but rarely image the high-angle normal faults that are well-known at the surface (e.g., Smith and Bruhn).

The normal faulting associated with Mesozoic extension--represented locally by the Pen Branch fault and regionally by a domain of extensional features along the eastern seaboard--is indicative of significantly extended continental crust. Studies of large earthquakes that have occurred within stable continental regions (SCR; Johnston et al.) show that all of the largest ($M > 7$) events have occurred within extended crust. Admittedly, the correlations given in Johnston et al. between the earthquakes and their tectonic associations were regional (that is, typically the large SCR earthquake can only be associated with a regional 'tectonic domain' and not with an individual fault--like the Pen Branch). Nevertheless, regardless of our inability to identify the exact causative fault, large SCR earthquakes must be occurring on faults and candidate causative faults within a domain can be identified.

2. The Pen Branch fault displays clear evidence for reactivation as a reverse fault. Geologic and geophysical studies of the Pen Branch fault provide perhaps the best documented evidence of reactivation of a Mesozoic normal fault as a post-Mesozoic reverse fault. This confirms that the fault was involved not only in the accommodation of regional extension associated with continental rifting, but, since then, has responded to post-rifting compressional stresses. These stresses were presumably induced by ridge-push forces following complete continental separation and continue to exist today in the continental crust of eastern North America. Detailed studies of some other Mesozoic normal faults (e.g., Ramapo fault) have shown that the most recent episode of brittle deformation occurred as normal faulting and did *not* include subsequent reactivation in a reverse sense (Ratcliffe).

The concept that Mesozoic normal faults might be reactivated as reverse faults--and might represent a contemporary seismic hazard--was first proposed by Wentworth and Mergner-Keefer. Based on the observation that the contemporary stress field appeared to be compressional and the--anecdotal at the time--limited evidence of recent faulting appeared to be along reverse faults, they suggested that a domain of reactivated reverse faults exists along the continental margin of the East Coast marked by Mesozoic basins. In the absence of much direct evidence, they postulated that future detailed studies of the basin-bounding faults might/would show evidence for reactivation in a reverse sense and, thus, an indication of potential activity in the present tectonic regime.

The Pen Branch fault clearly meets the conditions that are part of Wentworth and Mergner-Keefer's hypothesis (i.e., reverse reactivation of a Mesozoic normal fault), although, at the time, they believed that the maximum horizontal crustal stress direction was northwest-southeast, perpendicular to the northeasterly strike of the Mesozoic normal faults. We now have independent data that show that the axis of maximum horizontal compression lies in the northeast quadrant--essentially parallel to the strike of the Pen Branch fault. This orientation is probably most conducive to strike-slip faulting, with some component of reverse displacement. At present, there are virtually no data that confirm or deny a significant lateral component of post-Cretaceous slip on the Pen Branch fault. Therefore, the Pen Branch fault could well be a strike-slip fault, with a reverse component, consistent with the present tectonic crustal stress regime.

3. Dimensions of the Dunbarton Basin are sufficient to suggest the potential to generate significant earthquakes. The dimensions of a fault (downdip width and fault length) are an indication of the size of earthquakes that might be generated by the fault. It is also well-known that the dimensions directly scale with moment magnitude (e.g., Wells and Coppersmith). As discussed previously, the downdip width of the fault is likely crustal in extent because the Dunbarton Basin is a significant basin associated with continental extension and rifting. The thickness of the seismogenic crust in the vicinity of SRS is about 15 to 20 km thick. It is therefore suggested that the downdip width of the Pen Branch fault is also approximately of this dimension.

It could be argued that the Pen Branch possibly connects downdip with the Augusta fault and soles out at relatively shallow depth into a low angle fault. Assuming that only the updip high-angle part of the fault is seismogenic (i.e., that the low-angle part of the Augusta fault has not been reactivated since the Paleozoic), this would limit the downdip dimensions--and, hence, maximum earthquake potential--of the Pen Branch fault. However, as discussed earlier, a common problem with the interpretation of seismic reflection data in extensional regimes superimposed on compressional regimes is that the low-angle reverse faults are the dominant reflectors in the seismic data (Smith and Bruhn). For example, deep reflection profiles across large, active normal faults such as the Wasatch fault, Utah, and the Lost River fault, Idaho, image large regional low-angle reverse faults associated with previous episodes (primarily Laramide) of compressional deformation. Often, these reverse faults sole into regional detachments at relatively shallow depths (5-10 km). In most cases the active normal faults at the surface can be projected downdip to the steeper portions of the reverse faults but they are not well-imaged in the reflection data.

For example, in the case of the Lost River fault, the coseismic fault plane is well-imaged from the pattern of aftershocks to the 1983 Borah Peak earthquake. The coseismic fault dips steeply (~45-50 degrees) to the east and extends downdip to depths of about 15 km. There is no sign that the dip is listric. In contrast, seismic reflection profiles across the Lost River fault image an east-dipping Laramide reverse fault that is listric and soles into a subhorizontal reflector at depths of about 8 km. There is simply no good agreement between the faulting interpreted in the reflection data and the seismogenic fault mapped at

the surface and in the subsurface from aftershocks. It is suggested that a similar circumstance could be the case with the Pen Branch fault. The seismic reflection data clearly image the compressional Paleozoic structures and the high-angle (probably lesser cumulative slip) Mesozoic extensional structures are not well-imaged. However, the tectonic role that the normal faults played in continental rifting suggest that they do, in fact, extend to significant depth.

In addition to the width, the *length* of the Pen Branch fault is also likely significant enough to allow for the generation of moderate-to-large earthquakes. The location and length of the Dunbarton Basin is interpreted from geophysical data and subsurface geologic data to be about 30 km long. Although it is not known with certainty that the Pen Branch fault extends along the entire length of the basin, the tectonic position of the fault in the vicinity of SRS—a basin bounding normal fault—would suggest that it does bound the entire length of the basin. Further, the seismic reflection line that runs down the Savannah River indicates the presence of the fault at least beyond the boundary of the SRS.

The combination of a 15-20 km downdip width and a 30 km length would imply a potential rupture area that is about 450-600 km². This area would be capable of sustaining a moment magnitude of about 6 1/2 to 7, based on the empirical regressions between rupture area and magnitude given in Wells andoppersmith (1994).

4. The absence of observed seismicity is not a good indicator of the lack of future earthquake potential. The Pen Branch fault and the Dunbarton Basin lie within a diffuse regional zone of seismicity, as noted by Domoracki et al. Although there is some chance that the two small local earthquakes recorded at the SRS may have been associated with the Pen Branch fault (Domoracki et al.), there is no clear alignment or association of seismicity with the fault over and above the levels of the diffuse zone.

A clear association of seismicity with a fault is a good indication of its future earthquake potential (if not in magnitude, at least in terms of whether or not the fault is seismogenic). In contrast, the absence of observed seismicity may or may not be an indication of future earthquake potential. Numerous cases can be found—particularly along Quaternary-active normal faults of the Basin and Range province—where clearly “active” (i.e., Quaternary) faults are not associated with observed seismicity. This may be the case for the Pen Branch fault.

In the absence of observed associated seismicity, other information (e.g., geologic evidence for the recency of faulting, tectonic relationships, etc.) become the primary mechanism for assessing whether or not a fault should be considered potentially seismogenic. Quaternary geologic studies conducted thus far for the Pen Branch fault suggest that the Pen Branch fault has not displaced Quaternary deposits of the Savannah River and, therefore, is not a Quaternary-active fault. Unfortunately, these studies are preliminary and the level of resolution of the geologic mapping could allow for a small amount of Quaternary deformation below the threshold of resolution of the geologic and geomorphic techniques that have been applied thus far.

5. Probabilistic seismic hazard analyses should incorporate a wide range of tectonic hypotheses. Despite the brilliant (if not persuasive) arguments made in this white paper for why the Pen Branch fault is, in fact, a seismogenic fault, there is admittedly significant uncertainty surrounding the issue. A key goal to any PSHA should be to properly characterize alternative tectonic hypotheses and to quantify the associated uncertainties in a manner that is appropriate to hazard analysis. Popular counter-arguments to the notion of actually attempting to include the tectonic hypotheses in the analysis is that "it probably won't affect the hazard results anyway" or "a local source zone should cover the possibility of a local fault."

Purely from the standpoint of hazard analysis (i.e., mean hazard), these arguments are often correct. For example, most of the arguments surrounding the Pen Branch fault deal with whether or not it is seismogenic (that is capable of generating significant earthquakes). Even allowing for this uncertainty, the Quaternary geologic studies that have been done in the SRS area would suggest that, if the fault is active in Quaternary time, its rate of slip during the this time has been very low. Thus, a PSHA that uses slip rate as a constraint on earthquake recurrence rate (as most do these days) would show that, because of the low recurrence rate, the Pen Branch fault makes an insignificant contribution to the hazard at the Vogtle site. Therefore, "it doesn't affect the hazard results anyway."

This is true but there is some real value in properly and comprehensively incorporating all credible tectonic models and hypotheses into the PSHA. The arguments are the following. First, our intuition about what is important and unimportant to PSHA is not always correct. PSHA is a complicated convolution of the probability of activity, source-to-site distances, earthquake recurrence rates, and ground motion attenuation laws. Even the most sage hazard analysts are occasionally surprised by the results. Second, including all tectonic hypotheses can help satisfy the larger technical community that all viewpoints have been considered and--indeed--represented in the hazard analysis. This can enhance the technical credibility of the study and help diffuse contention and polarization about controversial issues. Third, although a particular model or hypothesis may not affect the mean hazard at certain probability levels, it could significantly affect the uncertainty distribution of the hazard and might have significance at other probability levels of interest. For example, the concept of a large-magnitude earthquake rupturing the regional Paleozoic detachment along the eastern seaboard (an hypothesis that has lost favor in recent years) might only be significant to calculated hazard at low probability levels (say, $10E-4$ per year). Finally, often the best way to show that a particular tectonic hypothesis is insignificant to hazard is, in fact, to include it in the analysis. Sensitivity studies can then isolate its contribution to the hazard results and, if found to be significant, can identify those aspects that are most important. For example, once the Pen Branch fault is included in a PSHA for the Vogtle site, it may be shown that the fault is a minor contributor to the hazard; or, if it is significant, that the most important aspect of its characterization is the assessment of whether or not it is seismogenic. This type of sensitivity analysis can help to focus subsequent data-collection efforts.

Conclusion

The Pen Branch fault--and perhaps other local faults--should be considered as potential seismic sources in the PSHA. This is a tectonic hypothesis that should be properly included in the analysis. We can debate the alternative ways that this hypothesis might best be represented (e.g., a discrete fault, a local source zone, a zone of faults, etc.).

APPENDIX B: WHITE PAPERS ASSIGNED TO EXPERTS IN PREPARATION OF WORKSHOP #3

Extrapolating rates for small magnitudes to large magnitudes

Pro: Klaus Jacob:

Con: Martin Chapman

Estimating maximum magnitude:

— Strong position on using fault plane area/length for ETSZ Gil Bollinger

—Using global data (not developed)

Estimating magnitudes from Paleoliquefaction

Pradeep Talwani

LIMITATIONS TO ESTIMATING THE RATE OF LARGE EARTHQUAKES FROM THE RATES OF SMALL EVENTS.

Klaus H. Jacob

Lamont-Doherty Earth Observatory of Columbia University, Palisades NY 10964
E-mail: jacob@ldeo.columbia.edu

PREAMBLE.

The author was assigned to the task of presenting the arguments AGAINST the widely held opinion that one can readily infer the rate of occurrence of large earthquakes from the rates of smaller earthquakes. Martin Chapman (1997) was assigned to the task of presenting the opposite arguments, i.e. IN SUPPORT of the notion that such extrapolations can be readily made.

Note: In this script we use the following notations: m is magnitude; M stands for seismic moment; the symbol \sim means "proportional to", and $^{\wedge}$ implies "raised to power" (of what ever follows in parentheses).

Summary

It is shown that if self-organized criticality is a process that applies to earthquake phenomena, than one needs to know the mode of criticality of the strain release process before one can decide whether it is possible to extrapolate from the rate of small earthquakes to the rate of the largest possible earthquakes in any given region.

Introduction.

In the interior of plates and "stable continental regions" (SCR) the sparse seismicity is -by definition- not associated with plate boundaries whose relative plate motion rates are generally well constrained; nor is such SCR seismicity generally associated with major through-going fault systems whose slip rates are constrained from geologic or geodetic data. Therefore geologic/geodetic constraints do not generally exist for the moment rate that may be released by earthquakes. Since *large* earthquakes tend to release most of the strain energy available, while small earthquakes contribute little to the strain release, there are little useful constraints on the occurrence rate of potentially large earthquakes other than what can be learned and inferred from the instrumental, historic, or paleoseismic record of the earthquakes themselves. However, in most regions of the eastern U.S. (i.e. east of the Rockies), the historic record is at best only 200 to 300 years old which is thought to be only a small fraction of the recurrence times of the largest earthquakes. And only in a few regions paleoseismicity has produced data for longer exposure times. Moreover, the paleoseismicity studies are geographically sparsely distributed; the

completeness of the record of large earthquakes detectable by paleoseismic methods is difficult to assess; and the spatio-temporal resolution of paleoseismically inferred events is often quite poor.

For these reasons, seismologists have been tempted to infer the expected rate of occurrence of potentially larger earthquakes (say, $m \geq 6$) from the rate of occurrence of smaller events (typically with magnitudes $m \leq 4$) by extrapolating the well known Gutenberg-Richter (G-R) relation

$$\log N = A - bm \quad (1)$$

to magnitude ranges $m \geq m^*$ where m^* is the magnitude of the largest earthquake so far observed at least once in the sample record for the specific region or seismic source zone under consideration. The validity of extrapolations to $m \geq m^*$ hinges critically on a number of assumptions. One of these is the notion that the slope b in the (G-R) relation (1) is constant over a sufficiently wide range of magnitudes that includes both the observed magnitudes and the magnitudes $m \geq m^*$ to which we wish to extrapolate.

Let us therefore look at some of the arguments that have been made in the literature about the validity of a constant b -value, deviations from constant- b models, and relevant observations and theoretical arguments. This brief commentary is only a sampling of the literature and does not claim to be a balanced and exhaustive survey; hence it may not be fully representative of the variety of arguments that may have been made on this subject.

Also, we do not touch here on other difficulties that can arise in addition to the question whether b is constant or not. These other difficulties tend to control the *uncertainties* associated with determining the A - and b -values of the G-R relation, stemming often from the related problems of catalog incompleteness, and of non-unique definitions of the magnitude and intensity scales. These practical issues do not call by themselves in question the existence of the constancy of b in the Gutenberg-Richter relation; but they can contribute to the uncertainty with which b can be determined and thus may make it impossible to resolve whether a constant b slope exists or not, over the range of magnitudes of interest.

The Physical Need for an Upper Magnitude Limit.

It has been shown by many authors (e.g. Main, 1995) that the seismic energy E (or moment M) is related to magnitude m and fault length L by relations of the form

$$\log E = cm + d \quad (2)$$

and
$$E \sim L^a \quad (3)$$

It can be shown that (1) through (3) imply a power law frequency distribution of energy

$$N(E) \sim E^{-B} \quad (4)$$

with $B = b/c$.

It also can be shown that for typically observed b-values $0.5 \leq b \leq 1.5$ a finite maximum earthquake size must exist, otherwise there would be infinite seismic energy release for a finite strain rate in the presence of the G-R law (1) and power-law distribution (4). Hence, finiteness of strain energy requires a truncation at some upper magnitude level, at least for typically observed b-value slopes.

Observations and Arguments For and Against a Constant b-Value.

Observations: Limited fault or source zone vs. "global" fault or source zone statistics.

A constant b-value slope in the powerlaw distribution follows if self-similarity applies to the earthquake process, i.e. if the processes involved apply equally regardless of scale.

Wesnousky et al. (1983) found from combining geologic, geodetic and seismicity data, that in Japan for a single fault zone, the frequency-magnitude distribution does not follow the classic constant b-value model. In particular they found, that the largest moment on a fault is substantially larger than that predicted from a G-R type relation. Similar results are known from the Mexican subduction zone seismicity, or from a European graben system (Lower Rhine embayment in the Netherlands / German border region) with low seismicity and events thought to be limited to about $m \leq 6.5$ (Camelbeeck and Meghraoui, 1996).

Schwartz and Coppersmith (1984) proposed the concept of "characteristic earthquakes" based on observations on the Wasatch (Utah) and San Andreas (CA) faults. The geologically inferred recurrence rates of the characteristic earthquakes were higher than those inferred from the known historic and instrumental seismicity (see attached Figures A).

Davison and Scholz (1985) used catalogs from the Alaska Aleutian arc to make the point that if one uses the catalog data from limited rupture zones, then the extrapolation from small earthquakes always underpredicts the moment rate implied by the occurrence of the largest earthquakes in this

subzone. If, on the other hand, all events, i.e. small and characteristic events are used in a single "global" Alaska-Aleutian arc seismic zone, than the rate of the largest earthquakes (in this case of the 1964 moment magnitude 9.2 Gulf of Alaska earthquake) is well predicted by the occurrence of all other earthquakes. The same holds for a global catalog which correctly "predicts" the largest known earthquake, the 1960 Chile earthquake (see attached Figures B).

It is interesting to note that Bollinger et al. (1989) tested the seismicity catalog for the southeastern U.S. (SEUS) as a whole, and for subregions of it, and came to what appears to be a somewhat differing conclusion for this SCR region: that if the entire SEUS catalog (exclusive of Charleston S.C.) is used, a higher rate of Charleston-type earthquakes is inferred for this region using a G-R type relation for the moderate and smaller earthquakes, than the local small-magnitude seismicity data would allow one to infer for the Charleston area (which in turn provides recurrence rates roughly consistent with the paleoseismic results for Charleston). The authors argue that therefore the local data for Charleston may provide a better estimate of the recurrence rate of the maximum-size event in the Charleston area, and that using the entire SEUS data, i.e. the "global" data in our earlier terminology, would over- (rather than under-) estimate the recurrence rate of Charleston-type events in the entire SEUS, if such events can occur outside the Charleston area proper.

In many other regions investigators often find general applicability of the G-R relations, i.e. that the occurrence rates of the largest events can be reasonably accurately inferred from the rates of smaller earthquakes. However, as pointed out by Pacheco and Sykes (1992) based on empirical data, caution must be exercised when the size of ruptures becomes so large (moment magnitudes ≥ 7.5) that they approach the down-dip dimension of the seismogenic zone of the crust and uppermost mantle. Many seismic scaling relations appear to change at this magnitude threshold, including the b-value slope of global seismicity catalogs from $b=1.04$ for moment magnitudes $7.0 \leq m \leq 7.5$, to $b=1.51$ for magnitudes $7.6 \leq m \leq 8.0$ (see attached Figures C).

In summary, we find cases of overestimating, underestimating or correctly estimating the rates of large events from the rates of smaller events. What are the possible explanations for and inferences from these seemingly diverging observations, for reasons other than those presented by Pacheco and Sykes (1992) ?

Fractals, Rock Mechanics, Physical Models, Computer Simulations. In the last two decades or so the earthquake process has been investigated from the different vantage points of a variety of disciplines: chaos theory for linear and nonlinear systems; rock mechanics; statistical mechanics;

fractal concepts; and computer simulations of the earthquake-loading and strain-release cycles of large coupled systems (so-called "automatons"). From these approaches has emerged the realization that earthquakes may represent a class of stochastic processes known as "self organized critical (SOC) phenomena" (e.g. Ito and Matsuzaki, 1990). However, deviation from strict SOC behavior is needed to explain the diverse observations. Such modified SOC processes can "explain", or at least mimic, the sometimes quasi-cyclic behavior, foreshock and aftershock sequences, size distributions, "characteristic events" and other features frequently observed in seismicity. In a recent paper, Main (1995) reviews several of the salient features of these models and some of their implications for seismic hazard assessments.

Following Rundle and Klein (1993) three states are distinguishable in such modeling efforts: subcritical, critical and supercritical. The three types of behavior are illustrated in Figures D taken from Main (1995). The three types of behavior can be analytically described by a generalized power-law (fractal) distribution for small events if modified by an exponential (Boltzmann) tail with negative, zero, or positive exponent of the form:

$$N(E) \sim E^{(-b)} e^{(-E/E_0)} \quad (5)$$

where E_0 is a characteristic energy (or moment) "reflecting the probability of occupying the different energy states E ". In computer modeling experiments, E_0 tends to increase with driving velocity, i.e. the rate of the tectonic strain loading. The cumulative or integrated form of the density distribution (5) is a generalized gamma distribution (for details see Main, 1995). If the distribution is subcritical ($1/E_0 > 0$), then the system sets its own upper magnitude and one obtains the exponentially truncated frequency-magnitude distribution currently most commonly used in seismic hazard analyses. If the system is precisely critical ($1/E_0 = 0$), then all states have equal chance of being occupied up to the limiting state, and a fixed sharp drop-off at a well defined maximum energy (i.e. moment magnitude) is needed to preserve total final energy. If the system is supercritical ($1/E_0 < 0$) there is a greater potential for the largest earthquake than expected from the power-law distribution of the smaller events, i.e. energy is deprived to occupy the fractal- or powerlaw-controlled energy states of smaller events. This supercritical mode corresponds to the characteristic earthquake model. The three cases are schematically illustrated in Figures E taken from Main (1995) and referred to as case (a) = subcritical, (b) = exactly critical and (c) = supercritical, with their corresponding probability (or frequency) density distribution (left) and moment density distribution (right) indicated. For details see Main (1995).

Discussion.

The simple analytical model of an exponentially tailored power law described above by (5) is based largely on equivalents to thermodynamic processes. But relatively simple automaton computer models of systems of sliding masses, springs and damping components, can simulate artificial "earthquake data" with properties that largely reproduce the classes of observations from real earthquakes made for many parts of the world.

If this type of modified self-organized critical model does indeed apply to the earthquake process, which at this time is an unproven hypothesis, then such models would have great implications for quantitative seismic hazard assessments. Also not known at this time is which of the possible tectonic factors control the mode of criticality, i.e. under what tectonic circumstances does the subcritical, critical, or supercritical case apply. Strain rates seem to have some controlling influence, but not solely. The degree of material heterogeneities may contribute among many other possible factors.

All three modes of energy release (subcritical, critical, and supercritical) require a truncated frequency vs. moment (or magnitude) distribution. But only in the subcritical and critical cases it is possible to use the fractal portion (the power-law or G-R portion) of the frequency-magnitude distribution to estimate from the rate of small earthquakes the rate of the largest earthquakes with reasonable confidence. Without knowing the critical energy E_0 and/or its controlling tectonic factors, it will be unknown whether the common practice of using the simple G-R relations for estimating large earthquakes is valid and applicable in any specific case. While it is likely that more often than not subcritical to critical conditions exist, there is currently no method available to assess *a priori* the mode of criticality, and hence one cannot exclude the possibility that a characteristic earthquake model may apply in any given region due to supercritical conditions tending to produce characteristic earthquake occurrences. If such supercritical conditions apply, the extrapolation of the G-R relation to large magnitudes under the assumption of a constant b-slope would tend to underestimate the rates of the largest (characteristic) earthquakes.

References.

- Bollinger, G.A., F.C. Davison, M.S. Sibol, and J.B. Birch (1989). Magnitude recurrence relations for the Southeastern United States and its subdivisions. *JGR* 94, 2857-2873, March 10, 1989.
- Camelbeeck, T. and M. Meghraoui (1996). Large Earthquakes in Northern Europe more likely than once thought. *EOS, Transactions of the Am. Geophys. Union*, Vol. 77, No. 42, October 15, 1996, pp. 405 & 409.
- Chapman, M.C. (1996). Can small magnitude shocks be used to infer the occurrence rates and locations of future damaging shocks? White paper for LLNL - TIP, Jan 7, 1997.
- Davison, F.C. and C.H. Scholz (1985). Frequency-moment distribution of earthquakes in the Aleutian Arc: A test of the characteristic earthquake model. *BSSA* 75, 1349-1362, October 1985.
- Ito, K. and M. Matsuzaki (1990). Earthquakes as self-organized critical phenomena. *JGR* 95, 6853-6860, May 10, 1990.
- Main, I.G. (1995). Earthquakes as critical phenomena: implications for probabilistic seismic hazard analysis. *BSSA* 85, 1299-1308, October 1995.
- Pacheco, J.F. and L.R. Sykes (1992). Seismic moment catalog of large shallow earthquakes, 1900 to 1989. *BSSA* 82, 1306-1349, June 1992.
- Rundle, J.B. and W. Klein (1993). Scaling and critical phenomena in a cellular automaton slider-block model of earthquakes. *J. Stat. Phys.*, 72, 405-413.
- Schwartz, D.P. and K.J. Coppersmith (1984). Fault behavior and characteristic earthquakes: examples from the Wasatch and San Andreas fault zones. *JGR* 89, 5681-5698, July 10, 1984.
- Wesnousky S., C.H. Scholz, K. Shimazaki and T. Matsuda (1983). Earthquake frequency distribution and the mechanics of faulting. *JGR* 89, 9331-9340.

Figure intentionally omitted

Figures A: from Schwartz, D.P. and K.J. Coppersmith (1984). Fault behavior and characteristic earthquakes: examples from the Wasatch and San Andreas fault zones. JGR 89,568 1-5698, July 10, 1984.

Figure intentionally omitted

Figures B: from Davison, F.C. and C.H. Scholz (1985). Frequency-moment distribution of earthquakes in the Aleutian Arc: A test of the characteristic earthquake model. BSSA 75, 1349-1362, October 1985.

Figure intentionally omitted

Figures B (continued).

Figure intentionally omitted

Figure B (continued).

Figure intentionally omitted

Figures C: from Pacheco, J.F. and L.R Sykes (1992). Seismic moment catalog of large shallow earthquakes, 1900 to 1989. BSSA 82,1306-1349, June 1992.

Figure intentionally omitted

Figures D: from Main, I.G. (1995). Earthquakes as critical phenomena: implications for probabilistic seismic hazard analysis. BSSA 85, 1299- 1308, October 1995.

Figure intentionally omitted

Figures E: from Main, I.G. (1995). Earthquakes as critical phenomena: implications for probabilistic seismic hazard analysis. BSSA 85,1299-1308, October 1995.

Can Small Magnitude Shocks be Used to Infer the Occurrence Rates and Locations of Future Damaging Shocks?

by

Martin C. Chapman

Jan. 7, 1997

Summary

Yes, if it can be assumed that certain elements of the seismogenic process are scale-invariant and stationary. Under those assumptions, extrapolation of small magnitude occurrence rates to higher magnitudes is consistent with hazard models wherein the locations of larger shocks are represented by area sources.

Introduction

Seismogenic sources in most areas of the eastern United States must be inferred indirectly from geophysical data, which in most cases is gleaned from small magnitude earthquakes. Given a data set consisting largely of the locations and dates of occurrence of small magnitude shocks, what if anything can be said, in a statistical sense, about the future occurrence times and locations of larger (potentially damaging) shocks? I argue below that because the seismogenic process is fundamentally scale invariant and stationary, the locations and occurrence rates of small magnitude shocks, can in principle, be used to infer the rates and locations of future large shocks.

Discussion

Scale invariance implies that a process has the same appearance, regardless of the magnification used to examine it. For this discussion, the process in question is faulting, and the key measurement is the size of the earthquake source (expressed as a rupture length, or area, or indirectly as seismic moment) and the length(s) of seismogenic faults. Stationarity implies that statistical properties of the process are constant. Stationarity is a basic

assumption of hazard analysis. It is assumed that occurrence rates (as well as the locations) of future damaging shocks can be predicted, in a probabilistic sense, using a data set comprised of past observations.

Scale invariance is a property of fractal sets, and implies a power law frequency distribution of the lengths of objects comprising the set. Several important attributes of seismicity (faulting) exhibit this property. For example, fault lengths in a given region have a power law frequency distribution. The Gutenberg-Richter frequency versus magnitude relationship is also a power law, when expressed in terms of seismic moment rather than magnitude. Earthquakes are scale invariant in terms of stress drop. Observations show a range of stress drop between a few 10's of bars to a few hundreds of bars, over several orders of magnitude of seismic moment.

Spatial Behavior:

Earthquakes exhibit clustering, both temporally and spatially. In particular, it is well established from observation in regions with high deformation rates that seismic energy release at all magnitude levels tends to occur on large, dominant faults. Some recent studies of the (statistical) physics of crustal scale deformation suggest that the evolution of the faulting process in a given volume results in the spontaneous emergence of spatially organized, dominant faults. For example, Cowie et al. (1993) developed a numerical rupture model to simulate the growth of crustal scale faults. The conceptual model was comprised of a lattice of 10x10 km crustal blocks interacting through both short and long range elastic forces, in response to a constant driving velocity at the model boundary. Initially, the lattice deforms by uncorrelated nucleation of small faults, reflecting the random, uncorrelated distribution of the material properties in the model. But as time progresses areas of the lattice become silent, while other areas contain all activity. The deformation is increasingly concentrated on large, dominant through-going faults. This occurs in spite of the fact that stress is simultaneously high elsewhere in the model grid. The system is driven to failure less often between the major faults. The faults in the simulation have a power law scaling, both of their size distribution and in the sizes of the earthquakes they

generate (Cowie et al., 1995). The results indicate that the (eventual) localization of rupture in space does not require preexisting zones of weakness.

The results of Cowie et al. are derived from two-dimensional, thin plate models: all faults in their simulations rupture the conceptualized brittle crust. Deformation rates used in the modeling are compatible with plate boundary rates. If similar results hold for a large range of scale lengths in 3-dimensions and for a range of strain rates, they may have important practical implications. For example, in a system that has evolved sufficiently, a short term snapshot of the recent seismic history could in principle be very useful for hazard analysis purposes: the locations of small shocks tend to illuminate the dominant faults, upon which large shocks will tend to occur. Thus, the results provide an experimental justification for the common practice in hazard assessment of using low magnitude seismicity to define potential sources of large shocks. Equally important however, is the result that for a system in some earlier state of evolution, the spatial correlation between the locations of the smallest shocks and largest faults could be very weak. In the context of the modeling results above, the usefulness of the historical catalog of seismicity in the southeast depends upon whether or not deformation in the region is in a stable: i.e., stationary, "self-organized" state.

The evolution of the model of Cowie et al. leads eventually to asymptotic behavior, where deformation occurs on a few through-going faults (which may be structurally complex). Areas between these major faults are stable. While this situation may be analogous to California, for example, it is not analogous to the east, at least for the scales conceptualized in the experiments. Clearly, the intraplate setting of the east does not represent the ultimate evolutionary state of the model. However, the point here is that in the model experiments, the transition from uniform "disorganized" deformation on small faults to "organized" deformation occurs at an early stage, and corresponds to a change in fault lengths from an exponential to a power-law frequency distribution.

The Gutenberg-Richter relationship for the southeastern U.S. is consistent with a power-law, with a "normal" b value of about 0.8 to 0.9, determined over

magnitudes from 2.0 to 7.0 (Bollinger et al., 1989). This suggests that seismicity in the region has indeed reached a state such that at least some clustering along dominant faults is occurring. This is supported by the observation that the instrumentally located shocks occurring during the past 20 years are obviously correlated with the pre-1976 seismicity pattern, which is distinctly non-uniform. Also, small magnitude shocks in the New Madrid seismic zone define a highly organized zone of crustal scale faulting. Similarly, seismicity in Giles County, VA indicates a steeply dipping planar zone, suggesting a crustal scale fault zone. The same situation applies to Charleston, SC. These examples represent seismicity in the "shadow" of relatively recent, large shocks. The New Madrid, Charleston and Giles County earthquakes occurred 187, 110 and 100 years ago, respectively, and it is conceivable that the current seismicity is somehow due to stress redistribution following the larger shocks. However, it is at least equally plausible the observed activity is in fact representative of an (approximate) steady-state rate of earthquake occurrence in those areas. The temporal stationarity of the seismicity is an important issue, to be addressed below. However, regardless of that aspect, small magnitude shocks in New Madrid, Giles County and Charleston tend to occur on planar features that in all likelihood represent seismogenic crustal scale faults. So, it would seem that for the purpose of predicting the locations of future damaging shocks, the locations of small magnitude shocks represent a highly relevant data set.

Temporal Behavior:

If seismicity were indeed a temporally stationary, scale invariant process, the accuracy of predicted rates of large earthquakes would depend only on random error in observed earthquake rates, which in principle could be estimated with no bias from small magnitude events. Unfortunately, the physics of the problem on a fault-specific scale indicates a very complex process. A finite maximum magnitude must exist for any given fault. The elastic rebound theory implies that strain energy is stored and released in a manner such that slip rates on faults in a given region must reflect the regional tectonic deformation rate. It is generally assumed that the regional rates are constant on the long term (several thousand years), because they are due to the mechanics of plate motion

and interaction. However, a (constant) regional deformation rate in principle might not be accurately represented by the frequency of the smaller shocks, because the deformation is dominated by slip that occurs in the largest shocks. Furthermore, comparisons of rates of large magnitude shocks with rate of smaller magnitude, recent shocks often show a discrepancy. The characteristic earthquake model for the largest shocks on a fault (Schwartz and Coppersmith, 1984; Youngs and Coppersmith, 1985) implies clustering of interevent times, and higher rates than would be predicted from a linear extrapolation of the observed Gutenberg-Richter relationship at small magnitudes.

Given the above, do rate estimates derived from catalogs containing only small magnitude events have any practical value for hazard assessment? Yes, I think they do have value. Although the linear Gutenberg-Richter relationship may break down on a fault specific basis, most seismic sources in the eastern U.S. are modeled as composites (i.e. as areas), representing assemblages of individual seismogenic faults. This spatial averaging invariably produces a linear recurrence relationship, for the population of faults. This population average is compatible with the use of a hazard model wherein the location of future damaging shocks is treated as a random variable.

References

- Bollinger, G.A., F.C. Davison, M.S. Sibol and J.B. Birch (1989), Magnitude recurrence relations for the southeastern United States and its subdivisions, *Journ. Geophys. Res.*, 94, B3, 2857-2873.
- Cowie, P.A., C. Vanneste, and D. Sornette (1993), Statistical physics model for the spatiotemporal evolution of faults, *Journ. Geophys. Res.*, 98, B12, 21,809-21,821.
- Cowie, P.A. D. Sornette and C. Vanneste (1995), Multifractal scaling properties of a growing fault population, *Geophys. J. Int.*, 122,457-469.

Schwartz, D.P. and K.J. Coppersmith (1984), Fault behavior and characteristic earthquakes: examples from the Wasatch and San Andreas fault zones, *Journ. Geophys. Res.*, 89, 5681-5698.

Youngs, R.R and K.J. Coppersmith (1985), Implications of fault slip rates and earthquake recurrence models to probabilistic seismic hazard estimates, *Bull. Seism. Soc. Am.*, 75, 939-964.

USE OF FAULT LENGTH AND AREA IN THE ESTIMATION OF MAXIMUM MAGNITUDES FOR THE EASTERN TENNESSEE SEISMIC ZONE

G. A. Bollinger

LLNL SSHAC Project White Paper - November 1996

INTRODUCTION

A key parameter for seismic hazard analysis is an estimate of the maximum possible earthquake for the fault segment or seismic zone under consideration. For some high strain-rate, interplate regions, e.g., California, estimates for specific segments of the causal fault system (San Andreas) can often be made with reasonable confidence. For low strain-rate, intraplate areas such as the eastern U.S., the lack of understanding of the causes of intraplate seismicity in general and the lack of knowledge concerning individual fault segments in particular are major problems in this estimation process.

A principal technique applied in both interplate and intraplate areas for the maximum magnitude estimation process involves the use of empirical relationships between magnitude and fault parameters. Tocher (BSSA, 1958) was probably the first to show quantitatively that such a correlation existed. Since that initial study, there have been numerous published relationships relating magnitude to various fault parameters. The most recent of these is a 1994 study by Wells and Coppersmith (BSSA). This is an especially thorough, well done investigation. From a worldwide data base of source parameters for 421 earthquakes (Shallow - less than 40 km), continental interplate and intraplate shocks with magnitudes greater than about 4.5, 244 earthquakes were selected for analysis. Log-linear regressions were developed between earthquake magnitude and surface/subsurface rupture lengths and rupture areas that are especially well-correlated, having standard deviations of 0.25-0.35 magnitude units. That standard deviation is comparable to what is observed in the worldwide measurements reported for an individual earthquake. The authors conclude that since the magnitude-fault length and fault area

measurements have a large enough data base to exhibit a statistical stability that makes it unlikely that the regressions obtained would change significantly in response to additional data.

Of special importance to this study, Wells and Coppersmith (1994) also investigated the possible effect of tectonic setting. They used t-statistics to demonstrate that, at the 95% significance level, there was no difference in the regressions between extensional and compressional stress regimes. They also investigated for possible differences in earthquakes occurring in stable continental regions (SCR) with those from non-SCR regions. They found that, at the 95% significance level, the differences in the regressions for those two very different tectonic environments resulted in an expected magnitude difference of less than 0.2M. I agree with their final conclusion that subdividing the data set according to various geographic regions or tectonic settings would not typically improve the statistical significance of the regressions.

Accordingly, we will use herein the Wells and Coppersmith (1994) regressions between Moment magnitude (M) and subsurface rupture length, subsurface rupture width and rupture area. Those regressions are :

$$\text{Subsurface Rupture Length (SRL ; km)} \quad M = 4.38 + 1.49 \log (\text{SRL}) \quad (1)$$

$$\text{Subsurface Rupture Width (SRW ; km)} \quad M = 4.06 + 2.35 \log (\text{SRW}) \quad (2)$$

$$\text{Rupture Area (RA ; sq km)} \quad M = 4.04 + 0.98 \log (\text{RA}) \quad (3)$$

Use of these relationships to make estimates of maximum magnitudes obviously requires that the input rupture parameter estimates themselves be maxima. Also, it is preferable to make multiple estimates for the same fault if at all possible. This provides a qualitative indication of the stability and range of maximum magnitude estimates that the fault measurements at hand provide and it can also contribute to uncertainty assessments.

sub-vertical. Chapman provided two sets of plots at different foci gather distances (20 and 30 km) and I selected the width dimension that was the larger between them. A fault plane area is then determined by the product of the length and downdip values. Application of equations (2) and (3) produces the following results :

<u>Fault</u>	<u>Downdip Length (km)</u>	<u>(M)</u>	<u>Fault Area (sq km)</u>	<u>(M)</u>
EW1	17	7.0	1,037	7.0
EW2	16	6.9	1,520	7.2
EW3	10	6.4	420	6.6
EW4	17	7.0	510	6.7
NS1	17	7.0	1,428	7.1
NS2	20	7.1	2,500	7.4
NS3	(Not available)		(Not available)	
NS4	10	6.4	1,180	7.1

Again, we have magnitude values in the 6 1/2 to 7 1/2 range:

A comparison of the three magnitude estimates derived for all the faults except one (NS3) is as follows :

<u>Fault</u>	<u>Rupture Length M</u>	<u>Downdip Length M</u>	<u>Fault Area M</u>
EW1	7.0	7.0	7.0
EW2	7.3	6.9	7.2
EW3	6.8	6.4	6.6
EW4	6.6	7.0	6.7
NS1	7.2	7.0	7.1
NS2	7.5	7.1	7.4
NS3	6.7	NA	NA
NS4	7.5	6.4	7.1

The three values for each fault generally agree very well with each other. The average difference within the sets of three values is 0.28. Excluding NS4, whose downdip length estimate is anomalous with respect to the other two values, that average is 0.20. This remarkable consistency indicates that the horizontal length/downdip length of the Eastern Tennessee Seismic Zone faults is in accord with what has been observed for seismogenic faults worldwide.

I judge these estimates to be very useful to the process of determining maximum magnitudes estimates for the Eastern Tennessee Seismic Zone. In particular, they demonstrate that the crustal seismogenic zone present there is unusually thick (17 km), that it extends to mid-crustal depths of 22 km. and, according to worldwide earthquake fault data, is, in principle, capable of generating shocks in the large (7 1/2) range.

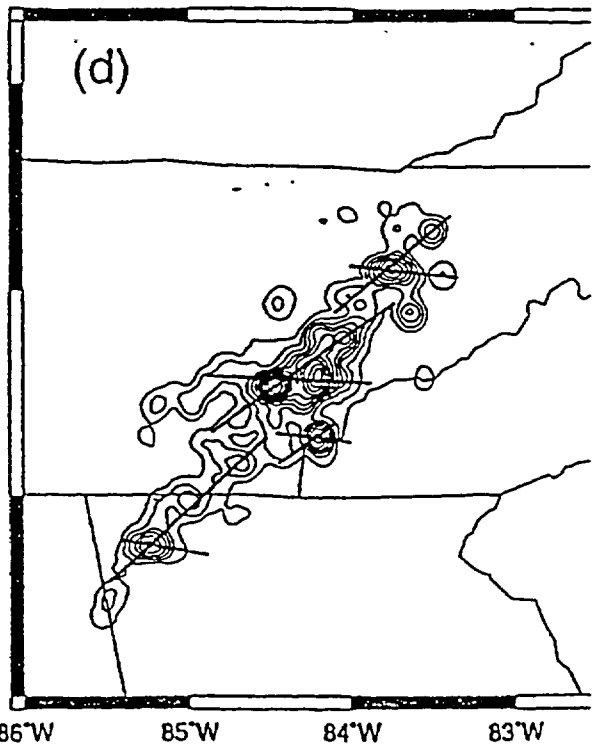
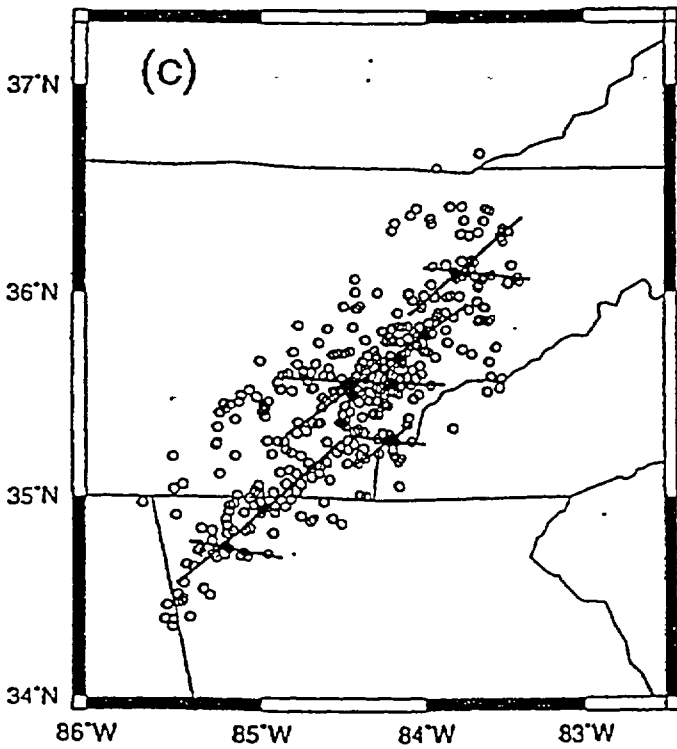
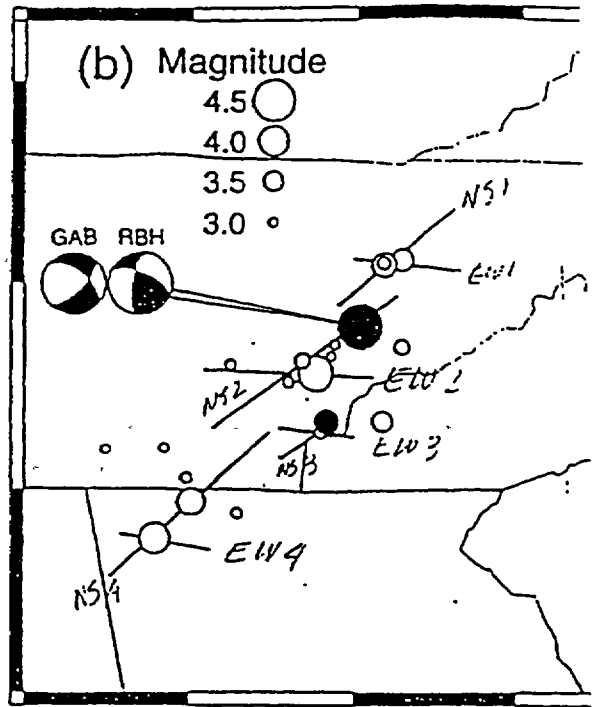
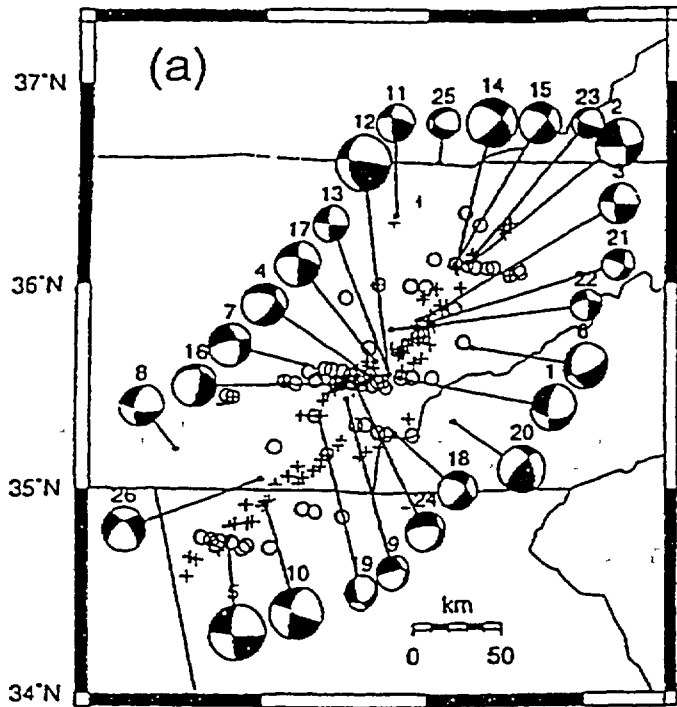


Figure 1

APPENDIX

Foci Plots for the Eastern Tennessee Seismic Zone Showing Horizontal and Vertical Distributions

(Provided by Martin Chapman, Oct 1996)

Figures on the following pages B-29 through B-40 were intentionally removed

Figure intentionally omitted

DRAFT

Estimating Magnitudes of Earthquakes From Paleoliquefaction

by

Pradeep Talwani
January 1997

1. Seismically induced liquefaction (SIL) features - lateral flows, explosion craters - are widely observed. The geometry, size and distance of these features from the earthquake source varies greatly attesting to the fact that seismically induced liquefaction is a very intricate process. Earthquakes of magnitude as low as 4.5 have been known to have caused liquefaction. Great earthquakes, e.g., 1905 Kangra, India are known to have caused widespread liquefaction at distances over 200 km, and there was an absence of liquefaction features at lesser distances. These observations are just to make a point that several factors control the location and incidence of liquefaction due to an earthquake. Contrariwise, determining the size and nature of an earthquake from an examination of SIL feature is problematic.
- 2.1. The occurrence of liquefaction at any site is controlled by several factors. These include:
 - a. Geotechnical characteristics of the soil - grain size, saturation, packing density, effective stress conditions, etc.
 - b. Thickness and density of overlying soil column.
 - c. Depth to the water table.
 - d. Amplitude of strong ground motion.
- 2.2. The amplitude of strong ground motion at any site, (besides the site conditions described in (i) above,) also depends on seismological factors:
 - a. The earthquake magnitude.
 - b. The hypocentral distance from the source.
 - c. The peak and duration of horizontal acceleration.
 - d. The crustal structure between the source and site. Several examples attest to this conclusion. Liquefaction occurred at distances 100 km or greater following the 1989 Loma Prieta, California, 1905 Kangra, India,

1934 and 1988 Bihar-Nepal, earthquakes. Catchings and Kohler (1996) showed that focussing of seismic waves, can amplify strong ground motion at large distances.

3. The above observations are made to point out that it is not a simple or easy task to estimate the magnitude of an earthquake from an examination of liquefaction features. However, if certain conditions are met it is possible to obtain a qualitative estimate of the size of a prehistoric earthquake. These include:
 - a. Knowledge of the location of the earthquake.
 - b. Widespread observation of liquefaction features relatable to a source.
 - c. Availability of a calibration earthquake, i.e., an earthquake whose location and magnitude are known and whose liquefaction effects can be compared with those of paleoearthquakes.

An example of such an earthquake is the 1886 Charleston earthquake which was associated with widespread liquefaction and various paleoearthquakes were associated with a similar distribution of paleoliquefaction features.

Obermeier and others (1989) noted that the dimensions and frequency of sand blows decreased away from Charleston. They interpreted that observation to suggest that the source of the prehistoric earthquakes was near Charleston.

4. Once the location of the source is known, under favorable circumstances, three methods can be used to obtain an estimate of the magnitude of a prehistoric earthquake from an examination of liquefaction features.
 - a. From the size and frequency of sand blows of the same age.
 - b. From Liquefaction Severity Index (Youd and Perkins, 1987).
 - c. From geotechnical measurements.

These are briefly described below:

- 4.a. The 1886 M_w 7.3 Charleston earthquake, was associated with liquefaction near Bluffton and near Georgetown, located 100 km to SW and NE of Charleston (Figure 1). The prehistoric earthquakes of 546, 1000, 3550 YBP were also associated with sand blows at these three locations. This observation was used to infer the size of the prehistoric earthquakes as being comparable to the 1886 event. The 1641 YBP paleoearthquake was only encountered in the sand

blows between Myrtle Beach and Georgetown and not near Charleston. It was assigned a M_w 6.0.

- 4.b. Using the size and nature of deformation of sedimentary features in a continuous distribution of liquefaction features away from sources of earthquakes in western US, Youd and Perkins (1987) developed the Liquefaction Severity Index (LSI) as a measure of horizontal ground displacement associated with subsurface liquefaction. By comparing epicentral distances to different liquefaction features for different magnitude earthquakes, they obtained LSI attenuation curves (Figure 2). These in turn can be used to estimate the magnitude of paleoearthquakes. However by comparing the LSI data for the instrumentally located Saguenay earthquake, Tuttle (1994) showed that the LSI curves are limited in their usefulness for estimating magnitudes for prehistoric earthquakes unless the source area can be defined.
- 4.c. Estimates of magnitudes from geotechnical tests. Magnitude estimates can also be obtained by comparing the results of geotechnical tests in areas of liquefaction (see e.g., Seed and Idriss (1982), Martin (1990), Amick and Talwani (1991) and Tuttle (1994)).

Based on an extensive body of data empirical correlations were obtained relating the occurrence and nonoccurrence of liquefaction to the intensity of ground shaking and the principal characteristics of cohesionless soils. Figure 3 shows the data for earthquakes with a $\sim M$ 7.5. Each point corresponds to one boring record. The intensity of ground motion at a site is represented by the vertical ordinate, τ_{av}/σ'_0 where τ_{av} is the average peak shear stress and σ'_0 is the initial vertical effective stress. The soil resistance is represented by the horizontal abscissa $(N_1)_{60}$ which is the blow count in a standard penetration test (SPT) corrected for the depth of the overburden.

The curve drawn in Figure 3 is used to divide zones of liquefaction and non-liquefaction. Using similar data for other earthquakes, Seed and Idriss (1982) obtained a family of curves for different magnitudes (Figure 4).

For a paleoliquefaction site, the results of SPT tests can be used to obtain the penetration resistance, and other tests are used to estimate the ground acceleration associated with the liquefaction (vertical ordinate), and hence the magnitude of the earthquake (see e.g., Martin 1990). These curves are generic and local site conditions can modify the results.

References

1. Amick, D.C. and P. Talwani (1991). The Use of Paleoliquefaction Features to Estimate Prehistoric Levels of Ground Motion. Proceedings of the Second International Conference on Recent Advances in Geotechnical Earthquake Engineering and Soil Dynamics, St. Louis, Missouri, March 11-15, 1991.
2. Catchings, R.D. and Kohler, W.M., (1996). Reflected Seismic Waves and Their Effect on Strong Shaking During the 1989 Loma Prieta, California Earthquake, *Bull. Seis. Soc. Am.*, 86, 1401-1416.
3. Martin, J.R. (1990). Implications From a Geotechnical Investigation of Liquefaction Phenomena Associated With Seismic Events in the Charleston, South Carolina Area. Ph.D. Dissertation, Virginia Polytechnic Institute and State University, 414 p.
4. Obermeier, S.F., Weems, R.E., Jacobson, R.B. and Gohn, G.S. (1989). Liquefaction Evidence for Repeated Holocene Earthquakes in the Coastal Region of South Carolina: *Annals of the New York Academy of Sciences*, 558, 183-195.
5. Seed, H.B. and I.M. Idriss (1982). Ground Motions and Soil Liquefaction During Earthquakes. EERI Monograph Series, Vol. 5, 134 p.
6. Tuttle, M.P. (1994). The Liquefaction Method for Assessing Paleoseismicity: Technical Report NUREG/CR-6258, Nuclear Regulatory Commission, Washington, D.C., 38 p.
7. Youd, T.L. and D.M. Perkins (1987). Mapping of Liquefaction Severity Index. *Journal of Geotechnical Engineering*, Vol. 113, No. 11, 1374-1392.

Figure intentionally omitted

Figure I Shows the location of paleoliquefaction sites from where radiocarbon dates have been obtained. Isoseismal lines for the 1886 Charleston earthquake are taken from Bollinger (1977).

Figure intentionally omitted

Figure 2 Liquefaction severity index (LSI versus distance for the 1988 Saguenay, Quebec, 1886 Charleston, SC, and 1811 New Madrid, MO, earthquakes, with least squares fit lines for each earthquake, as well as LSI for western US earthquakes (dashed lines) of equivalent magnitude (from, Youd et al., 1989). (Figure from Tuttle, 1994.)

FIGURE -3 Relationship between stress ratios causing liquefaction and (N1)60 values for clean sands for magnitude 7.5 earthquakes. Source: Seed et al. (1984).

Figure intentionally omitted

Figure 4- Chart for evaluation of liquefaction potential of sands for earthquakes of different magnitudes.
Source: Seed and Idriss (1982).

**APPENDIX C: PRELIMINARY SOURCE GEOMETRIES DEVELOPED
BY THE EXPERTS IN PREPARATION OF THE SEISMIC SOURCE
EXERCISE OF WORKSHOP #2**

Some of the maps displayed here were actually drawn by the experts during Workshop #1, then modified and documented for Workshop #2.

The remaining pages in Appendix C were copied from other sources. ⋮

DOCUMENTATION FOR SEISMIC SOURCE MAPS

by

Gil Bollinger

August 1996

for

Trial Implementation of SSHAC Guidelines Project - LLNL/FESSP

The basic rationale for my approach to the definition of Seismic Source Zones in the Southeastern U. S., along with detailed discussions for specific examples, is given in the *USGS Bulletin* 2017, 1992. In brief, my technique places primary emphasis on areas of concentrated historical and instrumental seismicity. That emphasis is based from three factors :

- (1) Those areas are the currently most active,
- (2) McGuire's 1979 study of the 1900-yr long Chinese catalog concluded that the most recent 50-100 year period was the best predictor of the felt-shaking hazard for the next 50 years,
- (3) There is good agreement spatially between the 200-yr+ historical seismicity and the most recent 20-years of network/instrumental seismicity in the southeastern U.S.

Points 2 and 3 bear directly on PSHA for structures with 50 yr and 100 yr lifetimes. However, current strain rate estimates for the eastern U.S. are too large to be sustained over geologic time - therefore, there must be some type of cyclicity or on/off character in the region's earthquake activity. Right now, we can only say that it is longer than 200 years. Since the much more active China region had a 300-yr periodicity, perhaps the much less active eastern U.S. will have even longer periods of variations in strain energy release.

I use data and results from Seismology, Geology, Geophysics and Tectonics to supplement the seismicity data for zonal boundary definition and parameter estimation on a case-by-case basis.

Instead of the use of alternate source zones to express uncertainty, I prefer to assign probabilities of existence (pe) to each zone - the more uncertain the zone the lower its pe.

A simple zonal boundary such as a closed-curve or a polygonal figure is judged to be adequate because :

- (1) When the epicenter error ellipses are plotted they occupy a much larger area than that of the epicentral point estimates,
- (2) The Southeastern US epicenter concentrations generally have a 'halo' type of surrounding activity thereby making the exact boundary of the zonal concentration less clearly defined, and
- (3) As the 1988 Saguenay earthquake demonstrated, moderate shocks can occur at appreciable distances from the main zonal epicenter concentrations (75 km from Charlevoix Zone).

The principal concentrations I identify as Seismic Source Zones in the Southeastern US are the sites of the two largest historical shocks in the region, the spatially largest epicenter concentration and a small cluster separate from the site of the region's largest earthquake :

- The Giles County, VA Zone (Zones RZ3 and RZ3A)
- The Eastern Tennessee Zone (Zones RZ1, RZ1A and RZ1B)
- The Charleston, SC Zone (Zones LZ1, LZ1A and LZ1B))
- The Bowman Zone (Zone LZ2)

More diffuse seismicity concentrations are identified as source zones in :

- Central Virginia (Zone RZ4)
- Central Appalachians (Zone RZ5)
- Western North Carolina (Zone RZ2)
- South Carolina. (Zones LZ3, LZ3A and LZ4)

Finally, because of their great seismic potential, zones should also be considered for :

- New Madrid, MO (Zone RZ6)
- Wabash Valley, IL-ID (Zone RZ7)

Documentation for Southeastern U. S. Seismic Source Zones

Following is a listing of each Zones' principal diagnostic features.

Giles County, VA Source Zone (RZ3 - pe 100%) :

- Concentrated linear zone of well-located instrumental seismicity -
Also, Define a causal fault zone (RZ3A - 75% pe)
- Zone of historical/poorly located seismicity ; Largest shock mb 5.6* in 1897.
- P and S reflection seismic data define steeply-dipping basement faulting in agreement with focal mechanism nodal planes,
Well-constrained focal depths 4-15** km - Implies average seismogenic crustal thickness and location beneath the Appalachian Overthrust,
- General agreement between NE strike of zone and strike of focal mechanism nodal planes - that strike is rotated some 20 deg from the ENE strike of the Appalachian structural grain,
- General uniformity of focal mechanisms - mixed strike-slip and reverse with northeasterly trending P-axes and
- Possible North-South intersection structure from instrumental seismicity.

* - Magnitudes herein from Stover & Coffman, USGS Paper 1527, 1992.

** - Focal Depths throughout are 10% and 90% fractile depths from Bollinger, 1992.

Eastern Tennessee Source Zone (RZ1 - pe 100%) :

- Concentrated 300+ km long linear zone of well-located instrumental seismicity,
- Zone of historical/poorly located seismicity ; Largest shock a mb 5.0 in 1865 (Chapman argues this shock was not in NC but rather near the NC-TN border),
- Well-constrained focal depths 8-21 km - Implies thick seismogenic crust below the Appalachian Overthrust rocks,
- Two groups of strike-slip, steeply dipping focal mechanisms : N-S/E-W and NE-SW/NW-SE, i.e., oblique and parallel to the zone, with well based preference for the NE-SW and E-W nodal planes as a conjugate set of causal faults,
- General uniformity of focal mechanism P-axes - northeasterly trend,

Very distinct correlation with regional through-going aeromagnetic anomaly lineations,

Define (1) A specific fault source zone (Chapman et al, subm BSSA, 1996) designated as RZ1A with a pe of 50% and also

(2) A low probability of existence (RZ1B - pe 10%) Zone for the possible development of a fault the full length of the zone resulting in a great earthquake (Mw 8).

Charleston, SC Source Zone (LZ1) - pe 100%) :

Concentrated cluster of well-located seismicity,

Zone of historical/poorly located seismicity ; Largest shock a Mw 7.3 in 1886;

Focal depths to 5-10 km - Average seismogenic crustal thickness, Focal mechanisms variable plus concentrated nature of recent seismicity suggests some type of intersection structure operative in localizing the strain.

Coastal Plain sedimentary wedge causes enhanced Intensity effects to the NW and reduced effects to the NE-SW and

Possible associated sources (or crustal amplification sites from the Charleston Source) from local liquefaction features northeast (Georgetown area - LZ1A - pe 50%) and southwest (Bluffton area - LZ1B - pe 25%) of the Charleston locale.

Bowman, SC Source Zone (LZ2 - pe 50%):

Concentrated zone (NW trend ?) of well-located seismicity ; Largest shock a mb 4.5 in 1972,

Not a historical zone - Has exhibited an 'on again/off again' habit since the early 1970's,

No focal mechanisms - Focal depths 2-6 km,

Only a few, small (M mostly less than 4) earthquakes and

Approximately 70 km from the Charleston source ; the 1988

Saguenay earthquake was some 75 km from the Charlevoix Zone.

South Carolina Piedmont & Coastal Plain Source Zone (LZ3 - pe 100%)

Diffuse seismicity of generally low-level ; Largest shock a mb 4.8 in 1913,

Persistent strain release throughout the historical record,

Reflection seismic data indicate structural/seismicity similarities with the Central Virginia Seismic Zone where strain release is occurring on multiple splay faults off a major detachment fault. Multiple sites of Reservoir-Induced Seismicity (RIS) and borehole stress measurements suggests high stress levels at shallow depths in the host crystalline Piedmont rocks. Presence of many intruded plutons in the basement rocks allows for sites of stress amplification and Alignment of RIS and other epicenter concentrations suggest the possibility of a Fall Line Seismic Zone (LZ3A - pe 20%).

Savannah River Site and Vogtle Seismic Zone (LZ4 - pe 20%)

Extensive geological, geophysical and seismological investigations at these two important sites have revealed the presence of multiple faults and other structural features, e.g., the Triassic Dunbarton basin and Pen Branch Fault, that are typical of the entire host Piedmont Province.

Very low level seismicity ; Largest shock an mb 3.3 in 1974 with mb 3.2's in 1972 and 1993.

Earthquake occurrences here have been interpreted as due to pockets of relatively high stress concentrations in the vicinity of buried plutons and/or a 'skin effect' of high stress regimes in the uppermost few kilometers of the high velocity Piedmont crystallines and

Recognized herein as a zone, with a pe of 20%, because of the known geologic structures and the critical facilities and storage materials present.

Western North Carolina Seismic Zone (RZ2 - pe 75%)

Diffuse earthquake activity of generally low level with larger shocks in 1861 (mb 5.0) and 1916 (mb 5.2),

Zone more active in pre-instrumental period prior to about 1960 than subsequently and

First identified as a zone by Gerald R. MacCarthy in 1956.

Central Virginia Seismic Zone (RZ4 - pe 100%)

Spatially isolated, coin-shaped seismogenic volume of persistent, low-level activity in the Virginia Piedmont,

Largest shock an mb 5.0 in 1875,
Focal mechanisms exhibit widely variable parameters and
Earthquake hypocenters and reflection seismic data show
excellent correlation with splay faults off the western flank of
a regional antiform structure (Foci shallower (3-7 km) and NE
trending focal mechanism P-axes) and with a separate, near-
vertical diabase dike swarm of Mesozoic age (Deeper foci (8-13
km and NW P-axes).

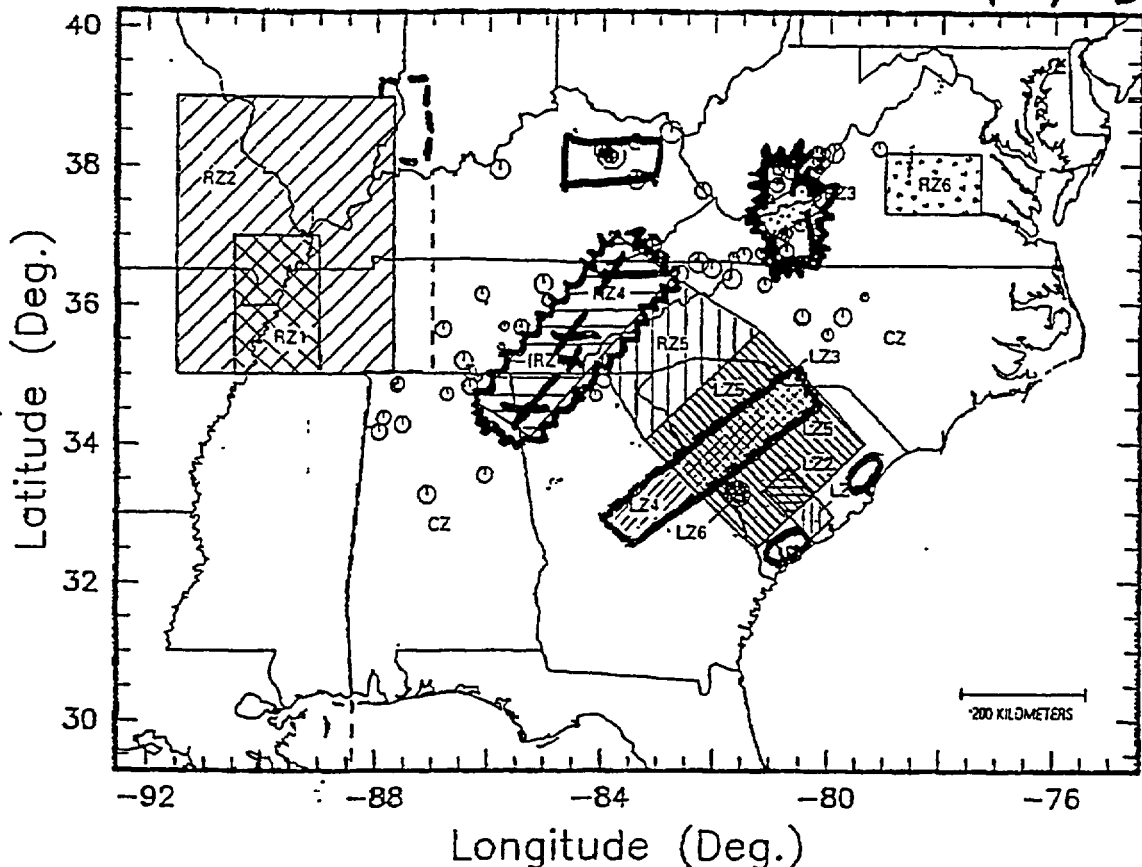
Appalachian Seismic Zone (RZ5 - pe 50%)

Diffuse earthquake occurrences that forms a regional 'halo effect'
about the area's more well-defined zones (Giles County, Eastern
Tennessee and Western North Carolina) and
Largest shock less than mb about 4 ; Low level seismicity historically
persistent.

New Madrid, MO Source Zone (RZ6 - pe 100%):

Concentrated zone - a complex 4-segmented zone of well-located
seismicity,
Zone of historical/poorly located seismicity ; Three largest shocks in
1811-12 in the Mw 7+ to 8 range,
Focal depths to 12 km. - Average seismogenic crustal thickness,
Focal mechanisms variable but uniform within each segment
Wabash Valley seismicity plus paleoliquefaction evidence argues
strongly for its own Seismic Source Zonal status (RZ7 - pe of
100%).

Bollinger
6/18/96



EXPLANATION

CZ	Complementary Zone	Background
LZ1	Local Zone 1	Charleston, South Carolina, seismic zone
LZ2	Local Zone 2	Bowman, South Carolina, seismic zone
LZ3	Local Zone 3	South Carolina Piedmont and Coastal Plain seismic zone
LZ4	Local Zone 4	South Carolina Fall Line seismic zone
LZ5	Local Zone 5	Area of Local Zone 3 minus area of Local Zone 4
LZ6	Local Zone 6	Savannah River Site
RZ1	Regional Zone 1	New Madrid, Missouri, seismic zone (small)
RZ2	Regional Zone 2	New Madrid, Missouri, seismic zone (large)
RZ3	Regional Zone 3	Giles County, Virginia, seismic zone
RZ4	Regional Zone 4	Eastern Tennessee seismic zone (RZ4A the same area as RZ4)
RZ5	Regional Zone 5	Northwestern South Carolina and southwestern North Carolina seismic zone
RZ6	Regional Zone 6	Central Virginia seismic zone

MAGNITUDE

○ (large)	5
○ (medium)	4
○ (small)	3
○ (very small)	2
○ (tiny)	1
•	0

34 Specification of Earthquakes Affecting the Savannah River Site in South Carolina

Preliminary Source Geometry

Martin Chapman

August 25, 1996

Zonation 1:

⋮

Spatial smoothing of seismicity, with source areas for the New Madrid and the Wabash Valley seismic zones (Figure 1).

Zonation 2:

⋮

Areas defined for all sources, with no spatial smoothing (Figure 2).

Zonation 3:

Modification to Zonation 2 above, where fault sources replace source areas A and D. Areas N and M replace areas C and E (Figure 3).

Discussion

Source A: (Eastern Tennessee Area Source)

The Valley and Ridge province of eastern Tennessee has been the most seismically active area in the southeastern United States since instrumental monitoring of the region became approximately uniform in the early 1980's. The pattern of epicenters defines a northeast trending zone, which correlates with regional scale potential field anomalies (King and Zietz, 1978; Nelson and Zietz, 1983, Powell et al., 1994). The earthquakes in eastern Tennessee show similarities to the seismicity of the Giles County, Virginia, zone (Bollinger et al., 1991). Focal depths are beneath the Appalachian sedimentary section in Precambrian basement.

Intentionally blank

Source A alternative: (basement faults)

The basement faults inferred by Chapman et al., (1996) are modeled as an alternative to a uniform area source.

Source B:

This source includes southwestern Virginia, western North Carolina, northeastern Tennessee, and northwestern South Carolina. Instrumental data from shocks in this area suggest that the earthquakes occur beneath the Appalachian thrust sheets, in Precambrian basement rock, as in Giles County Virginia and the adjoining eastern Tennessee seismic zones. The region overlies the inferred Eocambrian margin of North America, and reactivation of extensional faults that originally developed during the opening of the proto-Atlantic ocean may be responsible for modern seismicity (Bollinger and Wheeler, 1988).

The largest historical shock in this source area occurred on February 21, 1916. The epicenter of this shock is uncertain: it was strongly felt in Waynesville, North Carolina, which is the attributed epicenter. However, the shock was also strongly felt on the western side of the Smoky Mountains, in Sevierville, Tennessee. Stover and Coffman (1993) list a magnitude value of 5.2 (mb_{lg}), based on felt area.

Source C South Carolina - Georgia Piedmont.

A section of the Piedmont in South Carolina and eastern Georgia has experienced a higher level of seismicity than the Piedmont-Coastal Plain region as a whole. Probably the largest historical shock in the entire Piedmont occurred near Union, South Carolina on January 1, 1913. That shock threw down numerous chimneys in the epicentral area. The magnitude is estimated as 4.8 (Stover and Coffman, 1993). Source area C is defined here on the basis of historical and recent levels of seismicity.

Source D Charleston (1886 epicenter area)

Geological investigations have revealed evidence for several pre-1886 earthquakes in the coastal South Carolina area (Talwani and Cox, 1985; Obermeier et al., 1985; Weems and Obermeier, 1989; Amick et al., 1990; 1991, Rajendran and Talwani, 1993, Gelinis et al., 1994,). The evidence suggests that seismicity is recurrent in the immediate area near the epicenter of the 1886 shock. The area source D models the hypothesis of an active source limited to the epicentral area of the 1886 shock.

ZRA: (Alternative to Source D).

The fault models a potentially seismogenic structure associated with the zone of river anomalies discussed by Marple and Talwani (1993) and Marple (1994).

Source E: Piedmont and Coastal Plain

The Piedmont and Atlantic Coastal Plain areas exclusive of South Carolina and central Virginia exhibit a low level of seismic activity.

Source F: Central Virginia

The central Virginia seismic zone is an area of persistent seismicity that roughly trends along the James River. The largest historical shock was approximately magnitude 5.0 (mblg) on December 22, 1875, in Goochland County. The seismic zone has been instrumentally monitored since 1978. The data indicate a more complicated stress regime than that inferred for the Giles County, VA and eastern Tennessee seismic zones to the west. Also, central Virginia shocks tend to be at shallower depth, extending from the surface to mid-crustal depth.

Results to date indicate that the geologic causes of seismicity in central Virginia are substantially different from those operative to the west in the Appalachian mountain regions. Seismicity in central Virginia is related to

intensely deformed structures in the detached upper crustal rocks, whereas less deformed Grenville basement is aseismic. Much the opposite is the case in the Appalachian mountain region (Valley and Ridge and Blue Ridge), where the shallow crust above the detachment is aseismic, and earthquakes are inferred to occur due to reactivation of faults in Grenville basement.

Source G: Northern Virginia.

This area includes the Valley and Ridge and Blue Ridge areas of the central Appalachians. The area has a low level of historical seismicity.

Source H: Appalachian Foreland

This source area is simply defined on the basis of sparse historical seismicity. It represents the average seismicity characteristics of a large portion of the central United States.

Source I: Alabama

This source area includes the moderately active Appalachian Valley and Ridge province of Alabama and the extension beneath the coastal plain.

Source J: Giles County Virginia

The "Giles County" seismic zone is an area of concentrated seismicity near the West Virginia-Virginia border, lying mostly within Giles County, Virginia. This is the location of the second largest earthquake to have occurred in the southeastern United States during the historical period. It occurred on May 31, 1897, with an estimated magnitude of 5.8 (mblg). It caused intensity VIII MM damage in the epicentral area, near Pearisburg. The largest shock in recent times was mblg 4.6 on November 11, 1969.

Earthquakes occur at depths between 5 and 25 km and appear to define a 40 km long, steeply dipping structure which trends NNE, about 20 degrees

counterclockwise to the trend of the detached sedimentary structures mapped at the surface. The earthquakes are apparently unrelated to structure exposed at the surface, and are confined to the Grenville basement beneath the Paleozoic detachment. It has been proposed that seismicity in the zone is the result of reactivation of one or more Eocambrian extensional faults (Bollinger et al., 1993, 1991; Bollinger and Wheeler, 1988).

Source K: Wabash Valley

This area models the potential for large shocks in the Wabash Valley. Recent paleoseismic studies have discovered evidence for several large pre-historic shocks in this area (e.g., Obermeier, 1996).

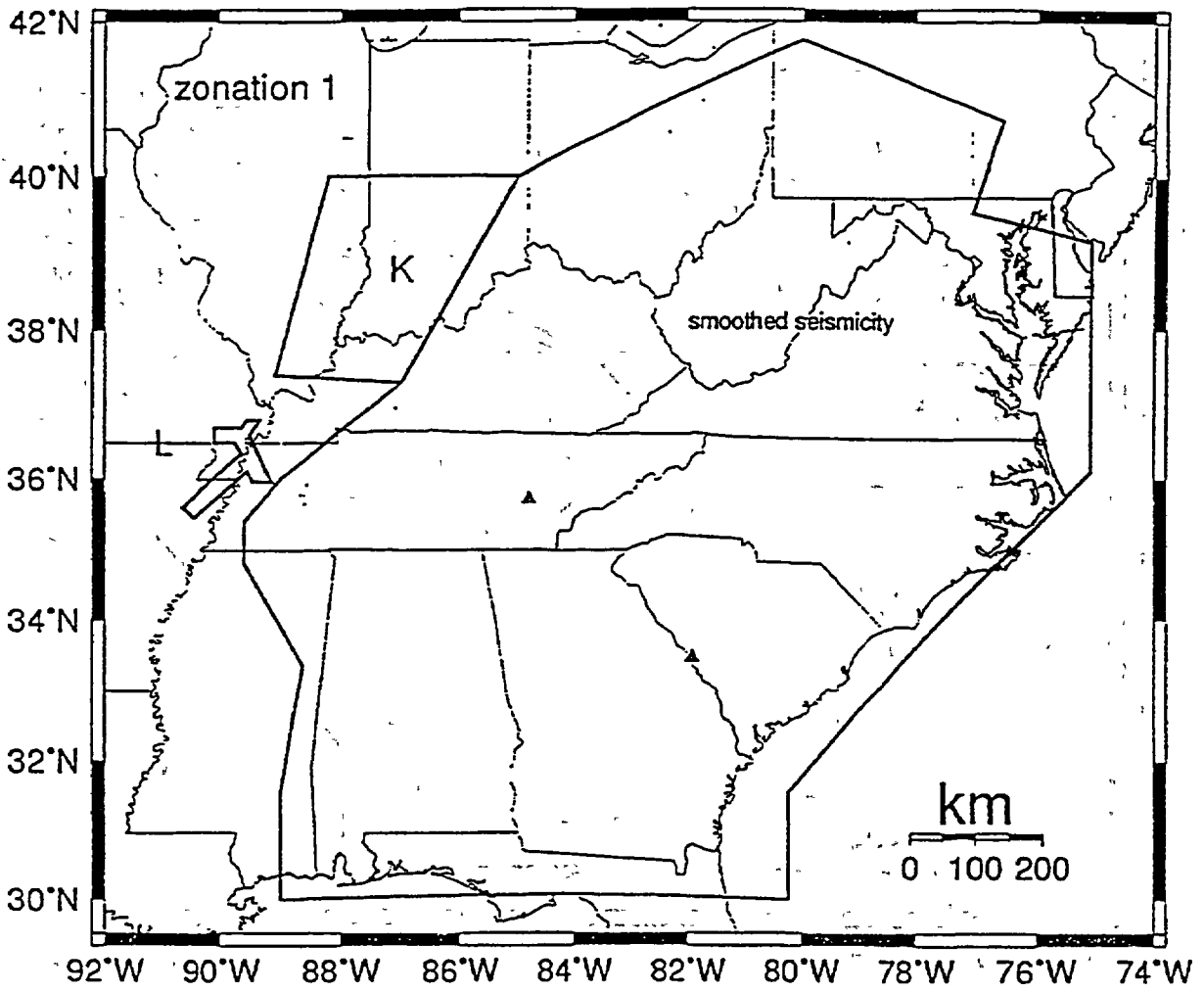
Source L: New Madrid

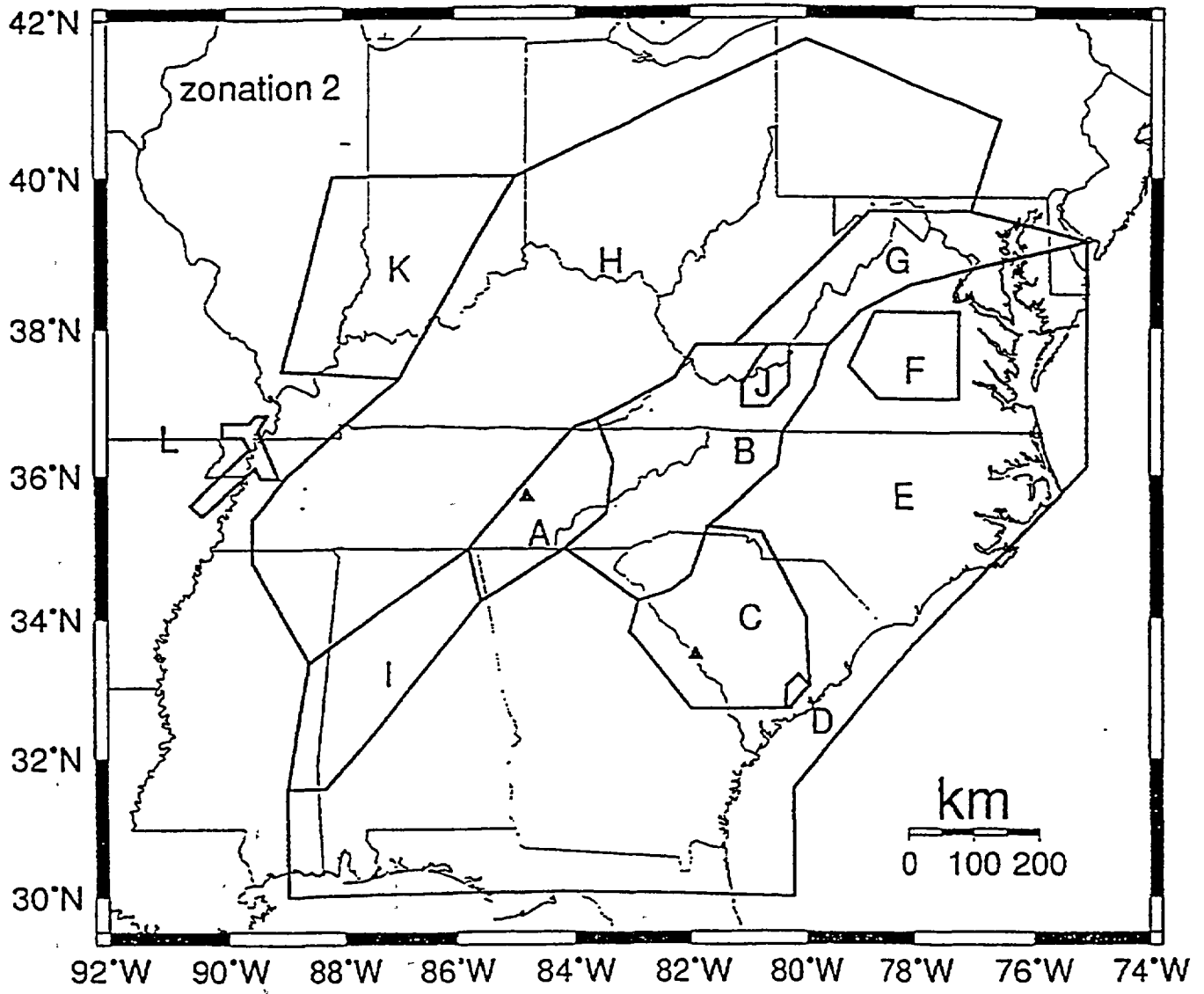
This source area models the seismogenic basement faults in the New Madrid seismic zone.

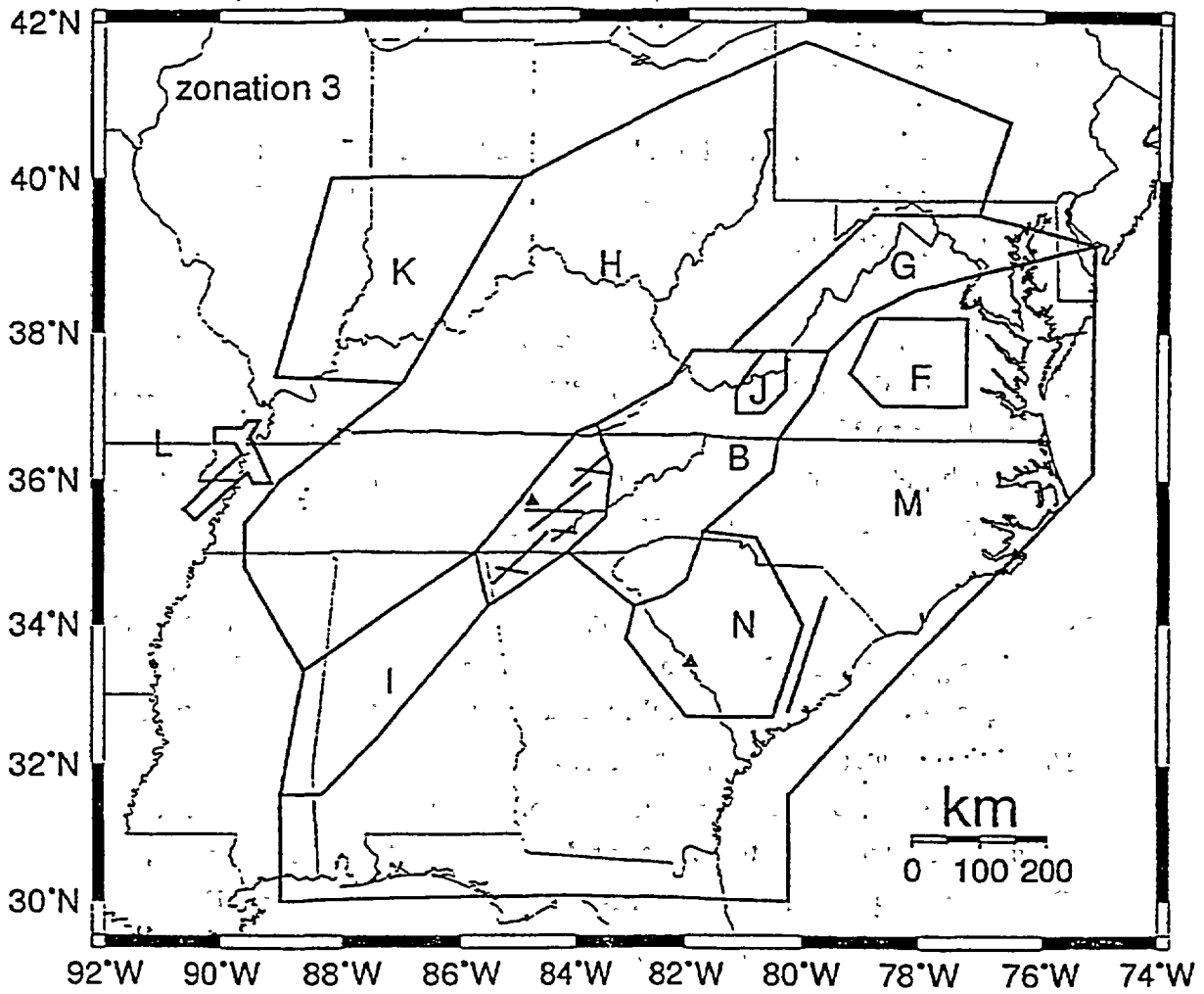
Source M: Alternative to Source E

Source N: Alternative to Source C

This slight modification is to be used in association with the ZRA source for Charleston and source E for the greater Piedmont areas.







References

- Amick, D., G. Maurath, and R. Gelinas, (1990), Characteristics of seismically induced liquefaction sites and features located in the vicinity of the 1886 Charleston, South Carolina, earthquake, Seismological Research Letters, v. 61, no. 2, pp. 117-118.
- Amick, D., R. Gelinas, and K. Cato, (1991), Magnitudes, locations and return periods of large prehistoric earthquakes occurring in coastal South Carolina, Seismological Research Letters, v. 62, no. 3-4, p. 161.
- Bollinger, G. A. and R. L. Wheeler, (1988), The Giles County, Virginia, seismic zone - Seismological results and geological interpretation, U.S. Geological Survey Professional Paper 1355, 85 p.
- Bollinger, G. A., A. C. Johnston, P. Talwani, L. T. Long, K. M. Shedlock, M. S. Sibol, and M. C. Chapman, (1991), Seismicity of the Southeastern United States; 1698 to 1986, in Neotectonics of North America, D. B. Slemmons, E. R. Engdahl, M. D. Zoback, and D. D. Blackwell, editors, Geological Society of America, Boulder, CO, Decade volume 1, pp. 291-308.
- Chapman, M. C., Powell, C. A., Vlahovic, G., and M. S. Sibol, (1996), The nature of faulting in eastern Tennessee inferred from a statistical analysis of earthquake epicenters and focal mechanisms, submitted to Bulletin of the Seismological Society of America, 1996.
- Gelinas, R., K. Cato, D. Amick and H. Kemppinen, (1994), Paleoseismic studies in the southeastern United States and New England, NUREG/CR-6274, Division of Engineering, Office of Nuclear Regulatory Research, U.S. Nuclear Regulatory Commission, Washington, D.C.
- King, E. R. and Zietz, I., (1978), The New York - Alabama lineament; Geophysical evidence for a major crustal break in the basement beneath the Appalachian basin, Geology, v. 6, pp. 312-318.

- Marple, R. T., (1994), Discovery of a possible seismogenic fault system beneath the Coastal Plain of South and North Carolina from an integration of river morphology and geological and geophysical data (Ph.D dissertation), Univ. South Carolina, 354 p.
- Marple, R. T., and P. Talwani, (1993), Evidence of possible tectonic upwarping along the South Carolina coastal plain from an examination of river morphology and elevation data, Geology, 21, p. 651-654.
- Nelson, A. E. and I. Zietz, (1983), The Clingman lineament, other aeromagnetic features, and major lithotectonic units in part of the southern Appalachian Mountains, Southeastern Geology, v. 24, pp. 147-157
- Obermeier, S. F., (1996), Seismically Induced Paleoliquefaction Features in Southern Illinois, (abst), Seismological Research Letters, 67 no. 2, p 49.
- Obermeier, S. F., G. S. Gohn, R. E. Weems, R. L. Gelinas, and M. Rubin, (1985), Geologic evidence for recurrent moderate to large earthquakes near Charleston, South Carolina, Science, v. 227, pp. 408-411.
- Powell, C.A., G.A. Bollinger, M.C. Chapman, M.S. Sibol, A.C. Johnston and R.L. Wheeler (1994). A seismotectonic model for the 300 km long eastern Tennessee seismic zone, Science, 264, 686-688.
- Rajendran, C. P., and P. Talwani, (1993), Paleoseismic indicators near Bluffton, South Carolina: An appraisal of their tectonic implications, Geology, 21, 987-990.
- Stover, C. W. and J. L. Coffman, (1993), Seismicity of the United States 1568-1989 (Revised), U.S. Geological Survey Professional Paper 1527, p. 418.

Talwani, P. and J. Cox, (1985), Paleoseismic evidence for recurrence of earthquakes near Charleston, South Carolina, *Science*, v. 229, pp. 379-381.

Weems, R. E. and S. F. Obermeier, (1989), The 1886 Charleston earthquake - an overview of geologic studies, in, *Proceedings of the 17th Water Reactor Safety Information Meeting*, v. 2, U.S. Nuclear Regulatory Commission, pp. 289-313.

**PRELIMINARY DEFINITION OF SEISMIC SOURCES
FOR THE VOGTLE AND WATTS BAR SITES**

TIP Project
Kevin Coppersmith
August 26, 1996

Regional Characterization (applies to both sites)

(See Map KC-1 for identification of sources)

Key Sources

- 1) MERR- Mississippi Embayment-Reelfoot Rift
- 2) New Madrid
- 3) Non-extended Craton
- 4) Ocoee Block
- 5) Iapetan rifted margin zone
- 6) Giles County
- 7) Central Virginia

Vogtle Characterization

(See map KC-1)

- 8) Extended crustal margin zone (runs east to slope break and East Coast magnetic anomaly)
- 9) NW seismicity zone
- 10) Model as either: Pen Branch fault (discrete fault along western boundary of Dunbarton Basin) or as a local source zone (as shown with dotted line)
- 11) Charleston mesoseismal zone
- 12) Marple's zone of river anomalies

Watts Bar Characterization

Three methods are suggested to characterize the spatial distribution of future seismicity in the Watts Bar region:

1. *Spatial smoothing* of observed seismicity, with the following characteristics:
Epanechnikov kernel, smoothing distance of 30 km, smooth counts (not 'a-values') including all events in the catalog (including dependent events)
2. *Seismic sources*, including the following sources (shown in Figure KC-2):
 - 1) Northeast-trending discrete faults (probability of activity of 0.3)
 - 2) East-west discrete faults (prob. activity of 0.2)

- 3) Red source zone (prob. activity of 1.0)
- 4) Yellow source zone (prob. activity of 1.0)

Dependences among the sources are the following:

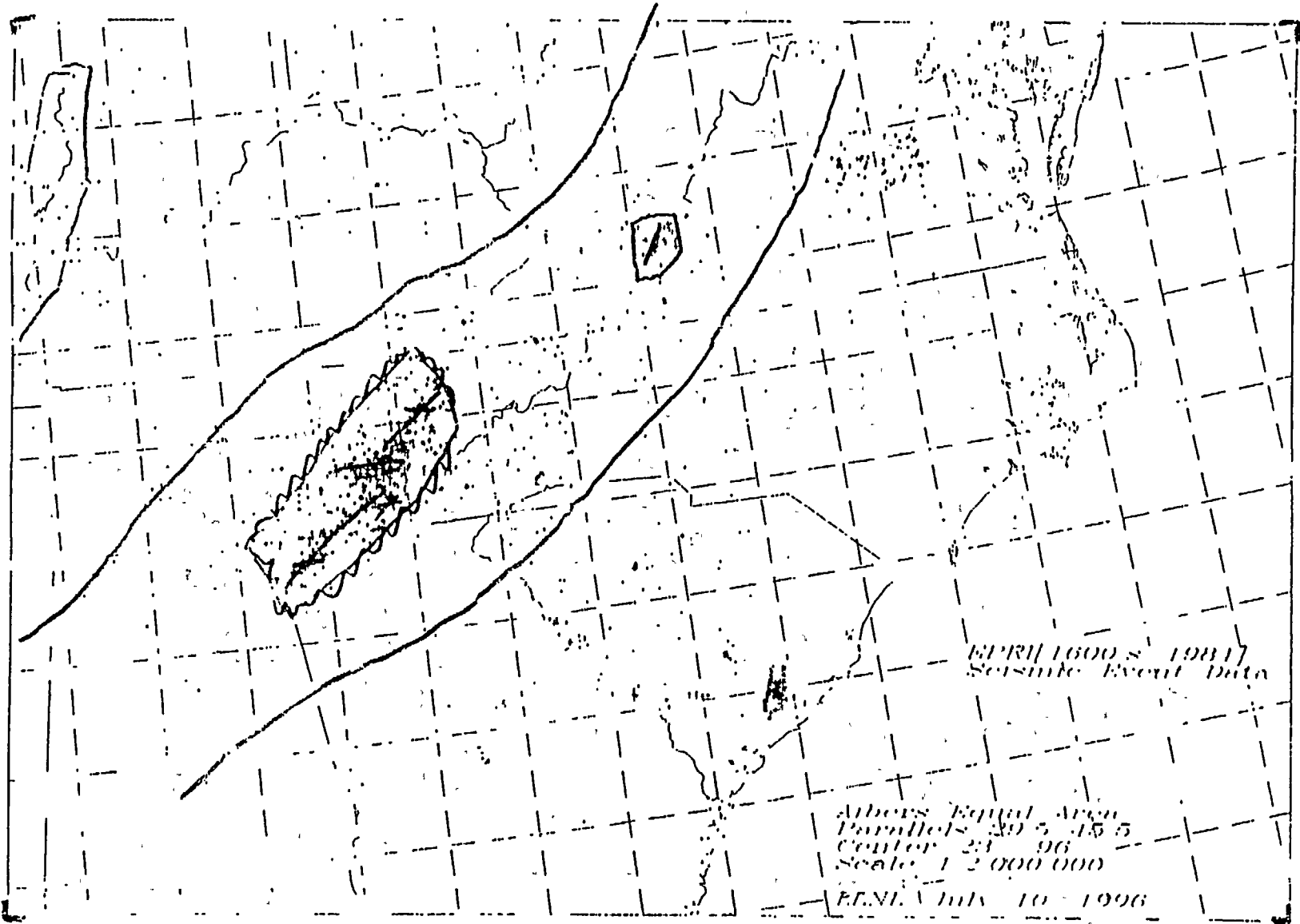
- Sources 1 and 2 are mutually exclusive.
- Sources 3 and 4 are alternative interpretations with weights of 0.4 and 0.6, respectively
- Sources 1&2 and 3&4 are mutually exclusive with each other

3. *Probability Density*

The contours drawn in Figure KC-3 are assumed to contain 70%, 95% and 100% of the probability density for the occurrence of future events (see attached pages for explanation)

M. CHAPMAN

Test Implementation Project - Map # 2



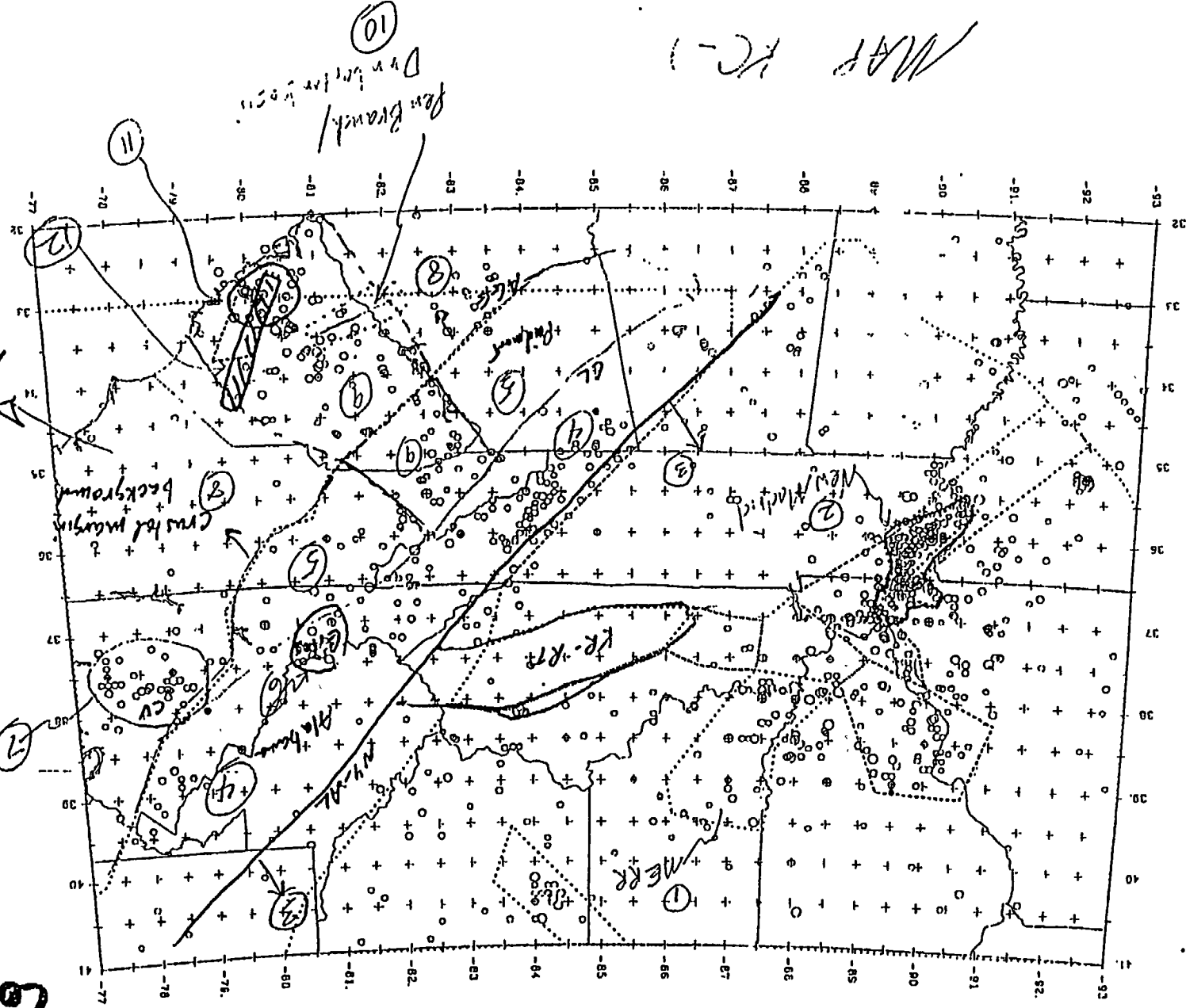
C-25

NUREG/CR-6607

Coppersmith
 1/8 6/18/19

- Magnitude Scale
- Int XI
 - ◊ Int X
 - ◊ Int IX
 - ◊ Int VIII
 - Int VII
 - Int VI
 - Int V
 - Int IV
 - Int III
 - Int II

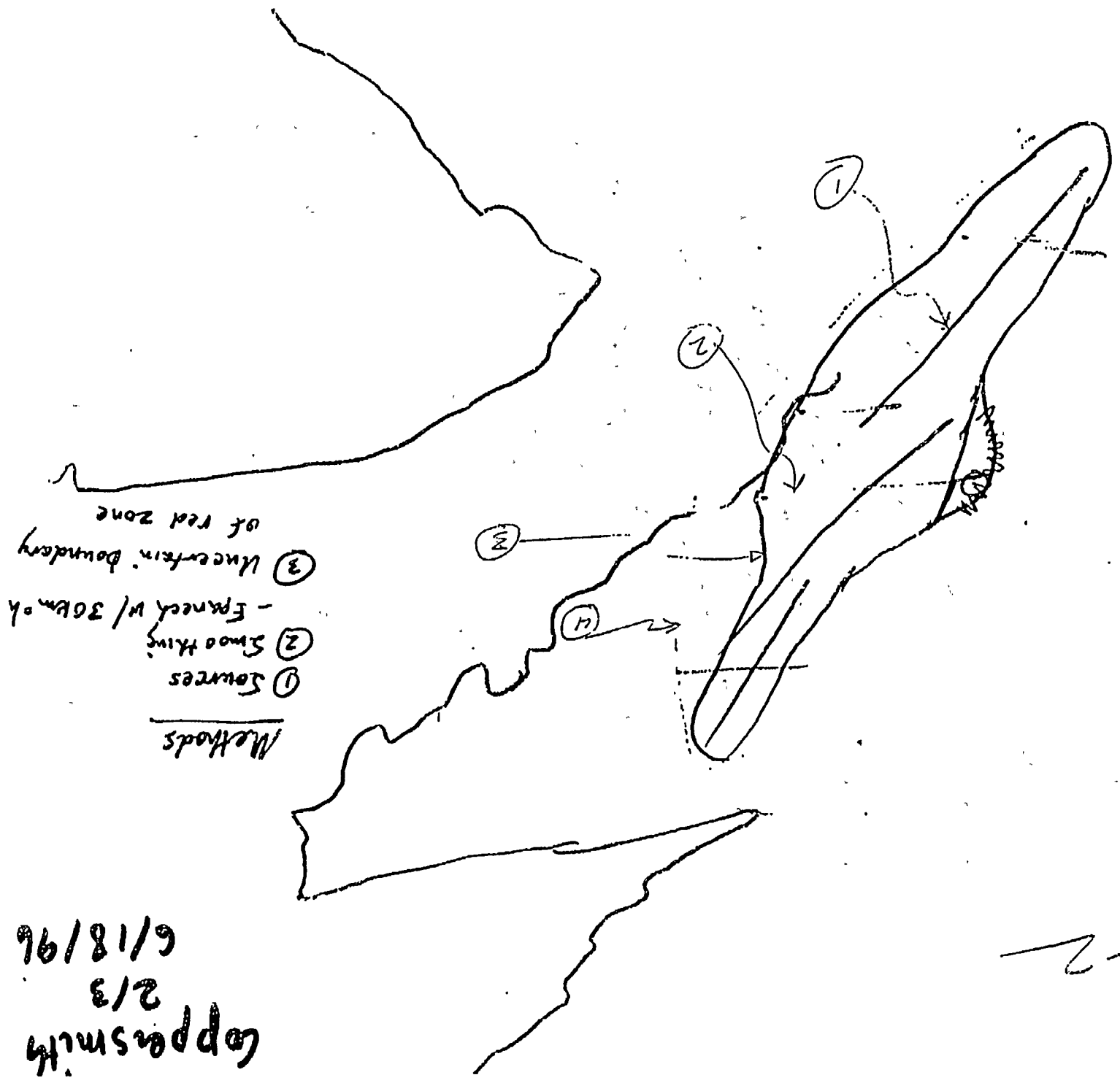
do slope break /
 may anomaly
 1:5,000,000
 Proposed Haysi Dam



MAR KC-1

Coppsmith
2/3
6/18/96

- Methods
- ① Sources
 - ② Smoothing - France w/ 30km ok
 - ③ Uncertain boundary of red zone



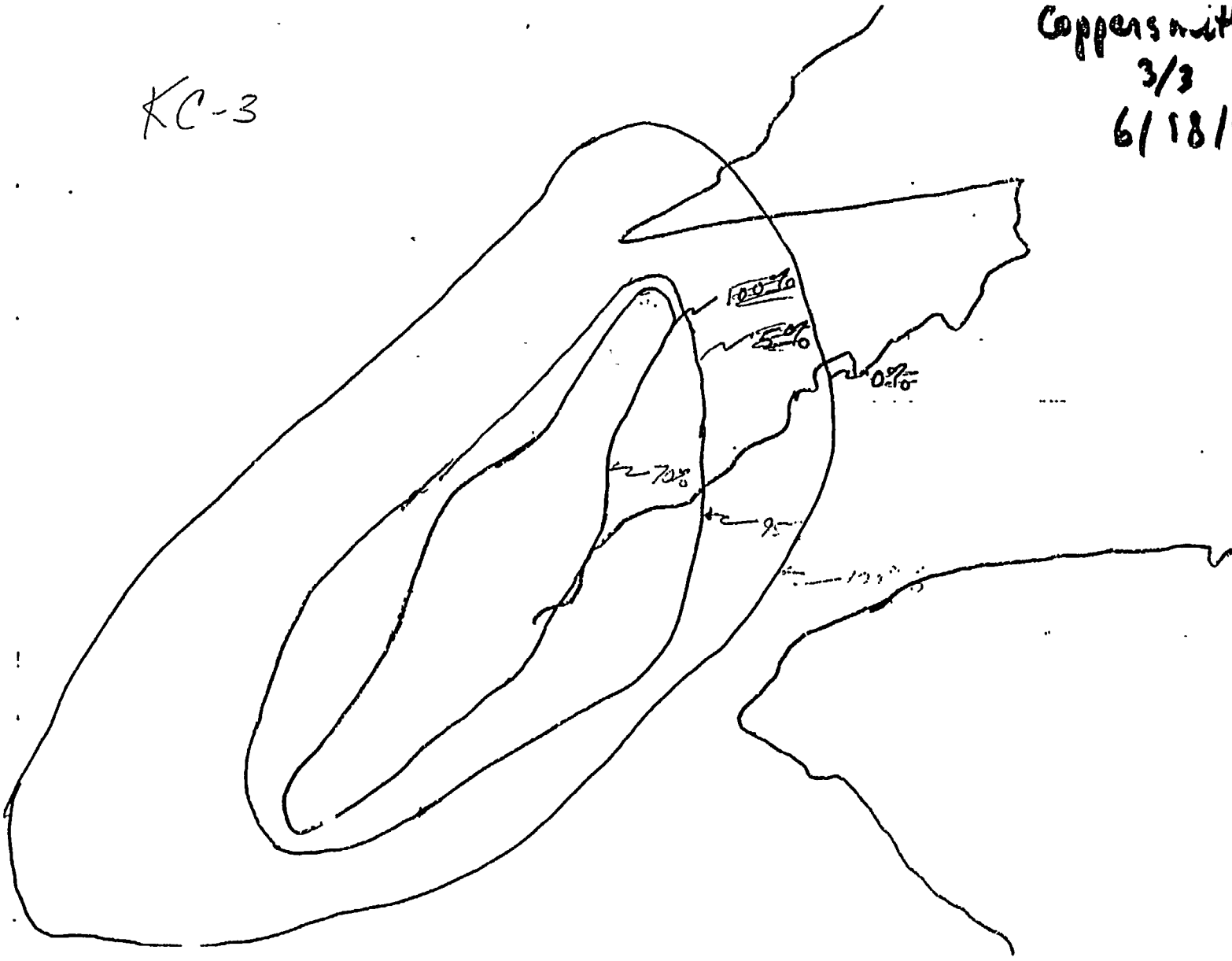
KC-2

NUREG/CR-6607

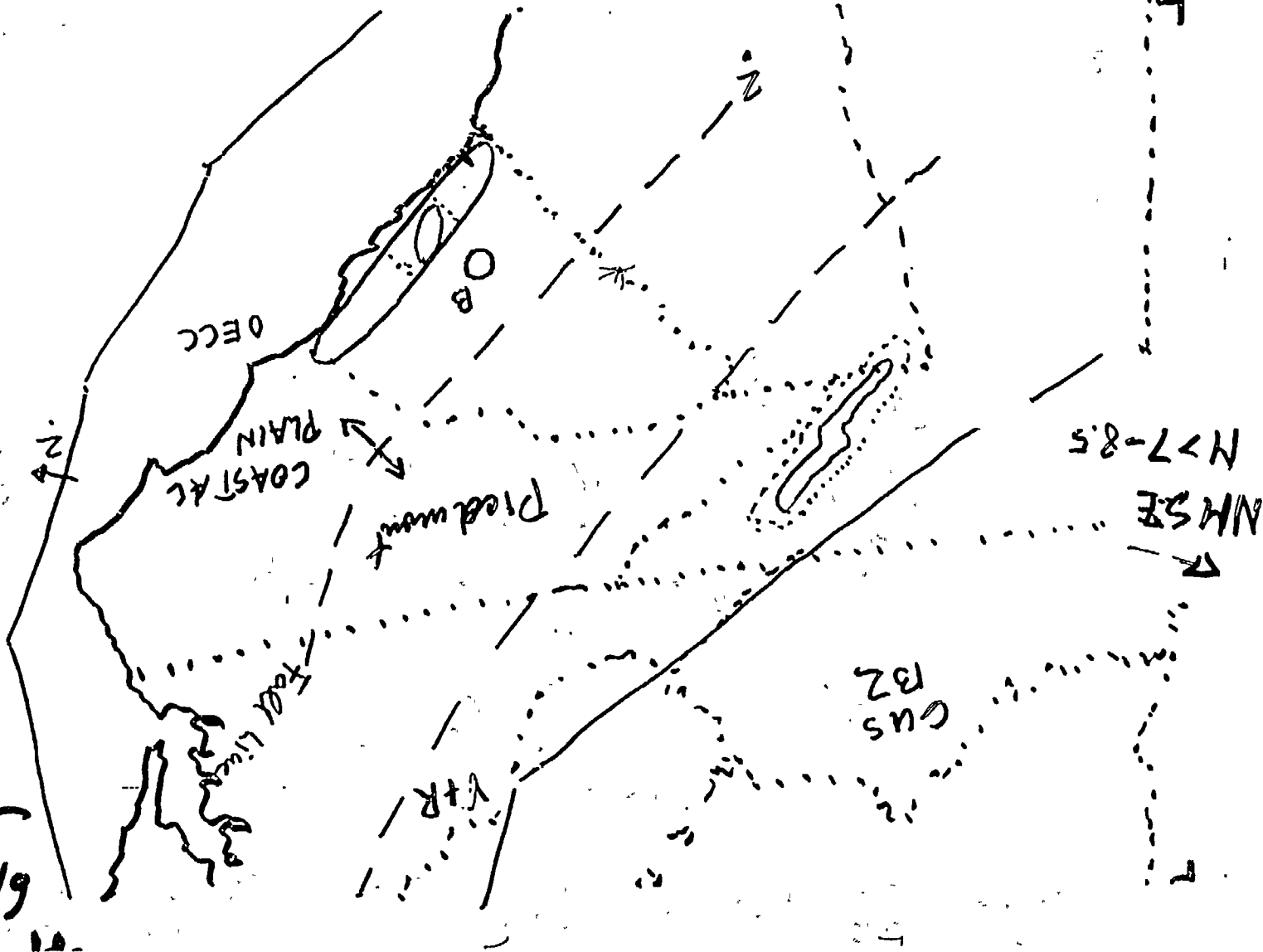
C-28

KC-3

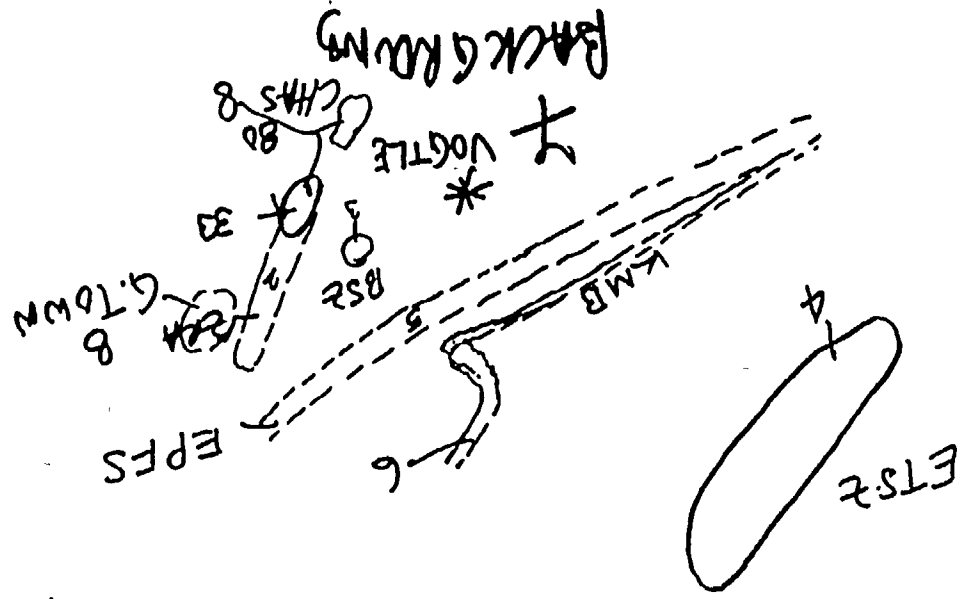
Coppersmith
3/3
6/18/96



6/18/96
Jacob



1. Charleston 2.5 3. B52 5.0 5 EPFS 5.0 7 BACKGROUND
 2 RA 4 ETS2 6.0 6 KMB 5.0 9
 A.S. + 670W
 RLU FTON.



+34
 #5

[RLW.N]
 2/18/96
 +

87
 +39

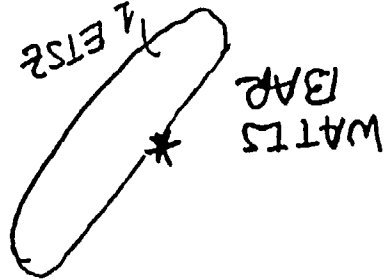
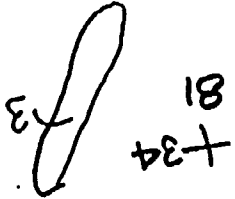
+

- 1. ETSZ 6.0
- 2. GCSZ 6.0

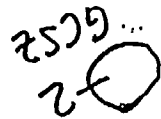
3. ZRA/C HARLESTAD 7.5

+

+



37.85
+



TRAVANI
+
5/18/96

+

**APPENDIX D: GROUND MOTION UNCERTAINTY IN
PROBABILISTIC HAZARD ANALYSES**

APPENDIX D: GROUND MOTION UNCERTAINTY IN PROBABILISTIC HAZARD ANALYSES

D.1 Introduction

In seismic hazard analyses all uncertainty may be categorized as either *aleatory variability* (not controlled by data) or *epistemic uncertainty* (controlled by the amount of available data). If it relates to limitations in the model, then it may also be labeled as *modeling*; if related to the chosen parameterization, then *parametric*. A convenient tool to visualize these decompositions is an uncertainty grid with one axis accounting for the classification as aleatory or epistemic, and the second for modeling or parametric. Aleatory variability is denoted by σ and epistemic uncertainty by U :

		Aleatory	Epistemic	
			Median	Standard Deviation
Modeling		σ_{model}	$U_{\mu\text{-model}}$	$U_{\sigma\text{-model}}$
Parametric		σ_{params}	$U_{\mu\text{-params}}$	$U_{\sigma\text{-params}}$

Although the terms variability and epistemic uncertainty may be unfamiliar, their use encourages precision in communication.

The following begins with a basic discussion of what aleatory variability and epistemic uncertainty are. Although simple in structure, the subject of uncertainty can rapidly become complex and confusing. To prevent the abstract aspects from becoming unwieldy, concrete examples are presented. These examples are all posed in terms of the development of strong ground motion attenuation relations, but the principles are equally relevant in other modeling applications.

D.2 Classification of uncertainty as aleatory or epistemic

Epistemic uncertainty is the uncertainty due to limitations of available data and is familiar to most scientists. Many parameters have a single, actual, true value based in physical reality. Some examples are the shear-wave velocity at a specific location in the real world, the mean of a distribution, and the probability distribution of a real-world population. Such items would be determinable to a near-certainty given perfect data, but as a practical matter we can only estimate what they are given existing data. Epistemic uncertainty is often called *scientific uncertainty* or, generically, *uncertainty*.

Aleatory variability cannot be eliminated by additional data and accounts for inherent limitations in the model. For instance, if faulting style is not a parameter in a simple magnitude-distance attenuation relation, the predicted ground motions will fit the data more poorly than if faulting style were included. This spread is aleatory variability due to unmodeled effects (σ_{model}): additional data will not remove the model shortcoming. Aleatory variability also may arise from model parameters that are multivalued by nature, when this attribute is not specified in the question asked. For instance, if stress drop is not specified, then the attenuation model predicts the ground motion for a "generic" stress drop, and uncertainty is introduced; this is described in greater detail in a later section. Aleatory variability is

sometimes termed *random* or *inherent*, perhaps because the ground motion that is unpredicted by the model looks like random scatter to the model and cannot be eliminated with this model. It may also be termed *random* because the actual stress drop associated with faulting in a future event (the stress drop value that "should" be used in the model) has no "true" value but only potential values, is not determinable at this time, and so in a sense will occur randomly.

In general, to decide if a contribution to uncertainty is aleatory or epistemic, consider if there is a single correct value of the parameter being considered. If a single, correct, factual value exists for a model parameter, but we simply don't know it due to lack of data, then there is epistemic uncertainty in the estimated value we use. If the parameter is not single-valued but rather has a range of potential values, and if the multi-valued nature is not included in the model, then the range causes aleatory variability. We also briefly note here, and explain in detail later, that *context* determines whether a parameter introduces aleatory variability or epistemic uncertainty into the model.

D.3 Three easy steps for empirical attenuation models:

At this point, calculating uncertainty for empirical attenuation models can be tackled. The classification grid makes assessing uncertainty for empirical attenuation models easy and systematic, and the divisions quite naturally reflect the structure of the problem. Any specific case will fit into one of three prototypes described below.

For a given magnitude and distance, an empirical attenuation relation produces an estimate of the median ground motion, μ , and the standard deviation of the ground motion, σ . A database of recordings at several sites for N earthquakes is used to construct the model. Known are some subset of the following: magnitude (M_j), faulting style (F_j), and stress drop (Δs_j) for each earthquake j , distance (d_j), site factor (S_i), and recorded ground motion (y_{ij}) for each site i .

In each case below, the question we ask is "what is the predicted ground motion given a magnitude, faulting style, distance and site type (M, F, d, S)?"

D.3.1 Case 1 : Inputs specified exceed model parameters

In Case 1, our model has three parameters, M , d , and S . Since by assumption the inputs specified are M , F , d , and S , in this case the inputs specified exceed model parameters.

The modeling aleatory variability, σ_{model} , is the amount of scatter not modeled, i.e. the data not matched by the model. It is given by the standard error of the model:

(eqn 1)

where y_{ij} is the predicted ground motion, y is the mean ground motion of all the recordings, and M_j is the number of recordings for event N .

The parametric aleatory variability, σ_{params} , is zero since we have specified a value for each model parameter. The parametric epistemic uncertainty, U_{params} , is similarly zero.

The modeling epistemic uncertainty is caused by a lack of data. With an infinite number of recordings we would know the true median ground motion and the true scatter about it. The limited data leads to uncertainty in our estimated values (denoted U_μ and U_σ). For now we assume U_μ and U_σ can be estimated by comparing credible models and by judgment.

Our uncertainty grid for Case 1 is:

Aleatory Epistemic

		Median	Standard Deviation
Modeling	σ_{model}	U_{μ}	U_{σ}
Parametric	none	none	none

D.3.2 Case 2 : Inputs specified equal model parameters

In Case 2, our model has four parameters, M, d, F and S. The assumed inputs specified are still M, d, F and S. Thus in this Case values for each model parameter, and no extra parameters, are specified.

The uncertainty analysis is identical to Case 1 and the uncertainty grid for Case 2 is:

Aleatory Epistemic

		Median	Standard Deviation
Modeling	σ_{model}	U_{μ}	U_{σ}
Parametric	none	none	none

D.3.3 Case 3 : Inputs specified exceed model parameters

In Case 3, our model has five parameters, M, d, F, Δs and S. The inputs specified are still M, F, d, and S. In this Case the inputs specified are fewer than model parameters: Δs is unspecified.

The modeling aleatory variability, σ_{model} , is still given by the standard error of the model as in equation 1 above.

The parametric aleatory variability, σ_{params} , for the parameters M, d, F, and S is zero since their values are specified. However, there is a non-zero $\sigma_{\Delta s}$. The parametric aleatory variability in Δs is given by the standard error in the predicted ground motion due to varying Δs. This is calculated by making multiple runs of the model and for each run picking a "random" Δs from a "known" distribution function of Δs:

(eqn 3)

Written in continuous terms,

(eqn 4)

As above, the modeling epistemic uncertainty due to limited data is U_{μ} and U_{σ} . The parametric epistemic uncertainties are due to uncertainty in knowing the true distribution function of Δs ($\mu(\Delta s)$ and $\sigma(\Delta s)$).

Our uncertainty grid for Case 3 is:

		Aleatory	Epistemic	
			Median	Standard Deviation
Modeling	σ_{model}		U_{μ}	U_{σ}
Parametric	$\sigma_{\Delta s}$		$U_{\mu(\Delta s)}$	$U_{\sigma(\Delta s)}$

D.3.4 Observations on uncertainty for empirical attenuation relations

The total aleatory variability for a given question cannot be reduced by addition of parameters beyond those specified in the question. Additional parameters merely shift uncertainty from aleatory modeling variability to aleatory parametric variability.

Models having more parameters will have less standard error than models with less parameters:

$$\sigma_{model}^{(3)} < \sigma_{model}^{(2)} < \sigma_{model}^{(1)}$$

is less than the modeling component of the aleatory variability for

$\mu^{(2)}$, the parametric aleatory error balances it out:

$$\sigma_{total}^{(2)} = \sigma_{total}^{(3)}$$

because

(eqn 5)

and

(eqn 6).

A summary of our results for a question in which 4 parameters are specified for model 1 (3 parameters), model 2 (4 parameters), and model 3 (5 parameters) is given below.

Calculation of σ_{total} :

$$\sigma_{total}^{(1)} = \sigma_{model}^{(1)}$$

$$\sigma_{total}^{(2)} = \sigma_{model}^{(2)}$$

$$\sigma_{total}^{(3)} = [\sigma_{model}^{(3)}]^2 + [\sigma_{\Delta s}^{(3)}]^2$$

Relations between models:

$$\sigma_{model}^{(3)} < \sigma_{model}^{(2)} < \sigma_{model}^{(1)}$$

$$\sigma_{total}^{(1)} > \sigma_{total}^{(2)}, \sigma_{total}^{(3)}$$

$$\sigma_{total}^{(2)} = \sigma_{total}^{(3)}$$

D.3.5 Calculation of the epistemic uncertainty for empirical attenuation models

Epistemic uncertainties in μ and σ arise because of the limited number of records in the data set used to develop the model. In practice U_μ and U_σ are usually not estimated explicitly, but rather are represented by using multiple attenuation relations with weights. This approach assumes that credible attenuation relations developed by different people represent both U_μ and U_σ . Although it may sound overly esoteric to talk about U_σ , the epistemic uncertainty in the aleatory variability, it is of practical importance to estimate how well we know the scatter of the ground motions. (For instance, this tells us about the possibility of extremely high accelerations.) In this approach the epistemic uncertainty is represented by alternative models and the aleatory variability is given by the standard deviation provided with the attenuation relation. This is a natural separation of uncertainty.

The main drawback to using alternative models with weights to represent the epistemic uncertainty is that many of the models are developed from similar data sets. The differences in the models may not be representative of the true underlying scientific uncertainty due to small data set sizes. For example, consider the four alternative attenuation models for soil sites in California: Abrahamson and Silva (1997), Boore et al (1997), Campbell et al (1997), and Sadigh et al (1997). These attenuation models for peak acceleration are shown in Figure A-1 for magnitudes 5.0 and 7.0.

Figure 1 shows that the models all produce similar ground motion values for a magnitude 7.0 event at short distances; however, there is very little data in this magnitude-distance range. The agreement of the median predictions by the models does not necessarily imply that the value for the median is well known; the epistemic uncertainty, U_μ , should not necessarily be small.

Explicitly asking for estimates of U_μ forces us to think about epistemic uncertainty due to limitations of data that may not be accurately represented by alternative attenuation relations. Basically, it is another way of asking how confident we are of their estimates. The same can be said for U_σ .

D.4 Further discussion of aleatory and epistemic uncertainty

In words, the above example implies the sources of uncertainty are:

		Aleatory	Epistemic	
			Median	Standard Deviation
Modeling	Unmodeled effects		Uncertainty in estimate of μ due to finite number of recordings	Uncertainty in estimate of σ due to finite number of recordings
	Parametric	none	Uncertainty in distributions of parameters for which values are not specified	Uncertainty in distributions of parameters for which values are not specified

D.4.1 Application of these classifications to modeling

It is tempting to conclude that all uncertainty in ground motion attenuation is epistemic. That is, if we had the right model (exact description of the source process, 3-D crustal structure, and site properties) then we could compute the ground motions exactly. This is the concept of the perfect model with perfect data. Perfect data will eliminate epistemic uncertainty. A perfect model will eliminate the problem of inherent aleatory variability due to unmodeled effects. If a very simple or very specific question is asked, aleatory variability associated with "random" variables will not be present. There would be no uncertainty in the predicted ground motion.

Unfortunately, once the question is moderately interesting or general, the perfect model cannot eliminate the uncertainty associated with "random" variables. For instance, we know that stress drop affects the ground motions. Therefore the perfect model must include a parameter for stress drop. However, since it is impossible to uniquely determine the correct value of a future stress drop from current conditions, perfect data will not enable us to determine what value to use for stress drop, and we cannot eliminate this aleatory variability. We could eliminate this particular uncertainty if we pose the relatively less useful and more specific question of predicting ground motions for an earthquake with a stress drop of 50 bars.

More importantly, on a practical level, the problem with the "perfect model" concept is that it does not consider the limitations of the information that is provided. Typically, the independent variables provided are simply tectonic region, earthquake magnitude, focal mechanism, site-to-source distance, and site classification. Since these simple parameters are not sufficient to completely characterize the source, path, and site effects, we cannot develop a perfect model of ground motion. Although with an infinite number of recordings we can reduce the uncertainty in our estimate of the median ground motion to zero, there will still be variability due to unmodeled effects such as the range of source properties, crustal velocities, and site properties that all have the same region, magnitude, mechanism, distance, and site class. This inherent variability due to unmodeled effects is aleatory variability.

D.4.2 Context-dependence of classification of uncertainty

The question that is asked by the model determines whether a model parameter contributes epistemic or aleatory variability. For example, if we want to know what ground motions will be generated by an event on the Whittier Fault and we think the dip is around 60°, the dip parameter introduces epistemic uncertainty that could be settled as a factual matter by digging a very deep trench (assuming a planar fault). On the other hand, if our question is what the ground motion will be from a generic earthquake, then the dip parameter introduces aleatory variability, because we do not uniquely specify the dip. (As an aside, the assumption of a planar fault introduces aleatory variability from unmodeled effects to the extent that the assumption does not reflect the real world, which is accounted for under the model's randomness, σ_{model} .)

D.5 Modeling and parametric uncertainty related to numerical models

We have implicitly discussed and made use of the division of uncertainty into modeling and parametric uncertainty in the above discussion. For complex models such as arise in numerical modeling procedures there are many components to each of our four basic uncertainties σ_{model} , σ_{params} , U_{model} and U_{params} .

D.5.1 Modeling uncertainty

Modeling uncertainty represents the limitations of the ground motion model. That is, even when the model parameters are optimized for a particular past earthquake, there are still differences between the predicted motions and observed motions (for example, the residuals are not all zero). These differences are attributed to the use of a simplified model of a complicated process.

Since modeling uncertainty is a measure of the limitations of the ground motion model, the only way we can measure it is through comparisons with ground motions from previous earthquakes. The comparison of the model predictions with recordings from past earthquakes has been called model *validation*, but it is more than that. Validation is also necessary to estimate the modeling uncertainty component of the total uncertainty of the ground motion predictions for future earthquakes.

The standard error of the residual represents uncertainty of the ground motions that is not predictable by the simple model. This uncertainty is considered to be random variation (aleatory) for that particular model. (As far as that particular model is concerned, these variations are random.) When predicting ground motions for a future earthquake, we need to account for this random variation that is not captured by the model (part of aleatory σ). There is also epistemic uncertainty due to the uncertainty in our estimation of the value of the standard error due to the limited number of recordings and earthquakes used in the validation exercise (component of U_e). In general, there is also uncertainty in the form of the probability distribution (e.g. other than lognormal), but that is outside the scope of this discussion.

Since modeling uncertainty is computed from comparisons to data, the modeling uncertainty is a catchall that in principle covers all of the shortcomings of the numerical simulation procedure. This is true only to the extent that the events used in the validation exercise are representative of future earthquakes. As the numerical models become more complete, the modeling uncertainty will be reduced, but the parametric uncertainty should then be increased because more event-specific parameters need to be randomized, as described below.

D.5.2 Parametric Uncertainty

The parametric uncertainty represents the uncertainty of ground motion due to variations of the parameters for future earthquakes. This variability comes from multiple realizations of the model with different values of the source parameters. Those source parameters that were optimized for individual events in the validation study are varied for future earthquakes. Parameters that are fixed in the model (either to constant value or constant scaling relations) are not varied because the effect of their variations is already captured as part of the modeling uncertainty if a sufficient number of events is used in the validation study. (The same holds for site and path parameters.)

We discussed above how parametric aleatory variability arises from unspecified values for a parameter with a range of potential values. There is also parametric epistemic uncertainty in the assumed distributions for the source parameters (mean and standard deviation of the source parameters).

D.6 Uncertainty in numerical simulation models

For numerical simulations, there are two parts to the modeling uncertainty: the mean of the residuals and the standard error of the residuals. The mean residual is an estimate of the bias of the model, i.e. whether or not the model tends to systematically over-predict or under-predict the ground motion. If there is a large bias, then the model may not be acceptable. The evaluation of the model bias is really what is commonly taken as the model validation. If the bias is acceptably small, then the model is said to be validated. If there is a significant model bias, then the model could be revised (improved) in the future to correct for this bias. Because the bias is reducible with additional information, the bias is considered as part of the epistemic uncertainty (a component of U_e).

For numerical simulations, there are two parts to the parametric uncertainty. Parametric aleatory variability is caused by not specifying values for the source parameters of the future event. Uncertainty in the values contributes epistemic uncertainty to U_e .

The sources of uncertainty for numerical modeling are:

	Aleatory	Epistemic	
	σ	U_μ	U_σ
Modeling (From comparisons with data)	σ_{model}	$\sigma_{\mu-method}$ σ_{bias}	$\sigma_{\sigma-method}$ $\sigma_{\sigma-model}$
Parametric (From multiple realizations of the model)	σ_{source}	σ_{disp}	Not considered

D.7 Total uncertainty

The total aleatory variability is given by summing the modeling variance and parametric variance:

$$\sigma_{total} = \sqrt{\sigma_{model}^2 + \sigma_{param}^2}$$

This assumes that the covariance between the modeling and parametric terms is zero, i.e. that they are independent variables.

In a hazard analysis, the epistemic and aleatory components of the uncertainty are kept separate. However, for an 84th percentile ground motion estimate, the total uncertainty is given by summing the aleatory variance and the variance in the median:

$$\sigma_{total} = \sqrt{\sigma_{model}^2 + \sigma_{param}^2 + \sigma_\mu^2}$$

D.8 Complex versus simple models

As more complex models are used, the modeling uncertainty is reduced, but there is a counteracting increase in the parametric uncertainty. That is, the total uncertainty cannot be reduced by adding more event-specific parameters to the model.

The advantage of using a complex model with additional event- and site-specific parameters is that it better explains past earthquakes. It provides a physical basis for the variations in the ground motion. We intuitively have more confidence in the model when we can explain the variations rather than just say that they are random.

The disadvantage of using a more complex model is that we need to develop *joint* probability distributions for all of the event-specific parameters used in the model. It is sufficiently difficult to develop probability distributions for the parameters independently from the limited data available; once we have multiple source parameters, we must develop joint distributions to account for their correlation. If the correlation of source parameters is ignored, then the variability will likely be overestimated.

**APPENDIX E: DOCUMENTATION OF EXCEL 5.0
SPREADSHEETS AND FORTRAN CODES FOR DEVELOPING
HYBRID EMPIRICAL GROUND-MOTION ESTIMATES FOR THE
MIDCONTINENT OF THE EASTERN UNITED STATES**

APPENDIX E: DOCUMENTATION OF EXCEL 5.0 SPREADSHEETS AND FORTRAN CODES FOR DEVELOPING HYBRID EMPIRICAL GROUND-MOTION ESTIMATES FOR THE MIDCONTINENT OF THE EASTERN UNITED STATES

Kenneth W. Campbell
EQE International, Inc.
2942 Evergreen Parkway, Suite 302
Evergreen, Colorado 80439

INTRODUCTION

I have developed several EXCEL 5.0 spreadsheets and a Fortran 77 code for calculating the various distance measures, adjustment factors, and empirical ground-motion estimates for application of the hybrid empirical ground-motion model, hereafter referred to as the Hybrid Model, to the Midcontinent region of the Eastern United States (EUS). The spreadsheets allow the user to interactively add distances and ground-motion parameters for which the estimates are to be made as well as to change the weights assigned to the various relationships and adjustment factors. The Fortran code allows the user to compute theoretical median adjustment factors and their standard deviations for specific values of seismological and crustal parameters. A brief description of the spreadsheets and Fortran code are given below.

DESCRIPTION OF SPREADSHEETS AND FORTRAN CODE

DIST_D5.XLS, DIST_D10.XLS, and DIST_D20.XLS

These spreadsheets calculate the three fault-distance measures required to estimate empirical ground motions using contemporary empirical strong-motion attenuation relationships for shallow-focus (DIST_D5.XLS), intermediate-focus (DIST_D10.XLS), and deep-focus (DIST_D20.XLS) earthquakes. Each spreadsheet contains two worksheets for fault dips of 90 and 45 degrees. Distances for other fault dips can be calculated by simply changing the value of the fault dip on any of the worksheets or by copying an existing worksheet to a new worksheet and changing the fault dip to the desired value. Significant parameters in these spreadsheets are defined below. Only those parameters that are required to use the spreadsheets are described. All depths, widths, and distances have units of kilometers.

alpha. The dip of the fault plane measured from the horizontal plane in degrees. The fault dips of 90 and 45 degrees were specified by the facilitation team.

d. Depth to the center of the fault-rupture plane. This depth is held constant for all rupture scenarios. These depths were defined as 5 km (shallow-focus earthquakes), 10 km (intermediate-focus earthquakes), and 20 km (deep-focus earthquakes) by the facilitation team.

dmax. Maximum depth of fault rupture. This depth was assumed to be 35 km to be consistent with rupture scenarios defined in the ground-motion study conducted by EPRI (1993) for the Midcontinent region of the EUS. This depth is also consistent with the maximum depth of faulting estimated by Arch Johnston (personal communication, 1997) for the 1811-1812 New Madrid, Missouri, earthquakes.

dseis. Depth to the top of the seismogenic portion of the fault. The seismogenic zone of rupture is not allowed to propagate to depths shallower than this value. This depth is set at 3 km, the minimum value recommended by Campbell (1997). The use of a smaller value may lead to unrealistic amplitudes of ground-motion parameters and should be used with caution.

Magnitude. Moment magnitude, M_w . The values of M_w and the corresponding values of horizontal distance (see below) were specified by the facilitation team.

Fault Width. The median estimate of the fault rupture width for the given value of moment magnitude (M_w). This width is calculated using a relationship between rupture width and moment magnitude developed by Wells and Coppersmith (1994) for all faulting mechanisms. This width is assumed to be centered about d unless constrained by the surface trace of the fault or by d_{max} , in which case the remaining width is accommodated by the unconstrained portion of the fault. When the width fills the entire fault plane, the excess width, if any, is disregarded.

Horizontal Distance. The horizontal distance (defined in other spreadsheets as R_{hor}) from the site to the surface trace of the fault. The values of R_{hor} and M_w were specified by the facilitation team.

Reps. The distance from the site to an equivalent point source defined as the down-dip center of the fault rupture plane. This is the distance measure used in the BLWN-RVT point-source stochastic simulation model (Silva and Lee, 1987) used to calculate the theoretical adjustment factors.

Rjb. The shortest distance from the site to the projection of the fault rupture plane on the surface of the earth. This is the distance measure used by Joyner and Boore (1988) and Boore et al. (1997). See Abrahamson and Shedlock (1997) for a brief description of this distance measure.

Rrup. The shortest distance from the site to the fault rupture plane. This is the distance measured used by Abrahamson and Silva (1997), Idriss (1991, 1996), and Sadigh et al. (1997). See Abrahamson and Shedlock (1997) for a brief description of this distance measure.

Rseis. The shortest distance from the site to the seismogenic part of the fault rupture plane. This is the distance measure used by Campbell (1997). See Abrahamson and Shedlock (1997) for a brief description of this distance measure.

HYBRD_5.XLS, HYBRD_10.XLS, and HYBRD_20.XLS

These spreadsheets calculate hybrid empirical ground-motion parameters for shallow-focus (HYBRD_5.XLS), intermediate-focus (HYBRD_10.XLS), and deep-focus (HYBRD_20.XLS) earthquakes using contemporary empirical strong-motion attenuation relationships for California and adjustment factors for applying the California ground-motion estimates to the Midcontinent EUS. The adjustment factors were calculated using the band-limited white noise (BLWN) point-source stochastic simulation model with ground-motion parameters estimated from random vibration theory (RVT). A single estimate of these parameters were developed for California for each magnitude and distance of interest using model parameters developed by Walt Silva (personal communication, 1997), which he developed by calibration to strong-motion recordings and to the ground-motion estimates given by the empirical attenuation relationship of Abrahamson and Silva (1997). A single estimate of these parameters were developed for the EUS for each focal depth using the median model parameters for the Midcontinent region given by EPRI (1993), the crustal model (shear-wave velocity and density as a function of depth) specified by the facilitation team, and a relationship between stress drop and shear-wave velocity in the source region specified by Norm Abrahamson (personal communication, 1997). Uncertainty in the adjustment factors were taken directly from EPRI (1993) and were not calculated independently.

Each spreadsheet contains five worksheets. The first three worksheets give empirical estimates for the specified ground-motion parameters, magnitudes, and horizontal distances for fault dips of 90 and 45 degrees, the latter for both the hanging wall and the foot wall of the fault plane (not the earthquake rupture plane). The fourth worksheet (Factors) gives the calculated adjustment factors and their standard deviations. The standard deviations are 0 because only one estimate is calculated for each stress drop. The

fifth worksheet (Hybrid Estimates) gives the calculated hybrid empirical estimates for the same set of ground-motion parameters, magnitudes, and distances.

Significant parameters in these spreadsheets are defined below. Only those parameters that are required to use the spreadsheets are described. Parameters common to more than one worksheet are defined only once.

Empirical Estimates Worksheets (Dip=90; Dip=45, Hanging Wall; Dip=45, Foot Wall)

Attenuation Relationships. Identification of the attenuation relationships used to develop the empirical ground-motion estimates. Attenuation relationships developed by Abrahamson and Silva (1997), Boore et al. (1997), Campbell (1997), Idriss (1991,1996), Sadigh et al. (1997), and Joyner and Boore (1988) are included. The user can add additional relationships if desired. The Joyner and Boore (1988) relationships, although superseded by Boore et al. (1997), are included because they include a relationship for peak ground velocity. All of the listed relationships can be considered to represent California strong-motion recordings.

Dip. The dip of the fault plane measured from the horizontal plane in degrees.

Style of Faulting (F). The style of faulting parameter F used in all of the empirical attenuation relationships. $F = 0$ corresponds to strike-slip faulting. Most relationships do not include many normal-faulting earthquakes, but the authors of these relationships generally recommend that $F = 0$ be used for normal-faulting events. All of the authors recommend $F = 1$ be used for reverse and thrust-faulting earthquakes. Some authors recommend $F = 0.5$ be used for reverse-oblique faulting. The BLWN-RVT model parameters for California were determined for an average faulting mechanism, consistent with $F = 0.5$, and a median stress drop of 59 bars (Walt Silva, personal communication, 1997). In these worksheets, a value of $F = 0.5$, to be consistent with the way the California model parameters were developed, is used with median stress drops developed independently for the EUS by EPRI (1993) and Gail Atkinson (Norm Abrahamson, personal communication, 1997).

Depth to Hard Rock (D). The depth to basement (hard) rock defined by Campbell (1997). This parameter was set to 2.0 km, which is believed to be generally representative of the "generic" rock site used to calibrate the California BLWN-RVT point-source model parameters used to estimate the adjustment factors. The appropriate value of D for the Midcontinent EUS is inherently incorporated in the crustal model used to estimate the adjustment factors.

Mw. Moment magnitude. This magnitude measure was specified by the facilitation team.

Rhor. Horizontal distance to the surface trace of the fault plane. The values of these distances were specified by the facilitation team.

Reps, Rjb, Rrup, Rseis. The equivalent point-source and fault-distance measures defined previously. The values are those calculated in the DIST_D5.XLS, DIST_D10.XLS, and DIST_D20.XLS spreadsheets for the specified values of Mw and $Rhor$.

PSA. The average horizontal component of 5%-damped pseudo-absolute acceleration in g for the oscillator frequencies specified by the facilitation team (i.e., 1.0, 2.5, 10.0, and 25.0 Hz).

PGA. The average horizontal component of peak ground acceleration in g.

PGV. The average horizontal component of peak ground velocity in cm/sec. This parameter was not requested by the facilitation team. It is included for information only.

Median Ground Motion Estimates. The median estimates of PSA, PGA, and PGV from the selected attenuation relationships. Only Campbell (1997) and Joyner and Boore (1988) developed attenuation relationships for PGV. The values of PSA at a frequency of 25 Hz were estimated by interpolating between estimates at 20 Hz and PGA (assumed to represent a frequency of 33 Hz) for those relationships that did not have coefficients for 25 Hz.

Standard Errors. The standard errors (i.e., aleatory uncertainty) associated with the empirical estimates of PSA, PGA, and PGV. Interpolation was used to estimate standard errors at 25 Hz as discussed above for *Median Ground Motion Estimates*.

Subjective Weights. The weights assigned to each of the attenuation relationships and each of the ground-motion parameters. These weights must add up to 1, but can be 0 for those attenuation relationships which are not used. The user should select these weights according to his or her belief that the relationship is appropriate for the given ground-motion parameter, magnitude, and distance. Equal weights are assumed. The Joyner and Boore (1988) relationship is not used to estimate PSA and PGA because it has been superseded by Boore et al. (1997). It is used only to estimate PGV. Changing the weights will automatically adjust the weighted estimates in the spreadsheet.

Weighted Median. There are two sets of weighted medians, each weighted by the subjective weights assigned to the attenuation relationships: (1) the weighted median of the median ground-motion estimates, with weights applied to the logarithm of the ground-motion parameters assuming a lognormal distribution of medians; and (2) the weighted median of the standard errors (i.e., aleatory uncertainty), with weights applied to the standard errors assuming a normal distribution of standard errors. An attempt to provide 'unbiased' estimates for the median and standard error of PGV was implemented by applying the median ratio of these estimates with respect to PGA to the weighted median estimate for PGA estimated from all of the attenuation relationships selected by the user. The estimates of aleatory uncertainty are provided for information only. The calculated values of this uncertainty were not used in the hybrid estimates. Instead, the "randomness" component of standard deviation specified by EPRI (1993), which includes both parametric and modeling aleatory uncertainty, was used to estimate total aleatory uncertainty.

σ . There are two sets of σ s: (1) the standard deviation of the median ground-motion estimates (i.e., epistemic modeling uncertainty), and (2) the standard deviation of the standard errors. The σ s are not weighted, instead they are calculated from the total number of estimates that are available in order to avoid predicting too small a standard deviation if too few attenuation relationships are selected. The σ s are adjusted by the number of degrees of freedom (i.e., $N-1$, where N is the number of values used to determine the median). When $N = 1$, the number of degrees of freedom is assumed to be equal to 0.5. The estimates of epistemic modeling uncertainty are provided for information only. The calculated values of this uncertainty were not used in the hybrid estimates. Instead, the "uncertainty" component of standard deviation specified by EPRI (1993), which includes both parametric and modeling epistemic uncertainty, was used to estimate total epistemic uncertainty.

Adjustment Factors Worksheet (Factors)

$\Delta\sigma$. Stress drop in bars. Calculations were done for median stress drops of 120, 150, and 180 bars, consistent with the shear-wave velocity in the source region of the three focal depths. The median stress drops of 120 and 180 bars correspond to focal depths of 5 km ($V_s = 3.52$ km/sec) and 20 km ($V_s = 3.75$ km/sec), respectively. The smaller value is consistent with the shear-wave velocity of about 3.5 km/sec and the median stress drop of 120 bars specified by EPRI (1993) for the Midcontinent region of the EUS. The larger value is consistent with the shear-wave velocity of about 3.8 km/sec and the median stress drop of 180 bars specified by Gail Atkinson (Norm Abrahamson, personal communication, 1997) for northeastern North America. The intermediate values correspond to a focal depth of 10 km, near the boundary of the lower-velocity and higher-velocity source regions. Although adjustment factors for all

three stress drops are included in each spreadsheet, the value that is consistent with the appropriate focal depth is selected through use of a weighting factors (see *Subjective Weights* below). Each stress drop corresponds to a consistent value of shear-wave velocity and density in the source region and an associated crustal model (i.e., set of crustal amplification factors).

Adjustment Factors. The multiplicative adjustment factors for estimating ground-motion parameters for the EUS from the parameters estimated for California. These factors were developed using the BLWN-RVT stochastic simulation model as described above. The median represents the estimates obtained from the median model parameters for California and the EUS. The σ represents the standard deviation of the median factors (i.e., epistemic parametric uncertainty), assuming no uncertainty in the California model parameters. This value is 0 because the uncertainty in these factors resulting from the EUS model were adopted from EPRI (1993) and were not calculated independently. The assumption of no uncertainty in the California model should be evaluated by the user. The reasons for not including any uncertainty in the California model estimates are: (1) the model parameters were constrained by calibrating the model to the California strong-motion records and the Abrahamson and Silva (1997) attenuation relationship, so modeling uncertainty that would result from calibrating these parameters to other attenuation relationships is believed to be already accounted for in the parametric modeling uncertainty calculated by EPRI (1993) (Note that there may be a bias between the ground-motion estimates from this attenuation relationship and the weighted median of all of the attenuation relationships which has not been included); (2) the set of California parameters cannot be replaced with independent assessments of these parameters because of inter-parameter correlation, and (3) the same model is applied in both California and the EUS, so presumably uncertainty in the appropriateness of the stochastic simulation model does not contribute significantly to the modeling uncertainty in the calculated adjustment factors, provided that the source scaling relations are the same in both regions.

Subjective Weights. The weights assigned to each of the stress drops. This weight must be 1 for the stress drop that corresponds to the specified focal depth and must be 0 for all other stress drops.

Weighted Median. The weighted median of the median adjustment factors. This is simply the value that corresponds to the specified focal depth, selected by the use of the *Subjective Weights*.

Example Hybrid Estimates Worksheet (Hybrid Estimates)

Median. The weighted median empirical ground-motion estimate times the weighted median adjustment factor for the given ground-motion parameter, magnitude, and horizontal distance. Estimates are provided for all of the ground-motion parameters, magnitudes, and horizontal distances specified by the facilitation team for a vertical strike-slip fault and for the hanging wall and the foot wall of a 45-degree dipping fault plane. As requested by the facilitation team, estimates are also provided for a site randomly located on the hanging wall and foot wall. The user can modify or extend this table to include other magnitudes and distances of interest. This may require that additional empirical estimates be developed in the first three worksheets.

σ . The standard deviations of the empirical ground-motion estimates (aleatory uncertainty), the hybrid empirical estimates (epistemic uncertainty), and the aleatory standard errors (σ) for the given ground-motion parameter, magnitude, and horizontal distance. All of the standard deviations are given in terms of the natural logarithm (log base e). Except for PGV, the aleatory and epistemic uncertainty was taken from EPRI (1993). The aleatory uncertainty for distances greater than 20 km was used at shorter distances because the increased uncertainty at short distances given by EPRI was due to uncertainty in focal depth, whereas, for this application, the focal depth was specified by the facilitation team. Since EPRI did not provide uncertainty estimates for PGV, estimates of aleatory and epistemic uncertainty for this parameter were taken to be the same as that for the 2.5-Hz PSA for $M_w = 5.0$ and 6.0 and the average of the square root of the variances of the 1.0 Hz and 2.5 Hz PSA for $M_w = 7.0$ and 7.5, consistent with the empirical

attenuation relationships. The standard deviation of σ is the standard deviation of the weighted standard errors of the empirical ground-motion estimates.

Ratios. Ratios of PGV to PGA are provided for information.

FACTORS.FOR

This Fortran 77 computer code calculates the theoretical adjustment factors between the Midcontinent EUS and California for the ground-motion parameters of interest. It requires one additional executable Fortran code, EQERASCL.EXE, for calculating ground-motion parameters using the band-limited white noise (BLWN), random vibration theory (RVT), point-source stochastic simulation model developed by Silva and Lee (1987), with modifications recommended by Walt Silva (personal communication, 1995). EQERASCL.EXE is called from within FACTORS.FOR. This may require replacing the Lahey Fortran system call to DOS with the equivalent system call for the Fortran used to compile the code. The executable file, FACTORS.EXE, is provided to avoid having to recompile the code. FACTORS.FOR also requires an input file that lists the moment magnitudes and equivalent point-source distances for which the adjustment factors are calculated.

Input File

The name of the input file is provided by the user in response to a screen request when the main program is run. Only the main file name should be provided, not the extension (i.e., the part of the filename to the right and inclusive of the decimal point). The file extension for this input file must be '.IN' (e.g., FACT_D5.IN, FACT_D10.IN, or FACT.D20.IN). This file is free format so the only formatting constraint is that multiple entries on a given line be separated by one or more spaces. The data required in this input file are as follows:

First Line. The number of magnitudes followed by the number of distances for each magnitude.

Second Line. The moment magnitudes.

Third and Subsequent Lines. The horizontal distances (*Rhor*) followed by the equivalent point-source distances (*Reps*) corresponding to the horizontal distances (one line for each magnitude). The values of *Reps* are computed in the spreadsheets DIST_D5.XLS, DIST_D20.XLS, and DIST_D20.XLS.

Output Files

Two output files are generated, each with the main file name specified upon program execution, one with an extension of '.OUT' and one with an extension of '.DAT'. Each file is comma delimited for ease in importing to other programs (e.g., EXCEL). A description of these files are as follows:

'OUT' File. This file contains the following parameters: magnitude (MW); horizontal distance (RHOR); stress drop (SDROP); Q at 1 Hz (Q0); the exponent of frequency in the power-law Q function (ETA); the number of the crustal amplification model ('CRUST' ISDROP); the upper crustal attenuation parameter (KAPPA); calculated horizontal spectral accelerations (PSA) for all frequencies of interest (ordered from low to high frequency), peak horizontal ground acceleration (PGA), and peak horizontal ground velocity (PGV) for the Midcontinent EUS; the same ground-motion parameters (H_PSA, H_PGA, and H_PGV) for California; and the adjustment factors, or ratios between the ground-motion parameters listed in the same order as above, between the Midcontinent EUS and California (FACTOR). There is one line for each combination of magnitude, distance, and model parameters.

'DAT' File. This file contains the following parameters: magnitude (MW); horizontal distance (RHOR); stress drop (SDROP); and, for PSA at all frequencies of interest (ordered from low to high frequency),

PGA, and PGV, the median (AVG) and standard deviation (STDDEV) of the calculated adjustment factors. There is one line for each combination of magnitude, distance, and stress drop.

EQERASCL Files

There is one file that is provided by the user and several files that are automatically generated for use with EQERASCL. These files are described as follows:

FREQ.DAT. This file contains the frequencies for which ground-motion parameters are calculated by EQERASCL. The first two values in this file are "dummy" values that indicate PGA and PGV. The remaining values are the frequencies at which PSA and other spectral parameters are calculated. This file must be provided by the user.

INPUT.TXT. This file contains the names of the generic file names that are opened by EQERASCL (generated by FACTOR).

INPUT.DAT. This file contains the input data file for EQERASCL (generated by FACTOR).

OUTPUT.DAT. This file contains the output file from EQERASCL (generated by FACTOR).